

Doctor Thesis
Shibaura Institute of Technology

**Evaluation of Upper Limb Muscle Activation
Using Musculoskeletal Model
with Rehabilitation Assistive Device**

2022/September

Muhamad Fadzli Bin Ashari

Shibaura Institute of Technology
Graduate School of Engineering and Science

September 2022

Doctoral Thesis

Evaluation of Upper Limb Muscle Activation
Using Musculoskeletal Model
with Rehabilitation Assistive Device

Name	Muhamad Fadzli Bin Ashari
Student ID	NB18110
Major	Functional Control Systems
Department	Graduate School of Engineering and Science
Supervisor	Prof. Akihiko Hanafusa

To my parents for everything, they have supported me.

To my little family, wife, and children for their love
and expectation on me.

I dedicated this thesis to my late father, who has always
been there whenever I needed him
during his time in this world.

ACKNOWLEDGMENTS

I would like to express my deep gratitude to
Professor Akihiko Hanafusa,
my research supervisors for their patient guidance,
enthusiastic encouragement, and valuable critiques.

I would also thank him for allowing me to get enrolled in
this project. I appreciate the collaboration of all the
volunteers that made the study possible.

Finally, I wish to thank my family and friends for their
support and encouragement throughout the study.

Table of Contents

Contents	
ACKNOWLEDGEMENT	V
TABLE OF CONTENTS	VI
LIST OF FIGURES	IX
LIST OF TABLES	XI
RESEARCH ACHIEVEMENT	XII
ABSTRACT	1
CHAPTER 1	3
INTRODUCTION	3
1.1 Background study	3
1.2 Rehabilitation Assistive Device	6
1.3 Upper Limb Orthosis	7
1.4 Musculoskeletal Modeling and Simulation	9
1.5 Motivation	11
1.6 Objective	13
CHAPTER 2	14
LITERATURE REVIEW	14
2.1 Introduction	14
2.2 Effectiveness of rehabilitation robots	15
2.3 Rehabilitation robots background	16
2.4 Orthoses for the upper limbs	17
2.4.1 Classification of Upper Limb assistive device	17
2.5 Simbody	20
2.5.1 Mathematical Inside Simbody	20
2.5.2 System and States	22
2.5.3 System and Subsystems	23
2.5.4 The Realization Cache	24
2.6 OpenSim	27
2.6.1 Importing Experimental Data	29
2.6.2 Scaling	29

2.6.3 Inverse Problem	30
2.6.3.1 Inverse Kinematics	30
2.6.3.1 Inverse Dynamics	30
2.6.4 Static Optimization	30
2.6.5 Computed Muscle Control (CMC)	30
2.7 Biomechanical requirements	32
2.7.1 Biomechanics of Upper-limb	34
CHAPTER 3	36
RESEARCH METHODOLOGY	36
3.1 Overall Methodology	36
3.2 Experimental Set-up	37
3.3 Experimental Protocol	38
3.4 Motion Recording	42
3.5 Markers protocol	43
3.6 EMG Recording	45
3.6.1 Electromyography (EMG) signals of Human Muscles	47
3.6.2 Characteristics of EMG signals	47
3.6.3 Detection of Surface EMG Signals	47
3.6.4 Feature Extraction of Raw EMG Signals	49
3.7 Data Processing	50
3.8 Biomechanical Model	51
3.8.1 Working with OpenSim	52
3.8.2 Inverse Kinematics	52
3.8.3 Computed Muscle Control	53
3.9 Simulations of Experiments	55
3.9.1 Muscle force estimation	56
3.9.2 Validation of simulations	57
3.9.3 Simulation workflow	57
Conclusion	58

CHAPTER 4	59
RESULTS AND DISCUSSIONS	59
4.1 Introduction	59
4.2 Test cases evaluation for model validation	60
4.2.1 Simulation results	61
4.3 Simulation with an assistive device	63
4.3.1 Upper limb motion - 90-degree elbow flexion and extension	65
4.3.2 Upper limb motion - Maximum shoulder flexion and extension	66
4.3.3 Upper limb motion - Inward elbow flexion and extension	67
4.4 Statistical Analysis	68
4.4.1 Wilcoxon signed-rank test (Task 1 : 90 degree elbow flexion and extension)	68
4.4.2 Wilcoxon signed-rank test (Task 1 : 90 degree elbow flexion and extension)	69
4.5 Discussion	74
Chapter Conclusion	76
 CHAPTER 5	 77
Conclusion and Future Recommendation	77
 REFERENCES	 79
APPENDIX	87

List of Figures

Figure 1 <i>Upper Limb Orthoses Armeo® Spring</i>	7
Figure 2. <i>Rehabilitation Robot ARMin.</i>	8
Figure 3. <i>OpenSim platform for advance biomechanical simulation</i>	9
Figure 4 <i>Example of the musculoskeletal model created with OpenSim</i>	12
Figure 5 <i>Upper limb right-hand assistive device and a subject wearing the device.</i>	19
Figure 6 <i>System that once built is immutable, and everything that changes is stored in separate state objects.</i>	22
Figure 7. <i>Representation of a System and its Subsystems.</i>	24
Figure 8. <i>Organization of the different stages. The order is considering the stage that has to be computed to acquire the following stage.</i>	25
Figure 9 <i>Screen record shows OpenSim's GUI with different musculoskeletal models</i>	27
Figure 10 <i>The Three Interface Layers of OpenSim Built on SimTK</i>	28
Figure 11 <i>Flowchart of data processing.</i>	31
Figure 12. <i>Human upper limb.</i>	34
Figure 13. <i>Elbow complex and elbow motions. (a) Elbow antomy. (b) Elbow flexion/extension motion. (c) Forearm supination/pronation motion.</i>	35
Figure 14 <i>Subject performing reach forward motion</i>	38
Figure 15 <i>Assistive device developed in our laboratory</i>	39
Figure 16 <i>Assistive device motion range according to its degree of motion.</i>	39
Figure 17. <i>Method and the load cell position for tension force measurement.</i>	40
Figure 18. <i>Subjects wearing an assistive device were asked to flex their elbow close to 90 degrees and return to the initial position. Data (b) shows measured elbow flexion angle and tension force versus time.</i>	41
Figure 19 <i>Subject wearing an assistive device performing maximum shoulder flexion and extension. This movement acquires the subject to flex the elbow to the close 90 deg, and then the upper arm will be brought to the upper limit of the arm's reachable motion and then return to the initial position. Data (b) shows measured elbow flexion angle, shoulder flexion angle, and tension force versus time.</i>	41
Figure 20 <i>Subject wearing an assistive device performing maximum shoulder flexion and extension to the initial position. The arm's initial position was kept in front of the inner side of the frontal body of the subject. The elbow was flex to the maximum and returned to the initial position. Data (b) shows measured elbow flexion angle, shoulder flexion angle, and tension force versus time.</i>	41
Figure 21 <i>Motion recording experimental setup</i>	42
Figure 22. <i>10 markers locations following the International Society of Biomechanics (ISB).</i>	43
Figure 23. <i>Musculoskeletal model of the upper limb. The dynamic model incorporates 7 degrees of freedom, including (A) shoulder rotation and elevation (thoracohumeral angle) and wrist flexion, (B) wrist deviation and elbow flexion, and (C) elevation plane of the shoulder and forearm rotation.</i>	45
Figure 24 <i>The configuration of 6 channels EMG electrodes for upper arm.</i>	46
Figure 25 <i>A subject with the right upper limb attached with EMG electrodes and marker for motion capture.</i>	46

<u>Figure 26</u> <i>Detection procedure of surface EMG signals. EMG electrodes, an eight-channel input box, a multi-channel EMG amplifier, and a personal computer are used to detect the EMG signals.</i>	48
<u>Figure 27.</u> <i>Example of a raw EMG signal and its RMS value.</i>	49
<u>Figure 28.</u> <i>Musculoskeletal model of the upper limb. The dynamic model incorporates 7 degrees of freedom, including (A) shoulder rotation and elevation (thoracohumeral angle) and wrist flexion, (B) wrist deviation and elbow flexion, and (C) elevation plane of the shoulder and forearm rotation.</i>	51
<u>Figure 29 :</u> <i>Schematic of the Computed Muscle Control Algorithm.</i>	54
<u>Figure 30</u> <i>EMG data and estimated muscle forces for the same reach forward motion.</i>	61
<u>Figure 31</u> <i>Comparison of muscle activity for the same muscle cluster.</i>	62
<u>Figure 32.</u> <i>The required data for closed-loop simulation of a human-device system.</i>	63
<u>Figure 33</u> <i>Three predominant muscles activating the elbow DoFs were selected to be the test's muscle: biceps, triceps, and brachioradialis muscle.</i>	64
<u>Figure 34</u> <i>Comparison of EMG from experimental and muscle activations computed from Opensim resulting three muscle force brachioradialis (green), biceps (magenta), and triceps(blue) for 90-degree elbow flexion and extension motion with and without the assistive device.</i>	65
<u>Figure 35</u> <i>Comparison of EMG from experimental and muscle activations computed from Opensim resulting three muscle force brachioradialis (green), biceps (magenta), and triceps(blue) for maximum shoulder flexion and extension motion with and without the assistive device.</i>	66
<u>Figure 36</u> <i>Comparison of EMG from experimental and muscle activations computed from Opensim resulting three muscle force brachioradialis (green), biceps (magenta), and triceps(blue) for inner elbow flexion and extension motion with and without the assistive device.</i>	69
<u>Figure 37</u> <i>Mean and STD (error bars) plot of the muscle activation (brachioradialis) for subject performing 90 deg elbow flexion and extension with assist and without assistive device conditions.</i>	69
<u>Figure 38</u> <i>Mean and STD (error bars) plot of the muscle activation (biceps) for subject performing 90 deg elbow flexion and extension with assist and without assistive device conditions.</i>	70
<u>Figure 39</u> <i>Mean and STD (error bars) plot of the muscle activation (brachioradialis) for subject performing maximum shoulder flexion and extension with assist and without assistive device conditions.</i>	71
<u>Figure 40</u> <i>Mean and STD (error bars) plot of the muscle activation (biceps) for subject performing maximum shoulder flexion and extension with assist and without assistive device conditions.</i>	73

List of Tables

Table 1 Model Available in OpenSim Software	10
Table 2 Subject properties detail	37
Table 3 Markers corresponding names	42
Table 4 Mean (\pm SD) normalized EMG and Muscle Force for all tested muscles with and without device condition (Flexion).	68
Table 5 Mean (\pm SD) normalized EMG and Muscle Force for all tested muscles with and without device condition (Extension).	69
Table 6 Mean (\pm SD) normalized EMG and Muscle Force for all tested muscles with and without device condition (Flexion).	71
Table 7 Mean (\pm SD) normalized EMG and Muscle Force for all tested muscles with and without device condition (Extension).	71

RESEARCH ACHIEVEMENT

International Conference

1. Oral presentation (26 August 2019)

International Conference on Biomedical Engineering (ICoBE), Penang, Malaysia,
Preliminary Study on Muscle Force Estimation using Musculoskeletal Model for
Upper Limb Rehabilitation with Assistive Device for Home Setting.

Muhamad Fadzli and Prof. Akihiko Hanafusa.

2. Oral presentation (23 February 2022)

The 14th International UNIMAS Engineering Conference 2022 (EnCon2022),
Malaysia

Simulation of a Human-device Biomechanical Model to Estimate Muscle Activities
for Upper Limb Dynamic Movement.

Muhamad Fadzli, Prof. Akihiko Hanafusa and AP Dr. Shahrol Mohamaddan.

3. Poster presentation

IEEE Engineering in Medicine & Biology Society (EMBC), Berlin, Germany,
Muscle Force Estimation for Upper Limb Assistive Device for Home Setting.

Muhamad Fadzli, and Prof. Akihiko Hanafusa.

Domestic Conference

1. Poster presentation

The 58th Annual Conference of Japanese Society for Medical and Biological
Engineering, Okinawa, Japan.

Study of Muscle Force Estimation for Upper Limb Rehabilitation for Home Setting

Muhamad Fadzli, and Prof. Akihiko Hanafusa.

Journal (Q4, Impact Factor 1.71)

M. F. Ashari, A. Hanafusa, S. Mohamaddan, "Evaluation of Upper Limb Muscle
Activation Using Musculoskeletal Model with Wearable Assistive Device", Hindawi,
Applied Bionics and Biomechanics, vol. 2022, Article ID 8908061, 10 pages, 2022.
<https://doi.org/10.1155/2022/8908061>.

ABSTRACT

The number of stroke survivors in this world is quite large, and most of these survivors experience impairment impact on the upper limb function. Patients who suffer from upper limb impairment usually have difficulty performing daily activities that require using the upper limb, such as feeding, washing, etc. Some patients may recover some functionality of the upper limb function following the rehabilitation. The recovery of arm movements is one of the most important goals during stroke rehabilitation to avoid long-term disability that may restrict daily living activities (ADL), social and occupational activities that can lead to depression.

In order to regain the function of motor skills, many rehabilitation approaches are proven and being used widely such as locomotor training which uses task-specific and repetitive training such as using the treadmill to perform tasks repetitively. With recent advanced technologies, there is a lot of interest in using robots and wearable devices for rehab purposes. An assistive device that applies forces to the body to assist with motor tasks is one approach that may assist people with upper limb disorder or prevent injury as well as improve task economy. Recent studies show that mechanically cable-driven devices which are more affordable and suitable for use around the home could affect muscle activation during the tasks to help with rehabilitation, especially for the upper limb. Many of these wearable passive devices are designed to support and give assistance to assist the upper arm movement for the static task. However, the effect of the assistive force on the muscle output was not widely investigated and it is unclear whether this device built for static tasks would be suitable for supporting dynamic arm movements, which include activities of daily living and rehabilitation exercises.

Wearable devices are systems that are in close contact with the human body. Thus, their performances are influenced by many factors. It also offers numerous challenges to its design, evaluation, and modification including difficulty analyzing the effectiveness of the device and discovering the effect of changes in parameters on human muscle behavior. Therefore, numerical simulations play an important role in solving these challenges and have the potential to improve treatment strategies and medical decision-making.

In this study, the work focuses on the evaluation of upper limb muscle activities using a developed human-device model has been carried out. A human-device model is developed and this model is further validated and used in biomechanical software OpenSim to simulate the effect of the assistive device on the upper limb motion. An experimental protocol consisting of a series of motions was executed with five healthy subjects. Muscle activation on the brachioradialis, biceps, and triceps muscles was measured by using surface electromyography (EMG) and analyzed. The simulations with a human-device model to estimate muscle output were performed for three tasks. The desired assistive force is translated to the arm joint along with a tendon routing structure. Assisting movement by the wearable device was evaluated by measuring muscle activation with-assist and without-assist conditions.

Results showed that a musculoskeletal model with and without an integrated assistive device could produce muscle activation patterns more similar to the EMG measured for all muscles of interest during the simulated upper dynamic tasks. The human-device model results show that muscle force values for two primary arm muscles (Biceps and Brachioradialis) were reduced during the simulated task when wearing the assistive device. These results are congruent with expectations, with the assistive device that supports the upper limb movement, providing practical assistance. In addition, the group data were tested for differences using statistical analysis Wilcoxon signed-rank test reveals main activated muscles brachioradialis and biceps muscle shows differences in measured data when comparing the subject with and without wearing the device.

A comparison of measured EMG muscle data and human-device models revealed that, although the model did not fully incorporate similar muscle physiology completely, muscle force generated from the biomechanical simulation is comparable with measured muscle activity from the experimental. The results of this study contributed to the importance of evaluating muscle output using the biomechanical simulation, which could reduce the resource-intensive and time consumed with the experimental testing.

Chapter 1

Introduction

1.1 Background study

According to the World Health Organization, an estimated 5 million people are stroke survivors annually, and a high percentage of these are permanently disabled. Stroke often causes permanent and complex long-term disability in adults, placing a burden on families, health professionals, and communities in general [1].

Most of these survivors experience impairment impact on the upper limb function [1]. For severe cases, the restoration of arm motor skills is often incomplete, and more than 65% of patients usually have difficulty performing daily activities that require using the upper limb, such as feeding, washing, etc. [2]. Some patients may recover some functionality of the upper limb function following the rehabilitation. The recovery of voluntary arm movements is one of the most important goals during stroke rehabilitation to avoid long-term disability that may restrict activities of daily living (ADL), social and occupational activities and lead to depression.

Complete mobility recovery of a limb resulting from impairment is indeed a challenging goal to achieve, in some cases even impossible. Nevertheless, current technology allows making rehabilitation easier. Specially adapted devices such as exoskeletons and the assistive device can enhance the rehabilitation process by assisting the patient in executing motor tasks [5], and it was shown that weight-support in upper limb exoskeletons benefit motor function recovery [6], especially if

the load is varied during the therapy [7]. Recently, wearable assistive devices have also started to play an essential role as rehabilitation devices [2-4].

The assistive devices are promising but still too expensive to be the practice for treating disabling diseases where they have shown their potentials, like stroke, cerebral palsy, and spinal cord injury. Further development of this technology needs safe human-robot interaction, cost-effective and user-friendly nature could help patients with their rehabilitation training. Given the lack of the need for a therapist number, there are demanding that the assistive device be robust and easy to handle. Focusing on rehabilitation devices, it is essential that the development of the assistive device need to come together with an understanding of the muscle force and muscle activation of the target muscle during the rehabilitation training for stroke patients.

Presently, three main approaches, i.e., assessment scales, movement evaluation, and surface electromyography (sEMG) analysis, are widely applied to evaluate the upper extremities. As these assessments are mainly viewed and scored by the therapist, the evaluation results are often subjective and general. The movement evaluation method using the motion capture systems can provide data on the physical movement of the upper limb, which can then be used for monitoring the progress of the rehabilitation. However, this method cannot account for muscle characteristics in patients, and the neurological mechanism used to overcome the problems associated with their pathology is also still unknown. Although all these methods help assess upper limb function, they are still inadequate for quantitative evaluation due to the lack of deep muscle activation information and noise contamination from the movement artifact. Moreover, direct interaction with the subject is needed in order to gain the information, and this could be a limitation based on the patient's condition, time consumed to set up the system, and the cost for the actual test involving many equipment and subjects.

This study aims to evaluate muscle activation with and without assistive devices during defined upper limb movements. This study presents a method using a musculoskeletal model focusing on the upper limb to predict muscle force during the upper limb motion with the assistive device. Individual muscle force was investigated

during the upper limb movement with the healthy subject using the assistive device, and the results were compared with those of the one not using any assistive device. Through this approach, the specific functional muscle involved during the movement can be known, making it possible to improve the assistive device for rehabilitation training purposes.

1.2 Rehabilitation Assistive Device

Assistive and rehabilitation device is the new frontier of robotics development. It is a field of research dedicated to understanding and augmenting rehabilitation through the application of robotic devices. Over the last years, numerous rehabilitation exoskeletons for stroke survivors were developed, but only a few are used in clinical routines [8]. The robotic systems in rehabilitation can be classified as follows:

- Upper Limbs
 - Hands Support
 - Exoskeleton

- Lower Limbs
 - Treadmill
 - Exoskeleton

These devices are designated with applications of techniques the adaptability level of the patient. There are many types of training during the rehabilitation practices used :

- **Active assisted exercises:** the patient moves his hand in a predetermined pathway without any force pushing against it.
- **Active constrained exercises:** the patient arm's movement finds an opposite force exercised by the device.
- **Passive exercises:** passive range of motion; this means how far you can move your joints in different directions.
- **Adaptive exercises:** the device has to adapt to the exercises because it has never been done before and adapt to the new unknown pathway.

1.3 Upper Limb Orthosis

Exoskeletons are a clear example of robotic orthoses contribute as a recovery assistance. One of the few commercially available passive upper limb exoskeletons is the Armeo® Spring by Hocoma, based on the principle of the T-WREX exoskeleton, using a parallelogram linkage with elastic bands for arm weight compensation [9], [10]. By providing arm weight support, the Armeo Spring enables patients to use any remaining motor functions and encourages them to achieve a higher number of reach and grasp movements based on specific therapy goals. As all activity during the training is based on the patient's own movements, this repetitive training leads to better, faster results and improved long-term outcomes. Due to its dimensions and weight, the Armeo® Spring can only be used as a stationary device and cannot be installed on a wheelchair or chair.



Figure 1 : Upper Limb Orthoses Armeo® Spring

Another exoskeleton example that widely use in upper extremities therapy in stroke patient is ARMin exoskeleton. The clinical evaluation of this exoskeleton was assessed on a questionnaire and how the patient rated the robot. The effects of the ARMin training reported seem to be quite individual.



Figure 2 : Rehabilitation Robot ARMin

1.4 Musculoskeletal Modeling and Simulation

Recently, different platforms have emerged to aid in the human musculoskeletal modeling and dynamics simulation to better understand the details behind the movement science and focus on the causes. Through this, we can achieve an in-depth knowledge of human biomechanics with primary focus on crucial areas to find solution to our problems. Some of the basic domains touched by such platforms are robotics, design, orthopedics, prosthetics, and rehabilitation. (OpenSim.stanford.edu, 2017).

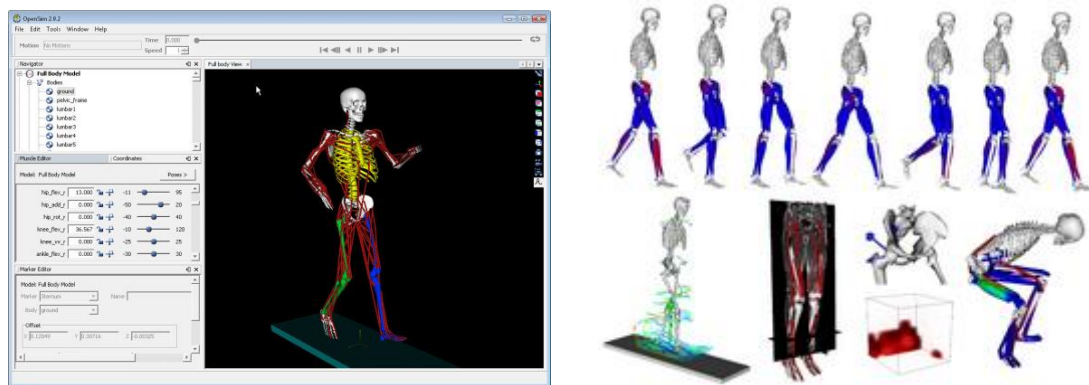


Figure 3: OpenSim platform for advance biomechanical simulation

OpenSimulator, abbreviated as 'OpenSim' is another such powerful musculoskeletal modeling platform which is an open source software. One can use a combination of springs, dampers, joints, controllers, actuators etc. to create a human musculoskeletal model. This platform uses a modified version of Hill-type muscle model, called 'Thelen2003Muscle' actuator, which captures the active and passive behavior of the muscles, and demonstrates the muscle-tendon dynamics efficiently. This platform also enables us to perform inverse kinematics, kinetics, static optimization and forward dynamic simulations of human movement. By using such powerful tools, one can analyze the variables or output of interest through its available analysis and probes functions. OpenSim, also, allows us to access its computational mathematic base through its extensible Application Programming Interface (API), using which the user can modify and edit the algorithms through plugins and programs (OpenSim, 2017).

This thesis utilizes computed muscle control (CMC) methods in conjunction with musculoskeletal modeling and experimental motion data to study the effects of active muscles in the human musculoskeletal model for selected movement when using the upper limb device.

OpenSim also has quite a few pre-existing musculoskeletal models that a developer made available for the user to use at his convenience. Few such models are listed in Table 1 below.

Table 1 Model Available in Opensim Software

Model Names	Years
Gait 2392 and 2354 Models	(OpenSim, 2017)
Lower Limb Model 2010	(OpenSim, 2017)
Full Body Running Model	(OpenSim, 2017)
Upper Extremity Model	(OpenSim, 2017)
Lower Extremity Model	(OpenSim, 2017)
Deformable Lower Extremity Model	(OpenSim, 2017)
MR-Based Models Lower Extremity Models	(OpenSim, 2017)
Human Neck Model	(OpenSim, 2017)
Human Shoulder Model	(OpenSim, 2018)

1.5 Motivation

As mentioned before, many stroke survivors suffer from upper limb physical impairment. Whether it is permanent or partial, there are some cases where there exists the possibility of recovery. In such case, the treatment to recover the lost limb requires time and a specialist that helps with it. Although in the future, a possible alternative could be based on new technologies, right now implementing hardware such as exoskeletons or assistive device still has some noteworthy disadvantages: it is very expensive, not only the device itself --hardware and software, but also the time that is needed to run necessary tests and find possible exercises which adapt the best as possible to the pathology that a person suffers. Moreover, working directly with an exoskeleton and to make progress with a patient can put him at risk of suffering some kind of injury.

In this way, there is a need to find alternative options in order to save both time and money when finding the best solution for each patient's pathology. For this reason, software simulators such as Matlab, Anybody, SimBody, OpenSim, and others, play an important role as these can model and hence simulate the physical systems which can lead to better understanding muscle activities during the rehabilitation training, improving orthosis designs, ultimately minimizing costs by saving time and money.

The project will be centered around two main software solutions, SimBody API and OpenSim. The first one is an open source C++ library that provides sophisticated treatment of articulated physical systems as mechanism, skeletons, etc. Likewise, OpenSim is also a comprehensive C++ library built from SimBody, that allows, among many other things, to develop models of musculoskeletal structures and create dynamic simulations of movement as well. Thus, OpenSim is often described as a software that is able to model humans, animals, and robots.

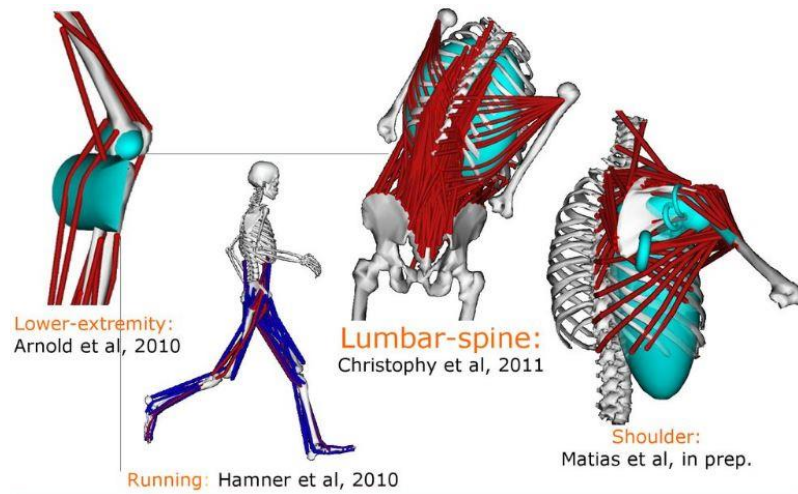


Figure 4 : Example of musculoskeletal model created with OpenSim

OpenSim is a good software tool to implement because of his applications in simulating and studying musculoskeletal body systems. Moreover, it is particularly interesting tool as the software has been developed by National Center for Simulation in Rehabilitation Research (NCSRR) where many people of different science branches converge working altogether in its development[5]. This means that OpenSim includes a lot of types of modeled real musculoskeletal bodies. Unfortunately, the main problem of OpenSim lies in the fact that the number of robotic orthosis implementations[8] --such as exoskeletons-- jointly with musculoskeletal bodies is much lower. Thus, to develop an OpenSim model in which interaction forces can be studied between a robot orthosis and a musculoskeletal body represent a great option to contribute in this field of studies.

1.6 Objective

Taking into account the previously described importance to understand the target muscle activity during the rehabilitation training solutions that minimize the costs associated with impairments recovery through the assistive device, the main objective of this project is to estimate the theoretical muscle activation that an individual can achieve while using the assistive device for rehabilitation purpose.

The novelty of this study could be described as follows objectives to be achieved :

- Develop a human-device musculoskeletal model to estimate muscle activities for upper limb dynamic simulation.
- Quantify muscle output with and without developed wearable assistive device during dynamic upper limb motion:
 - 90 degree elbow flexion and extension,
 - maximum shoulder flexion and extension,
 - inward elbow flexion and extension.
- Investigate the effect of assistive force on the upper limb muscle activity during the Activity of Daily Living (ADL) tasks.

Chapter 2

Literature Review

2.1 Introduction

This chapter will present an overview of the literature about the exoskeleton technology and its use in rehabilitation robotics. In addition, related works using musculoskeletal model approach will be described thus relate with the thesis works.

This chapter is organized as follows: section 2.2 explains Effectiveness of rehabilitation robots. Section 2.3 Rehabilitation robots' background. Section 2.4 describes some orthoses for the upper limbs. In section 2.5, introduction about Simbody. Section 2.6 is the introduction to the software that been used in this thesis which is OpenSim and how the workflow of using this software in this work. In section 2.7 the explanation of Biomechanical requirement in this study.

2.2 Effectiveness of rehabilitation robots

At the moment, there is a general lack of important clinical studies on the effectiveness of rehabilitation robotics, although many researchers are confident that robotic rehabilitation could have an effectiveness similar (or even better) to the traditional motor learning therapy. A study has been presented where more than one hundred stroke patients were treated with robotic machinery [34]. The result report that In patients with long-term upper-limb deficits after stroke robot-assisted therapy did not significantly improve motor function at 12 weeks, as compared with usual care or intensive therapy. In secondary analysis, robot- assisted therapy improved outcomes over 36 weeks as compared with usual care but not with intensive therapy. This means that robots can give the same benefits of treatments with expert therapists. However this result is not considered fully positive by some part of robotics community because there were expectations for even better outcomes. Some scientists are in fact convinced that this is mainly due to the not yet mature technology. Moreover there is a lack of knowledge about clinical outcomes with young patients and more complex pathologies such as cerebral palsy (CP) where lesion is not as specific as in stroke or spinal cord injury (SCI).

Similar results can be found in other literature works. In [5, 52] a systematic review confirms the potential for robotic assisted devices to improve motor functions of stroke in upper limbs. In [35] a review of recent developments for upper limb exoskeletons in patients with neuromuscular disorders is presented, with a discussion of potential areas for future researches where robots could be more effective and less expensive than traditional rehabilitation. In [45] authors found that training with passive devices in a gravity-reduced environment can provide comparable results to those achieved with robotic assisted rehabilitation. Also, there is evidence that training performed in virtual reality environment can induce cortical reorganization and associated recovery in stroke [62].

2.3 Rehabilitation robots background

Rehabilitation robots can be used with gain two distinct purposes: to improve motion performance or to learn new motor abilities. For instance, in stroke rehabilitation it was shown that an augmentation of errors can accelerate the learning process [21] because the mental representation of a given task is built in an adaptive error driven process ([47, 51]). So, in this case the focus is on learning (by means of brain plasticity) and usually the motion performance is downgraded. On the other hand robots that have the aim of improving performance are designed to augment human capabilities, such as force and endurance. These can often have also a positive effect on learning because enhancements of movements create more afferent feedback to the user.

The rehabilitation robots can be classified in two main categories, based on the mechanical interaction they have with the patients: prostheses, devices applied in series with human body to substitute some missing or damaged parts, and orthoses, working in parallel with human limbs and usually presenting a coordinated control between robot and human. Particular orthoses, where kinematic chain follows the human anatomy, are called exoskeletons since they usually provide an external shell that remembers the insect's one. Dealing with human anatomy, peculiar aspects of exoskeleton are ergonomic design and complex kinematic compatibility. In fact joint misalignment can cause undesirable interaction forces and pain. Otherwise, when the orthoses have a different kinematic from human, we have end-effector based orthoses (or peripheral actuated orthoses) in which the interaction with humans considers a single kinematic link. For these devices, the mechanical design can be simpler but there is only partial control of user movements [41]. Prosthesis and portable exoskeleton, grounded or not, are also called wearable robots. Non wearable robots are fixed to the ground, like most of the commercial rehabilitation systems, or mobile with moving base or appendix that are usually suited to carry the power source and other high weight parts [10, 32].

2.4 Orthoses for the upper limbs

The exoskeleton robot is an assistive device which is worn by the human user. It has external structural mechanism with joints and links correspond to those of the human body. It is a kind of a man-machine system centered by the human user. Since exoskeleton robots combine the intelligence of human user and the power of machine, it enhances the machine intelligence and power of the human user. As the name implies the upper-limb exoskeleton robot is an exoskeleton robot that can be worn on the upper-limb of the human user.

With the advances in recent technology in the fields of mechanical engineering, electronic engineering, biomedical engineering, and artificial intelligence the exoskeleton robot technology has acquired a rapid development in recent years. As a result, many upper-limb exoskeleton robot systems [31]-[83] and lower-limb exoskeleton robot systems [96]-[104] have been proposed for rehabilitation, haptic interaction, human-amplification and/or power-assist of physically weak individuals.

This section explains the biomechanics of human upper-limb and requirements and the design difficulties of an upper-limb exoskeleton robot are identified. Furthermore, currently developed upper limb device in our laboratory will be explained.

2.4.1 Classification of Upper Limb assistive device

Upper-limb exoskeleton robots can be classified in several ways considering features of their mechanical designs and/or control methods. In the literature of exoskeleton robots, the upper-limb exoskeleton robots are classified according to:

- **the applied segment of the upper limb**

Under this category the upper-limb exoskeleton robots can be classified as hand exoskeleton robot, forearm exoskeleton robot, upper-arm exoskeleton robot or combined segment exoskeleton robot;

- **the DOF**

In here, the upper-limb exoskeleton robots can be classified according to the number of active or passive joints or in other words DOF as 1DOF, 2DOF, 3DOF, etc.;

- **the power transmission methods**

Here the classification is such as gear drive, cable drive, linkage mechanism or other method;

- **the applications of the robot**

Upper-limb exoskeleton robots can be classified according to the intended purpose namely rehabilitation robots, assistive robots, human amplifiers, haptic interfaces or other uses;

- **the control methods**

This category classifies the upper-limb exoskeleton robots based on the used control methods such as impedance control, force control, fuzzy-neuro control or other control methods;

An upper-limb assistive device which is wire-driven by 2 servo motors has been developed in our laboratory [8]. The device can generate the motions of elbow flexion/extension movement and internal/external rotation movement, performed by pulling the wire hung on a pulley connected to the wrist part.

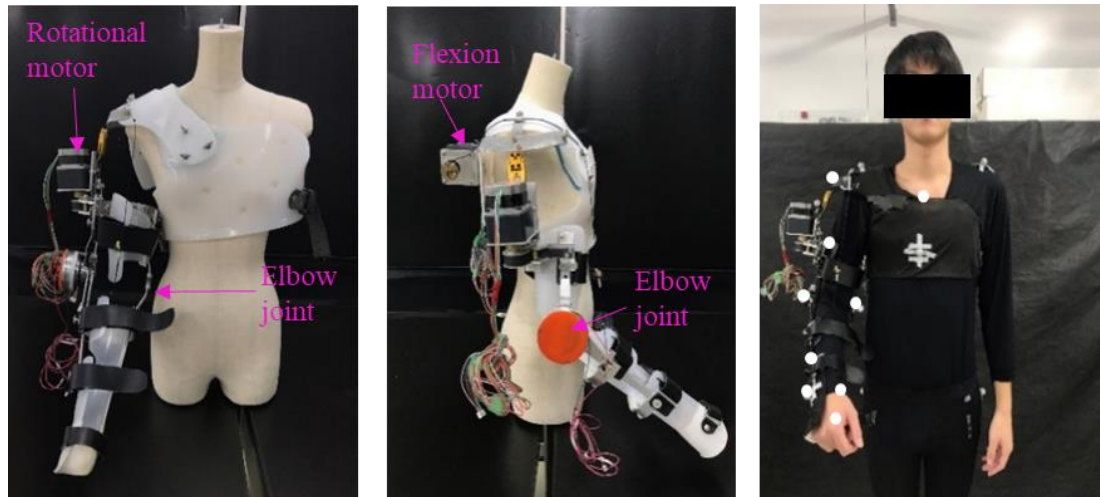


Figure 5 : Upper limb right hand assistive device and a subject wearing the device

The development of the upper limb device can be referred to in this publication [24]. Since the main focus of this thesis would be on the musculoskeletal model and simulations, no further explanation of device functioning and control will be explained.

2.5 Simbody

Digging deep into Simbody, we can find a set of application programs and Software Development Kit (SDK) embraced all of them with the name Simbios Biosimulation Toolkit (SimTK). The SDK includes a family of application programming interfaces (APIs) in which physics simulation can be done. Some examples of what can be done with them are: vector and matrix arithmetic, linear algebra, numerical integration, optimization, and so on. OpenSim API is one of the software that contains SimTK. It uses Simbody to build internal models of biomechanical systems.

2.5.1 Mathematical inside Simbody

Multibody system has to be seen as a system of equations that describes the behavior of a physic system. As a result, the state of the system at any moment in time is described by a vector of state variables. This is state vector is represented by \mathbf{y} and the main objective of simulating is to integrate the following equation:

$$\frac{d\mathbf{y}}{dt} = \mathbf{f}(t, \mathbf{y}).$$

Where:

\mathbf{f} : *reflects the forces acting on bodies and laws of physics.*

Digging into a vector of state variables and taking an human skeleton as example, it can be subdivided into:

- Generalized coordinates: it is represented with \mathbf{q} and taking as reference a skeleton would represent the set of angles for all the joints, and the orientation and position of the torso.
- Generalized speeds: it is represented with \mathbf{u} and it would correspond to angular and linear velocities.
- Auxiliary variables: it is represented with \mathbf{z} . Doing a simulation of a skeleton doing some sort of exercise, a possible example of auxiliary variable would be the

total energy done in this exercise. Thus, auxiliary variables do not give information about the configuration of the multibody system.

$$\mathbf{y} = [\mathbf{q}, \mathbf{u}, \mathbf{z}].$$

- As it has been said previously, the use of generalized coordinates avoids the need for most constraints, but in some cases additional ones are needed. These constraints has to accomplish the following equation:

$$\mathbf{c}(t, \mathbf{q}, \mathbf{u}) = 0.$$

- Simbody also contains event trigger functions. They are useful for reading multibody's data or turn on/off constraints. An event is said to occur when a trigger function crosses through 0:

$$\mathbf{e}(t, \mathbf{y}) = 0.$$

Thus, when an event occurs, the corresponding event handler is invoked, which can modify the state in arbitrary, discontinuous ways.

In order to track if constraints are turned on or not, a new type of variables called discrete variables d will be needed. Something important to highlight here is that these variables are not modified by equation 3.1. Only can be modified by event handlers. Thus, the equations (3.1, 3.3, 3.4) showed previously may all depend on discrete variables. So including these variables to these equations, we obtain:

$$\frac{dy}{dt} = f(\mathbf{d}; t, \mathbf{y}),$$

$$\mathbf{c}(\mathbf{d}; t, \mathbf{q}, \mathbf{u}) = 0,$$

$$\mathbf{e}(\mathbf{d}; t, \mathbf{y}) = 0.$$

As it will be noticed, there is a semicolon rather than a coma after \mathbf{d} . This is a reminder that discrete variables are held constant during continuous intervals when t and \mathbf{y} are changing.

2.5.2 System and States

In Simbody, we can distinguish between two things: those that remain constants and immutable during time simulation and those ones that change during the course of a simulation. The first ones are represented by the system and the second ones by the state.

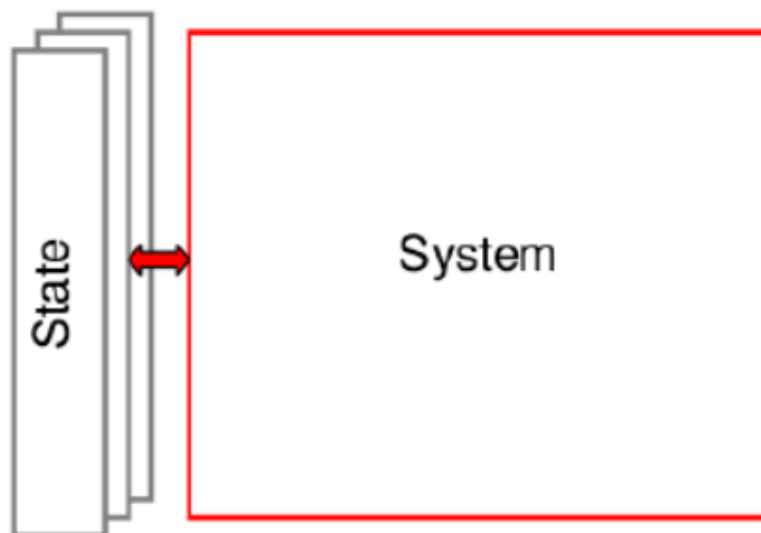


Figure 6 : This figure represents System that once build is immutable and everything that changes is stored in separate state objects.

In other words, a System object contains the bodies with all physical properties that defines them such as mass, inertia properties, dimensions, and so on. Moreover, System provides all the logic needed for simulation, instead a State object is purely a place for storing data.

- System provides the following logics for simulation:
 - Defines what information will be stored in a State.
 - - Provides routines to calculate force function, vector of constraints, and vectors of event trigger functions.
 - - Provides routines to handle events when they occur.

- State stores:
 - Time t .
 - Continuous state variables y .
 - Discrete state variables d .

2.5.3 System and Subsystems

Previously, it has been said that a System is in charge of giving all the basic logic to do the simulations, but actually who is in charge of it are the Subsystems not by the System itself. Thus, what Subsystems basically are, is those objects that compose a system. To understand in a better way of what we refer with Subsystems perform logic, it is going to illustrate it with an example: the total force calculated by the System is the sum of the forces calculated by all of its Subsystems. Check the figure 3.9:

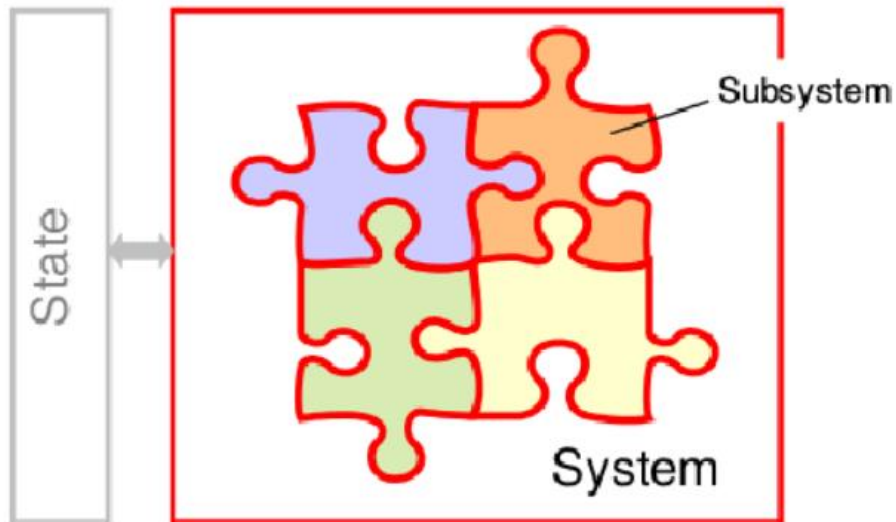


Figure 7 : This image shows a representation of a System and his Subssteams

Having Subsystems inside a System allows you to create it in a modular way since Subsystems can interact with each other. For example, Subsystem might define a subset of bodies, all the forces, constraints, and events related to them; another one can define all the state variables; a different Subsystem can define the forces acting on them, and so on.

2.5.4 The Realization Cache

In spite of the fact that state variables t , y , and d represent a complete description of the system's state at a given time, there are other variables that might be interesting to know. These variables are:

- Position.
- Forces acting on each body.
- Accelerations.
- Values of event trigger functions.

The previous variables can be computed using state variables. The main problem here is they need some computational time to acquire them. For this reason, a State object provides space for storing these derived values. This space is called realization cache, and the process of calculating the values stored in it is known as realizing the

state. Each of these variables cannot be computed at the same time, this means there is a sequence to compute each of them. Thus, the realization cache is therefore divided into a series of stages. When you want to get information from the cache, you must first make sure the state has been realized up to the stage that the information belongs to. Check figure 3.10.

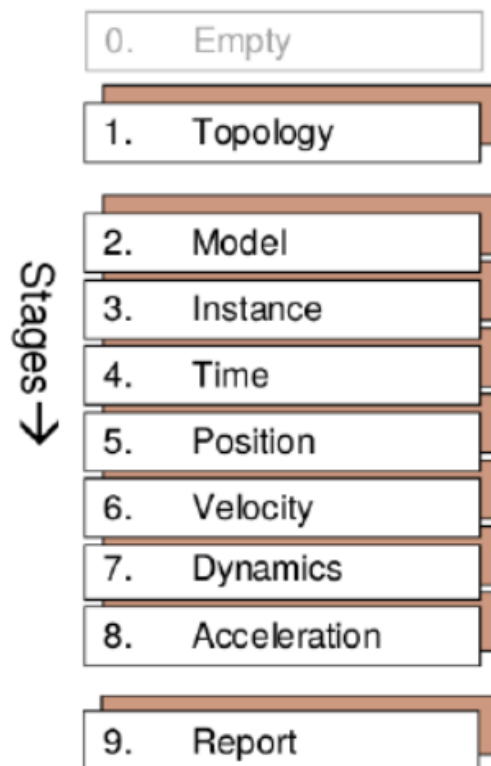


Figure 8 : Organization of the different stages. The order is considering the stage that has to be computed to acquire the following stage.

The first four stages are involved in the initial construction and initialization of the system. Thus, these first stages are not important during time simulation, but yes, when you are interested in writing extensions to Simbody. In the following lines we are going to dig into more detail explaining every stage:

- **Empty:** Before a new constructed State object has been realized, it belongs to an empty stage that contains no information at all, and is not specific to any particular System.

- **Topology:** When a State gets realized to this stage, it is set to become a particular System's State. This means, allocating space in the cache for the System's data that needs to be stored.
- **Model:** It defines how many state variables become fixed. For example, Simbody allows to choose to use between Euler or quaternion angles. Depends on the choice three or four generalized coordinates will be created, respectively.
- **Instance:** At this stage, it is known which forces, constraints, and events are enabled.
- **Time:** No information has been calculated yet. Only information about state variables t , y and d are available.
- **Position:** At this stage, the position of all the bodies in Cartesian coordinates are known.
- **Velocity:** At this stage, the velocities of all bodies in Cartesian coordinates are known, along with the amount by which the constraints are violated.
- **Dynamics:** At this stage, the force acting on each body is known, along with the total kinetic and potential energy of the system.
- **Acceleration:** At this stage, the time derivatives of all continuous state variables are known, along with the values of all event trigger functions.
- **Report:** It is a stage that it is not normally realized, but it is available in case a System can calculate values that are not required for time integration, but might be needed by an event handler or for later analysis.

2.6 OpenSim

As it has been said previously, OpenSim is a free open source software package that allows to build, exchange, and analyse computer models of musculoskeletal systems and dynamic simulations of movement. As Simbody package, OpenSim was created by Stanford University and the first version of it was introduced at the American Society of Biomechanics Conference in 2007. The latest version of OpenSim offers Graphical User Interface (GUI) to illustrate the simulation result and animation. In addition, create models and placing the different bodies easier when conducted in GUI rather than programming it.

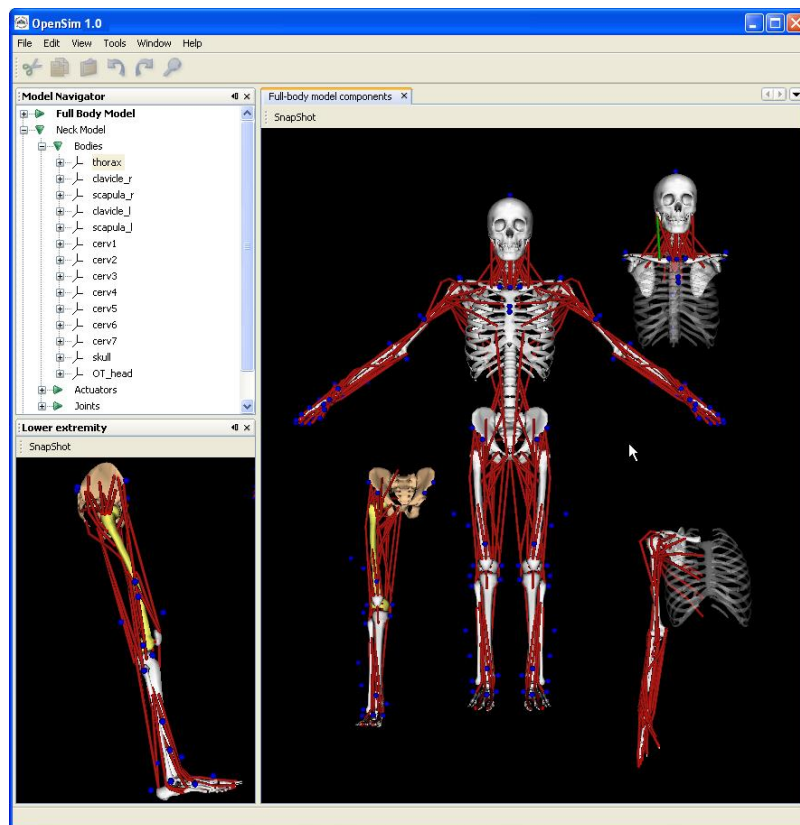


Figure 9: Screen record shows OpenSim's GUI with different musculoskeletal models.

As mention previously, OpenSim is built on the computational and simulation core provided by SimTK. This core includes low-level, math and matrix algebra libraries, such as LAPACK, as well as Simbody, the infrastructure that allows to

define a dynamic system and his states, and solve them. The following figure shows the three interface layers of OpenSim built on SimTK:

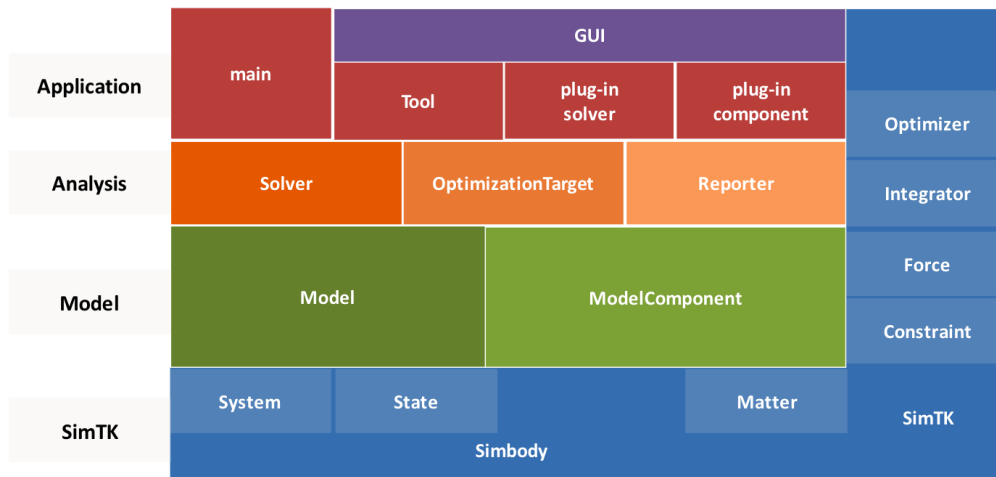


Figure 10 : The Three Interface Layers of OpenSim Built on SimTK

To understand better how OpenSim works, it is going to explain in more details the main parts which it is composed of:

- **Manager:** this class is in charge to manage the execution of a simulation.
- **Optimizer:** the target of the optimizer class is to find a local minimum to an objective function.
- **Analysis:** this class allows to the user creates some plugins in order to make force analysis.
- **Dynamics Engine:** it is a wrapper class to use the SimTK Simbody dynamics engine as the underlying engine for OpenSim.
- **Model:** One of the main classes because it is in charge of creating a model or to call an existing one. Thus, it specifies the interface to a musculoskeletal model and can read this in from an XML file and modify it via OpenSim's API.

- **ModelComponent:** This class is used for adding computational components to the underlying SimTK::System or called MultibodySystem, too. In other words, it specifies the interface that components must satisfy in order to be part of the system and provides a series of helper methods for adding variables such as states, discrete, cache among others.

Some features that OpenSim lets to implement are:

- Importing Experimental Data.
- Scaling.
- Inverse Kinematics.
- Inverse Dynamics.
- Static Optimization.
- Computed Muscle Control

2.6.1 Importing Experimental Data

OpenSim allows to analyse experimental data that has been collected from:

- Marker trajectories or joint angles from motion capture.
- Force data typically could be ground reaction forces and moments and/or centers of pressure.
- Electromyography

2.6.2 Scaling

There are lots of generic models that have been created for using with OpenSim. Sometimes, this model can be useful to use with the experiments. For this reason, the model can be scale to match the experimental data collected for the subject. The main reason to do that is to modify the model's anthropometry to match with the subject's one. It is an important step in order to solve inverse kinematics and inverse dynamics problems because these solutions are sensitive to the accuracy of the scaling step. The

things that are adjusted when an OpenSim model is scaled are the mass, the inertia tensors and the dimensions of the body segments.

2.6.3 Inverse Problem

Using experimental measured data from motion and forces of a subject to generate the kinematics and kinetics of a musculoskeletal model, OpenSim enables to solve the inverse Dynamics problem.

2.6.3.1 Inverse Kinematics

The Inverse Kinematics tool computes generalized coordinate values which position the model in a pose that best matches for a particular experimental data recorded of a subject.

2.6.3.2 Inverse Dynamics

The inverse Dynamics tool is in charge of determining the generalized forces that cause a particular motion, and its results can be used to infer how muscles are actuated to generate that motion.

2.6.4 Static optimization

Static Optimization resolves the net joint moments into individual forces at each instant in time. In other words, using a minimizing criteria finds the optimal force that should be applied in this time instance to a model's body.

2.6.5 Computed Muscle Control (CMC)

At user-specified time intervals during a simulation, the CMC tool computes muscle excitation levels that will drive the generalized coordinates (e.g., joint angles) of a dynamic musculoskeletal model towards a desired kinematic trajectory.

In this study, standard pipelines were used to scale the musculoskeletal model and to estimate the joint angles (inverse kinematics), and muscle forces (CMC) in the OpenSim environments. In OpenSim environment, OpenSim used a static trial to scale the individual segments based on the marker position. For estimating muscle forces, Computed Muscle Control (CMC) was solved in OpenSim by computes the muscle excitation levels that will drive the muscle towards the desired trajectory. Furthermore, a set of constraint preventing individual muscle forces from exceeding their physiological maximum is included. Figure below shows the flowchart of the pipeline used in this study.

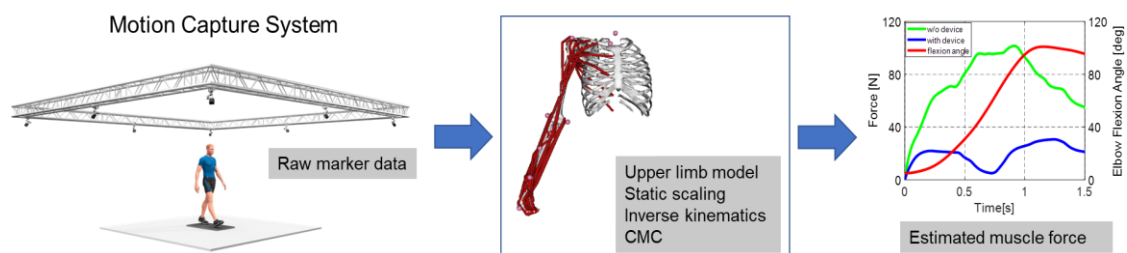


Figure 11 : Flowchart of data processing.

2.7 Biomechanical requirements

There is very few literature on formal studies carried out to determine the biomechanical requirements of an upper limb assistive device and specifically for after stroke rehabilitation training module. Concretely, four studies assessing some of the biomechanical requirements for ADL were found. Three of them study the kinematics and one focuses also on the dynamics.

The first is the one by Romily et al. [19], in which the range of arm joint angles for a variety of common tasks was evaluated in order to determine which of the angular degrees of freedom could be collapsed for the purpose of designing an anthropomorphic orthosis. They evaluated the range of motion (RoM) of 7 joint angles in 22 tasks, including shoulder, elbow and wrist.

The second is from Ramanathan et al. [20], where the trajectories of the elbow were analysed while doing different activities of the daily living in order to determine the elbow-position envelope. 9 tasks were performed and 2 joint angles (elbow flexion and lower arm elevation) were studied.

The next one, by Magermans et al. [21], was aimed to obtain the RoM of the shoulder and elbow for a selection of ADL. It is oriented to help in rehabilitation practice to determine the functional capacity of patients according to the RoMs obtained. The authors divided the tasks in range of motion tasks (7 tasks), where the aim was to reach a maximal joint angle, and ADLs tasks (5 tasks).

The last work is the only that studies dynamics and kinematics. It was elaborated by Rosen et al. [22]. The aim of this research was to study the kinematics and the dynamics of the human arm during ADL for the design of a 7-degree of freedom (DOF) powered exoskeleton for the upper limb. Angles, angular velocities and accelerations and finally, total, gravitational and inertial torques were calculated. It is the most complete study, 24 ADL tasks and 9 general motions, where the idea was to reach a maximal joint angle.

The main problem on directly applying these studies for the design of an upper limb exoskeleton for stroke patients is that they cover activities without knowing which muscle mainly activated during the movement. Even though the one from Ramanathan et al. is focused on patients that suffer neuromuscular diseases, it only studies the trajectories and angles of the elbow without analyzing the other upper limb. When designing an orthosis, or evaluating the training task during the upper limb motion other requirements apart from the biomechanical ones are needed. Some of these include comfort, easy donning and doffing, force transmission to the body, adjustability to the body, functionality, aesthetics, inconspicuousness, etc. [23,24].

2.7.1 Biomechanics of Upper-limb

Human upper-limb is made up of skeleton, muscles, nerves, skin etc. The skeleton mainly consists of clavicle, scapula, humerus, radius, ulna, carpal bones, metacarpal bones, and phalanges. Human upper-limb is shown in Fig. 12. It mainly consists of shoulder complex, elbow complex, and wrist joint. In addition, the hand consists of fingers which have several joints. Human upper-limb mainly consists of 7DOF: 3DOF in the shoulder, 2DOF in the elbow, and 2DOF in the wrist [116]. The main motions of upper-limb are shoulder flexion/extension, abduction/adduction, and internal/external rotation; elbow flexion/extension, forearm supination/pronation, wrist flexion/extension, and wrist radial/ulnar deviation.



Figure 12 : Human upperlimb

In this study, main movement would be focusing on the elbow complex. The elbow complex and its motions are shown in Fig. 13. Elbow complex includes the elbow joint and the radioulnar joints. The elbow joint is a compound joint consisting of two joints: the humeroradial, between the capitulum and radial head, and the humeroulnar, between the trochlea and the trochlear notch of the ulnar. The humeroradial joint is a ball-and-socket joint. However, its close association with the humeroulnar and superior radioulnar joint restricts the joint motion from 3 to 2DOF. The elbow complex allows 2DOF, flexion/extension and supination/pronation [17]-[19], [21]. In the elbow flexion motion, the angle between the forearm and the upper

arm is decreased whereas in extension motion the angle is increased [see Fig. 13(b)]. Pronation is the motion between the radius and ulna which permits the rotation of the distal end of the radius from the anatomical position across the anterior surface of the ulna. In pronation, the wrist and hand are moved from palm-facing-front to palm-facing-back [see Fig. 13(c)]. The opposing movement, which turns the palm forward, is supination. Average movable ranges of the human elbow are 5 degrees in extension, 145 degrees in flexion. Forearm supination and forearm pronation each has average movable range of 90 degrees [37].

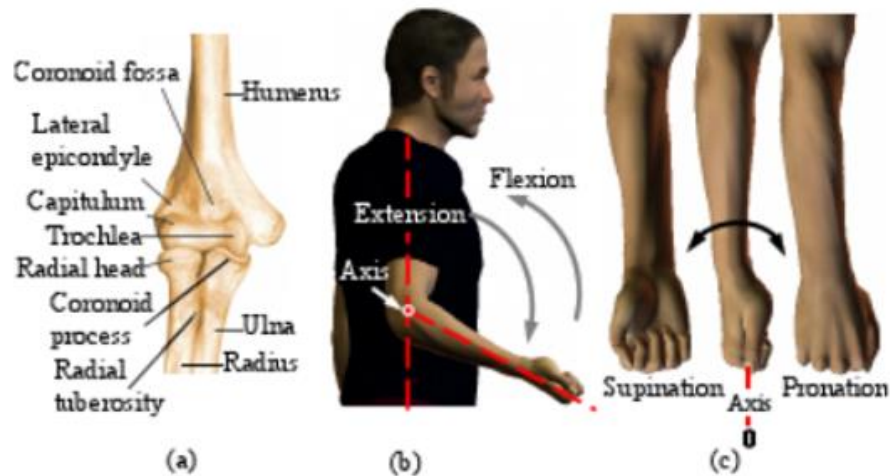


Figure 13: Elbow complex and elbow motions. (a) Elbow anatomy. (b) Elbow flexion/extension motion. (c) Forearm supination/pronation motion.

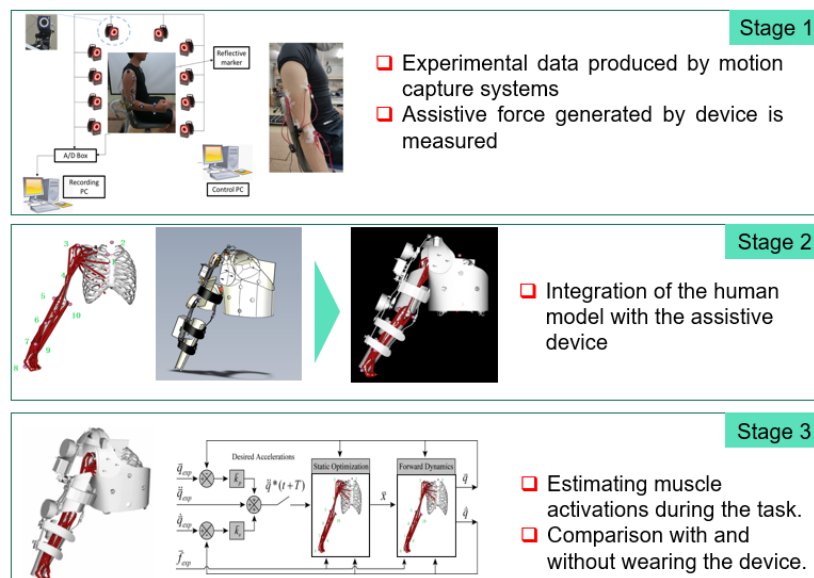
These biomechanics of upper limb movement will be taken into consideration during designing the task so that the muscle output and interested muscle activity could be observed accordingly. In addition, assistive movement provided by the developed assistive device also could follow few of the above elbow complex and elbow motions.

Methodology

3.1 Overall Methodology

The proposed method consists of three stages. In the first stage, Considering the sole effect of a device on each subject, the experimental data of a subject is produced by motion capture systems, and the assistive force generated by the device is measured. Since muscle activity will be evaluated further, EMG data for interested muscle has also been measured. In the next stage, the human generic model is integrated with the device to develop a human-device model. This human-device model will be further validated and used in OpenSim to simulate the effect of the assistive device on the upper limb motion. Muscle estimation from simulation and comparison with EMG data experimental is conducted in the final stage.

Overview of Methodology



3.2 Experimental Setup

In this study, five able-bodied subjects (all male, age ranging 23 -30-year old, 65 ± 9 kg) participated. All of them are right-handed dominant and have no reported neuromuscular disorders of their upper limb. They were ever instructed to practice the intended movements until they felt comfortable with the experimental setup.

Table 2 Subject properties details

Details	
<i>Gender</i>	Male (n=5)
<i>Age</i>	25.70 (± 4.42) years old
<i>Height</i>	170.43 \pm 6.63 cm
<i>Weight</i>	65.85 \pm 9.53 kg

3.3 Experimental Protocol

An experimental protocol was approved by the Shibaura Institute of Technology (SIT) Review Board. All subjects were told the aim of the experiments and provided written consent to participate in this study, and this consent procedure was approved by SIT. The individual in this manuscript has given written informed consent to publish these case details. Firstly, an upper limb motion was designed to validate the model used in biomechanical simulations. It is shown in figure 14 (reach forward motion).

During the experiment, the subjects were quietly seated in the chair with their torso keeping upright and their right-hand keeping relaxing. The motion was initiated when the right arm was freely hanging and close to the torso. The arm movements are repeated several times to capture both the commonality and the variability of the EMG and motion properties.

The muscles were allowed to relax shortly (around 1 min) before initiating the next motion repetition. Around 5-min rest was allowed before the start of the second test session. All the motions were performed naturally without any kinematic or dynamic constraints of the right arm. The subjects themselves controlled the exact duration of the single motion completion and the rest between adjacent motion repetitions as they felt comfortable.



Figure 14: Subject performing reach forward motion and return to the initial post

The primary goal of our study was to quantify muscle output with and without an upper limb assistive device during a simulated task. Moreover, measured assistive force provided by the device will be used in the simulations to study the effect of the assistive force on muscle activities. The design and parameters of the assistive device were imported into OpenSim for simulation tasks. We hypothesized that the resulting assistive force would cause muscle output to be lower for interested muscles with the device than without. The developed assistive device and its model in this study are shown in Figure 15 and Figure 16 below.

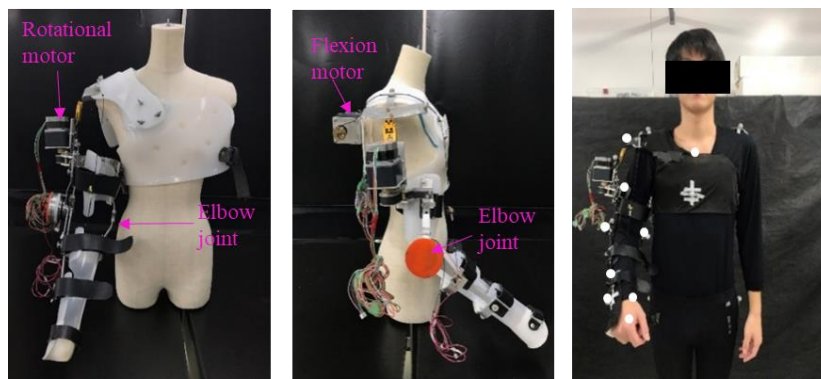


Figure 15: Assistive device developed in our laboratory

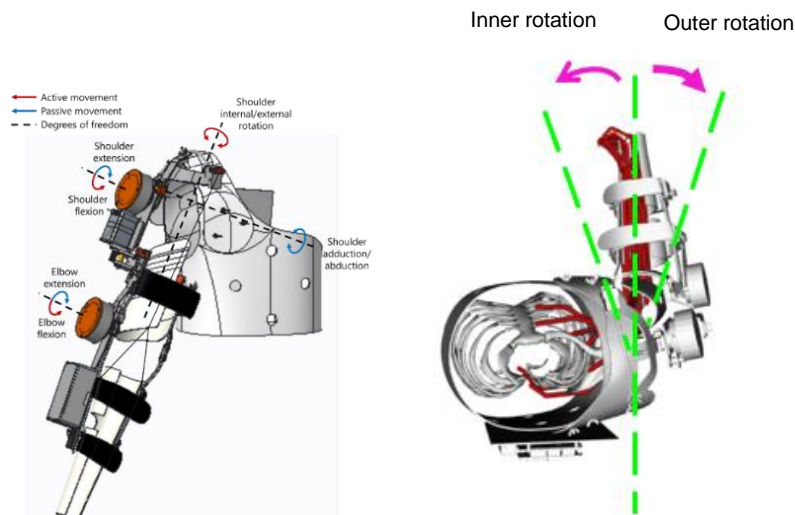


Figure 16: Assistive device motion range according to its degree of motion.

As mentioned in this study's objective, the relationship between the assistive force given by the assistive device and its relationship to the muscle output will be investigated further. Therefore, an experimental procedure has been conducted to measure the assistive force during the device's upper limb motion. Three specified

tasks: elbow flexion and extension, shoulder flexion and extension, and inner rotation with shoulder flexion and extension have been designed according to the device's capability, also associated with the training in rehabilitation upper limb movements. A load cell (TCS-20L) from Nec company, Japan, has been used to measure the tension force generated from the cable during the power transmission for the movements. The data is connected to the motion capture system so that every activity with the subject is recorded simultaneously for further analysis. Method and load cell position are shown below in Figure 17.

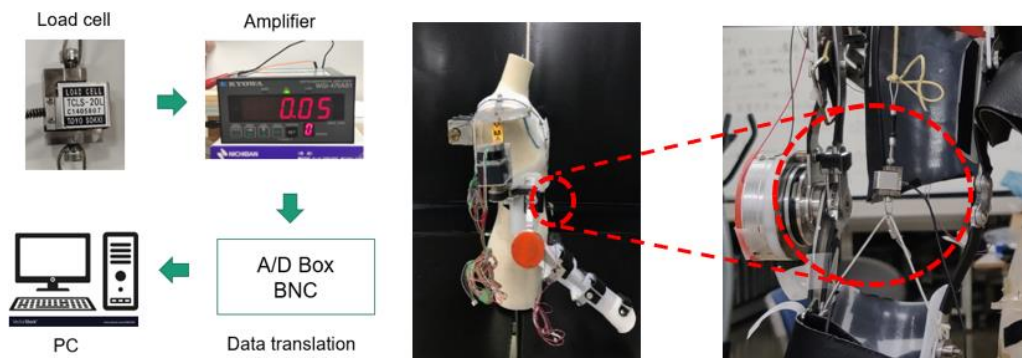


Figure 17: Method and the load cell position for tension force measurement

Three motions are shown in Figure 18, Figure 19, and Figure 20 were designed to obtain motion of the right upper limb. The traces in every Figure indicated the movement trajectory from the initial position to the destination position in a single trip of each motion and returned to the initial position

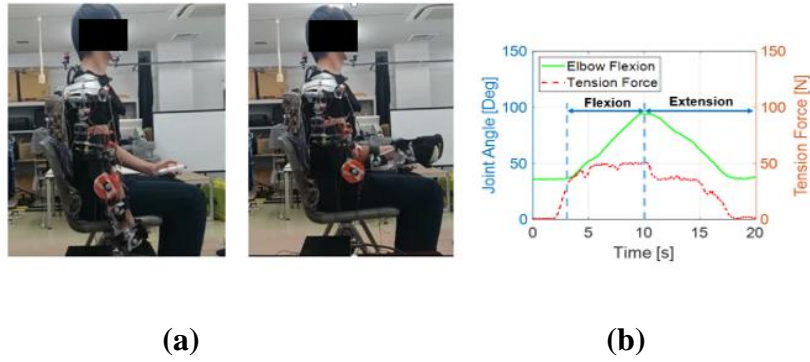


Figure 18: Subjects wearing an assistive device were asked to flex their elbow close to 90 degrees and return to the initial position. Data (b) shows measured elbow flexion angle and tension force versus time.

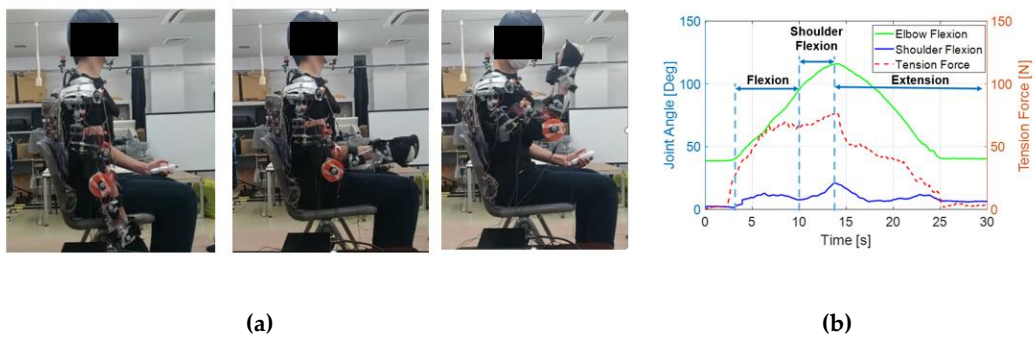


Figure 19: Subject wearing an assistive device performing maximum shoulder flexion and extension. This movement acquires the subject to flex the elbow to the close 90 deg, and then the upper arm will be brought to the upper limit of the arm's reachable motion and then return to the initial position. Data (b) shows measured elbow flexion angle, shoulder flexion angle, and tension force versus time.

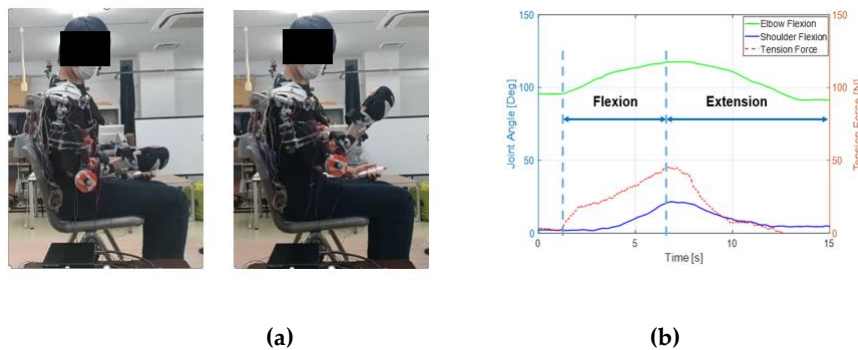


Figure 20: Subject wearing an assistive device performing maximum shoulder flexion and extension to the initial position. The arm's initial position was kept in front of the inner side of the frontal body of the subject. The elbow was flex to the maximum and returned to the initial position. Data (b) shows measured elbow flexion angle, shoulder flexion angle, and tension force versus time.

3.4 Motion Recording

Data were acquired in the Shibaura Institute of Technology (SIT) laboratory using the NAC 3D Motion Capture System. This equipment consists of a set of infrared cameras, which can capture the 3D position of the different markers over time. The infrared cameras have a sampling frequency of 100Hz, which is one measurement every 0.01 seconds. The markers are small reflective spheres that reflect the infrared light emitted by the cameras. This light is captured by an optical system of the cameras that determines the position of the markers on the perpendicular plane to the optical axis of the camera. From the information of the 10 cameras, the system computes the position of the markers at each instant of time. To have accurate result, it is essential to calibrate the equipment before doing the captures. In this study, each motion was captured several times until a clear one was obtained. Finally, one trial per person was analyzed.

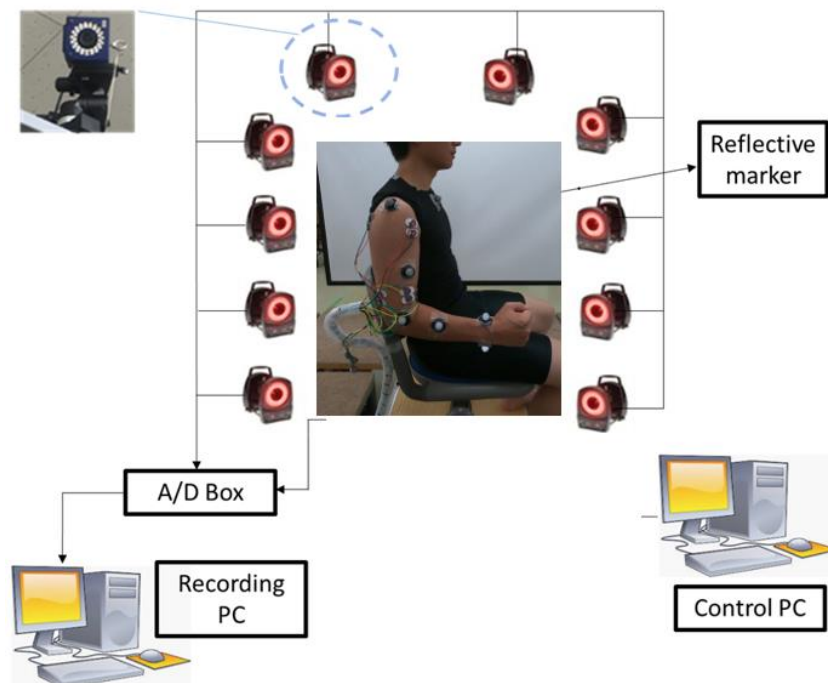


Figure 21: Motion recording experimental setup

3.5 Markers protocol

Ten markers are placed in the subject to capture the different motions analyzed. The number and locations of the markers were selected following the International Society of Biomechanics (ISB) recommendations that are based on the use of body landmarks to place the markers [28]. Body landmarks are points easy to find and close to the bones. So, these points do not have mobility associated with soft tissues, or it is significantly reduced. The markers on the scapula were not applied in this model because its motion is not analyzed in detail, and the fact that the subject was sitting on a chair might have blocked the view of these markers for the cameras. Moreover, two additional markers were placed in the middle of the segments as in the Helen Hayes model [29]. These two markers were added because three markers per segment are generally used to minimize motion capture errors. Finally, as just the motion of the right arm is studied, the markers are only placed in the right part of the body. Markers setup is shown in Figure below with the corresponding names.

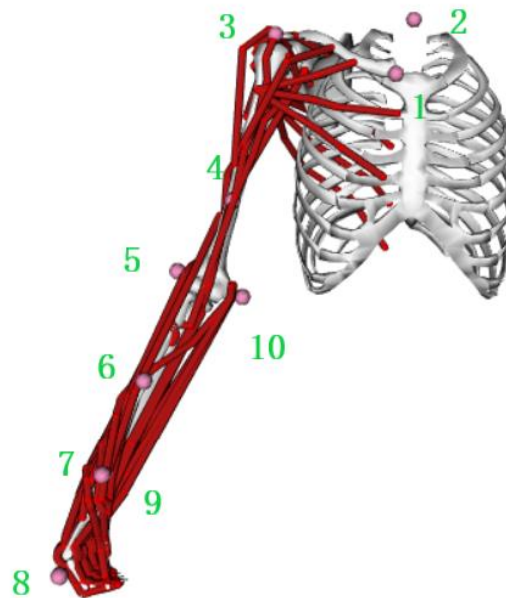


Figure 22: 10 markers locations following the International Society of Biomechanics (ISB)

Table 3 : Markers corresponding names

Marker Number	Names
<i>1</i>	Clavicle
<i>2</i>	C7
<i>3</i>	Shoulder
<i>4</i>	Bicep
<i>5</i>	Elbow.Lateral
<i>6</i>	Forearm
<i>7</i>	Radius
<i>8</i>	Hand
<i>9</i>	Ulna
<i>10</i>	Elbow.Medial

3.6 EMG Recording

Surface EMG signals were acquired by a commercial EMG acquisition system (P-EMG plus, Oisaka.co.jp, Japan).



Figure 23: P-EMG Plus System with EMG electrodes

In this experimental setup, the configuration of the EMG recording is shown in the Figure below. Eight predominant muscles activating the four shoulder and elbow DoFs were selected to be the muscle of test, that is, biceps, triceps, deltoid (anterior), pectoralis major(clavicular head), deltoid (middle), deltoid (posterior), trapezius, and teres major muscles. Eight channels (only 6 channels are used) of the bipolar differential amplifier were carefully placed on these muscles according to both the anatomy and hand touch experience according to SENIAM [50] guide. The active EMG electrodes of each channel were positioned at the muscle belly along the muscle fiber direction with the reference electrode orthogonal to the midline of the active electrodes according to the recommendation of Me6000. The skin underneath the electrodes was cleaned with an alcohol patch to reduce the resistance between the skins and sensors.

Ch.1: Deltoid (anterior part) Ch.4: Triceps (lateral head)
Ch.2: Deltoid (posterior part) Ch.5: Biceps (short head)
Ch.3: Biceps (long head) Ch.6: Triceps (long head)

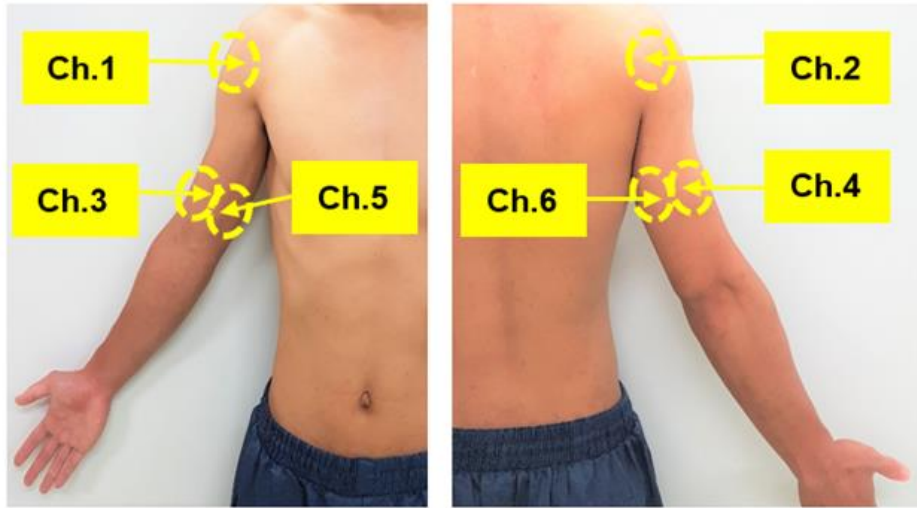


Figure 24: The configuration of 6 channels EMG electrodes for upper arm



Figure 25: A subject with the right upper limb attached with EMG electrodes and marker for motion capture

3.6.1 Electromyography (EMG) signals of Human Muscles

The electromyography signals, abbreviated as EMG, represent the amount of electrical potential generated by the muscle cells when they contract or when they are at rest. EMG signals directly reflect the human motion intention. They are usually evaluated for muscle activity for each movement. In this study, recorded EMG signals will be analyzed and compared with the muscle force estimated by the musculoskeletal model in order to validate the model for further simulation. . This section describes the characteristics, detection method, and feature extraction of EMG signals.

3.6.2 Characteristics of EMG signals

EMG signals can be classified into two types according to the place where they are extracted. The EMG signals detected from inside the muscles are called intramuscular EMG whereas EMG signals detected from the skin surface of the muscles are called surface EMG. The extraction procedure of intramuscular EMG signals is invasive. Although intra-muscular EMG signals give a better muscle activation pattern than that of the skin surface EMG signals, they are difficult to use practically, since the invasive extraction procedure. Therefore, the skin surface EMG signals of the muscles are measured in this study. The frequency of the EMG signal varies in the range of 10-2000Hz and the peak to peak value of the amplitude is within 0-10mV. Although the amplitude of the EMG signals is usually stochastic in nature, it can be represented by the Gaussian distribution function. The EMG signals vary from person to person. In addition, it differs for the same motion even with the same person. Physical conditions such as tiredness, sleepiness, etc., and psychological conditions such as stress, happiness, etc., affect the EMG signals. Therefore, the characteristics of the EMG signals should be carefully considered when comparing EMG signals as input information.

3.6.3 Detection of Surface EMG signals

Detection procedure of surface EMG signals is illustrated in Fig. 26. First step of the EMG signal detection procedure is attaching the surface electrodes [Co., Japan]

on the skin surface of the muscles. The electrode and the skin should be cleaned well before adhering to the skin. Usually, the alcoholic liquid is used for cleaning. In this study, ethanol is used. A conductive ionic paste is applied between the skin and the electrode to remove static electric insulation of dry skin. In this study, EEG paste is used as the conductive ionic paste. Usually, a pair of surface electrodes are adhered to the skin surface of the muscle with a separation of 1cm [117].

Additionally, a reference electrode is attached to electrically unrelated tissue (elbow bone). EMG signals are then passed to an input box. The input box consists of input channels for several electrodes and a reference electrode. The input box [P-EMG plus] used in this study has eight input channels for eight electrodes and one for the reference electrode. From the input box, EMG signals are passed to a multi-channel amplifier. The gain of the multi-channel amplifier [P-EMG plus] is set to 50 $\mu\text{V}/\text{V}$ in this study. Amplified EMG signals are then passed to a computer via USB by converting to digital signals. EMG signals are processed on the computer for feature extraction using P-EMG plus software.

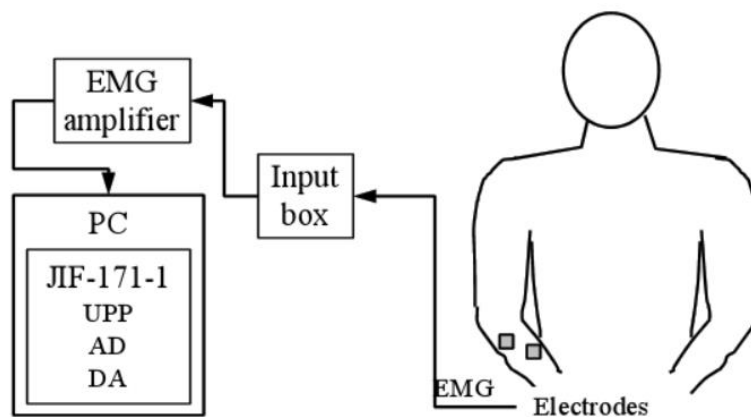


Figure 26: Detection procedure of surface EMG signals. EMG electrodes, an eight-channel input box, a multi-channel EMG amplifier, and a personal computer are used to detect the EMG signals.

3.6.4 Feature Extraction of Raw EMG Signals

Several feature extraction methods are available to extract features from the raw EMG data [118]. They are mean absolute value, mean absolute value slope, waveform length, zero crossings, and root mean square value. Root Mean Square (RMS) method is applied to extract features of raw EMG in this study. RMS value can be stated as follows.

$$\text{RMS} = \sqrt{\frac{1}{N} \sum_{i=1}^N v_i^2}$$

Where, v_i is the voltage value at the i th sampling, and N is the number of samples in a segment. The number of samples is set to be 100, and the selected sampling frequency is 1kHz in this study. Figure 22 shows an example of a raw EMG signal and its RMS value.

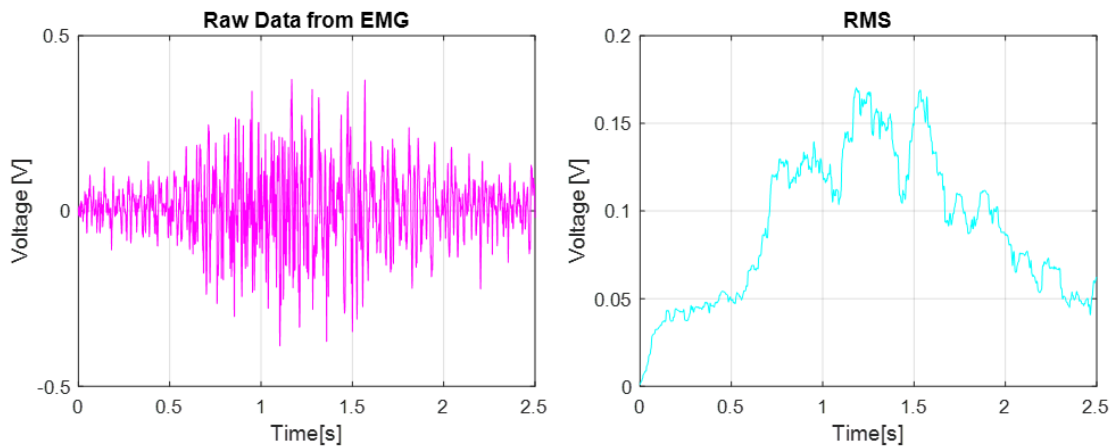


Figure 27 : Example of a raw EMG signal and its RMS value.

3.7 Data Processing

With the above EMG and motion recording strategies, the EMG and motion data were saved in a computer and treated offline in Matlab (The MathWorks, Version 7.10.0.499, 64-bit, 2017). The purpose of data processing is to extract suitable signal features for estimation model learning. In addition, the test data used for cross-validation were also processed, as did for the training data. The motion data was processed using the software provided together with the motion capture system.

From the motion captures the coordinates X, Y, and Z over time were known and used to calculate the kinematics and dynamics of each motion. The model described in Section 3.3 was first scaled and then adjusted in OpenSim according to each subject to have the exact body measurements and markers placed in the same location as the capture. Once the model per person was obtained, the motion data were imported to OpenSim to compute the kinematics and dynamics associated with each motion. This process was repeated for all the subjects. In terms of kinematics, relative or joint angles were extracted. The ones of interest were: elbow flexion and elbow extension. All this process was done using OpenSim. It is a powerful free software for modeling and simulating human movement used to uncover the biomechanical causes of movement abnormalities and to design improved treatments. Since its development in 2006, researchers have used OpenSim to address fundamental issues in movement science, focusing on critical areas of rehabilitation medicine, including stroke, spinal cord injury, cerebral palsy, prosthetics, orthotics, and osteoarthritis.

3.8 Biomechanical model

The model used consists of 9 solids: thorax, humerus right / left, ulna right / left, radius right / left, and hand right / left, and has 16 degrees of freedom. The thorax is the reference body, which is linked to the ground (inertial frame). So, it has 6 degrees of freedom with respect to the ground, 3 rotations, and 3 translations. The other degrees of freedom of the model is the relative rotations between the different bodies that constitute the model. The model is presented in Figure 28 below. The movement of the fingers and the wrist is not studied due to two main reasons: the considered arm support will not articulate the fingers, and those are the last part affected by the disease. Although just one arm is analyzed, both arms are modeled equally.

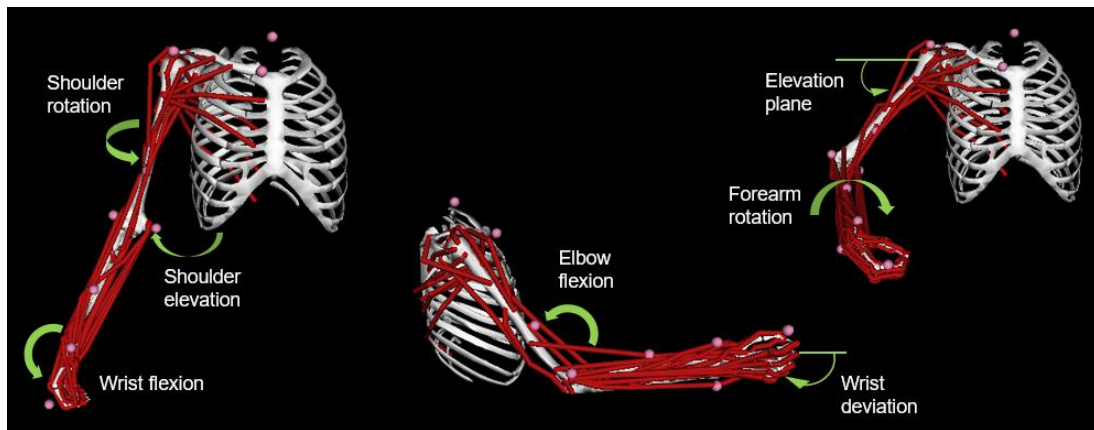


Figure 28: Musculoskeletal model of the upper limb. The dynamic model incorporates 7 degrees of freedom, including (A) shoulder rotation and elevation (thoracohumeral angle) and wrist flexion, (B) wrist deviation and elbow flexion, and (C) elevation plane of the shoulder and forearm rotation.

3.8.1 Working with OpenSim

OpenSim software is a robust framework that can be used to analyze and simulate complex dynamic models, such as biological structures. This subsection contains an overview of the approach used to estimate muscle activation using this software, including the model's validation. To summarize, OpenSim gives a library of biomechanical models that can be modified or written from scratch using the available components or user-defined ones. Starting from a musculoskeletal model, it is possible to simulate them, using movements taken by real data or synthesized from control signals, and analyze their behavior with the tools available from the framework. The remaining subsections will describe the tools used in this thesis.

3.8.2 Inverse Kinematics

The Inverse Kinematics (IK) Tool allows mapping the real sensor data of a movement to the simulated model to perform the required analysis Inverse on the motion. It is fundamental for many other tools, such as Dynamics (subsection 4.2.3) and Computed Muscle Control (subsection 4.2.4). The tool steps through each time frame of the experimental data and sets the joint coordinates of the model in a pose that best matches the experimental marker and coordinates data for that time frame. The best match is a pose that minimizes a sum of weighted squared errors of markers and coordinates. The marker error is the distance between an experimental marker and the corresponding marker on the model when its generalized coordinates are the ones computed by the tool. The coordinate error is the difference between an experimental coordinate value and the coordinate value computed by the tool; the experimental coordinate values can be the joint angles obtained directly from the motion capture system, a specialized external algorithm, or other measuring devices goniometer. It can also be a fixed desired value for a coordinate, for some user's purpose.

Moreover, the tool allows a distinction between prescribed and unprescribed coordinates: the first are coordinated whose trajectories are known and do not need to be computed by the tool; the latter, on the other hand, coordinates whose value is computed using the tool. Each unprescribed coordinate and each marker's associated weight, specifying how strongly its error should be minimized. Mathematically, the IK tool solves the weighted least squares problem stated as follows:

$$\min_{\mathbf{q}} \left[\sum_{i \in \{\text{markers}\}} w_i \| \mathbf{x}_i^{\text{exp}} - \mathbf{x}_i(\mathbf{q}) \|^2 + \sum_{j \in \{\text{unprescribed coordinates}\}} \omega_j |q_j^{\text{exp}} - q_j|^2 \right]$$

having $q_j = q_j^{\text{exp}}$ for each prescribed coordinate j . The tool finds for each time frame the generalized coordinates vector \mathbf{q} that minimizes the cost equation, where $\mathbf{x}_i^{\text{exp}}$ is the experimental position of the marker i , $\mathbf{x}_i(\mathbf{q})$ is the position of the corresponding marker on the model, function of the generalized coordinate values, and q_j^{exp} is the experimental value for the coordinate j . All the prescribed coordinates are set to their experimental values. The marker weights (w_i) and the coordinate weights (ω_j) are specified respectively by the `<IKMarkerTask>` and `<IKCoordinateTask>` tags of the XML settings file of the tool. The least-squares problem is then solved using a general quadratic solver, with a convergence criterion of 0.0001 and a limit of 1000 iterations.

3.8.3 Computed Muscle Control

The Computed Muscle Control (CMC) Tool has the purpose of computing a set of muscle excitations (or, more generally, actuator controls) that will drive a dynamic musculoskeletal model, trying to track as good as possible a set of desired kinematics in the presence of applied external forces (if any). It uses residual input data the ground reaction forces and the output kinematics of the Reduction Algorithm (RRA) Tool. This tool has the purpose of minimizing the effects of modeling and marker data processing errors that lead to large non-physical compensatory forces called residuals. The working principle of the algorithm that lies behind the tool has been described in [50]. At user-specified time intervals during a simulation, the CMC Tool computes muscle excitation levels that will drive the generalized coordinates of the dynamic musculoskeletal model towards a desired kinematic trajectory. CMC does this by using a combination of proportional-derivative (PD) control and static optimization (see figure 29).

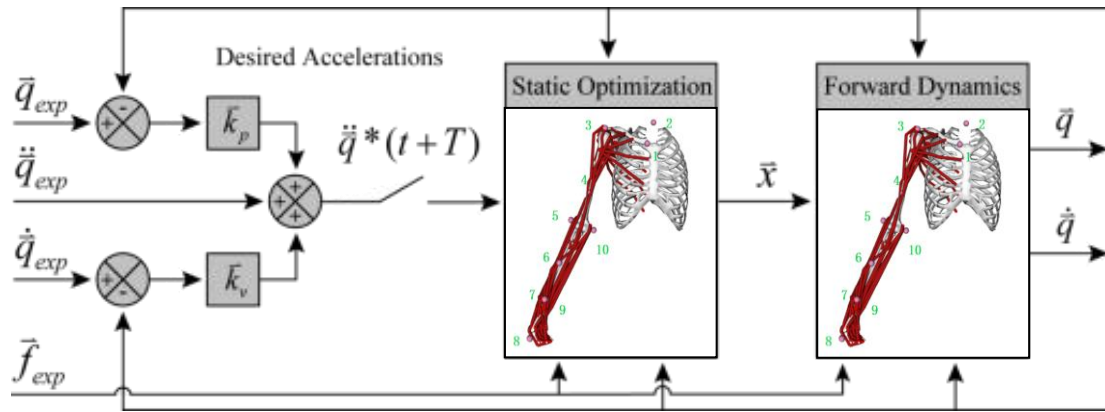


Figure 29: Schematic of the Computed Muscle Control Algorithm

Before starting the CMC algorithm, initial states for the model are computed. The states comprise the generalized coordinates, generalized speeds, and muscle states (i.e., muscle activation levels and muscle lengths). While the initial values of the generalized coordinates and speeds can be taken from the desired kinematics that you specify, the initial values of the muscle states are generally unknown. To compute viable starting muscle states, CMC is applied to the first 0.030 seconds of the desired movement. Because the muscle states are generally out of equilibrium and muscle forces can change dramatically during this initial time interval, the simulation results during this interval are generally not valid.

3.9 Simulations of Experimental tasks

We generated simulations of the upper limb model based on the experimental motion data. We refer to the simulations of the upper limb without a device attached as the baseline for the assisted simulations. We used a three-dimensional musculoskeletal model that is based on a model developed [34]. The model contains 27 degrees of freedom, though we locked 8 of them that we deemed nonessential for our study (wrist, hand).

Our simulation workflow began with scaling the geometry of the generic musculoskeletal model to match the anthropometry of each of our subjects, using the OpenSim Scale Tool. Additionally, we scaled the maximum isometric forces of the muscles according to a regression equation based on subject mass and height [42]. For each subject and condition, we simulated 3 of the overground trials. We generated joint angle trajectories for each of these trials using OpenSim's Inverse Kinematics (IK) Tool.

We used OpenSim's Residual Reduction Algorithm (RRA) Tool to reduce the residual forces. We ran RRA twice for each trial: first, to generate an adjusted model (RRA-model), and then to generate adjusted kinematics (RRA-kinematics). We combined all adjusted models from each run of the RRA-model for the same subject and condition (by averaging the suggested mass adjustments) to create a single adjusted model for each subject and condition. This strategy helps to avoid overfitting the model to the experimental data from any particular trial, which may occur when using a separate adjusted model for each trial. For the loaded condition, we used RRA-model to adjust the mass and location of the load. We then produced adjusted kinematics for each trial by running RRA-kinematics, using the single adjusted model and the kinematics from IK as input. Finally, we generated muscle-driven simulations of OpenSim's Computed Muscle Control (CMC) Tool [43], using the adjusted model and the adjusted kinematics.

CMC solves for muscle excitations that can produce the observed motion while minimizing the sum of squared muscle activations at regular intervals in the motion.

Precisely, CMC's objective function, J , consists of an effort term, J_{effort} , and a term associated with modeling and measurement error, J_{error} :

$$J = J_{\text{effort}} + J_{\text{error}}, \#$$

$$J_{\text{effort}} = \sum_{i \in M} a_i^2, \#$$

$$J_{\text{error}} = \sum_{i \in R} \left(\frac{f_i}{w_{f,i}} \right)^2 \cdot \#$$

The effort term (Eq 2) depends only on the activation of the set of muscles M in the model. The error term (Eq 3) penalizes the force or moment f applied by the set of reserve and residual actuators R in the model. Reserve actuators apply small joint moments to compensate for unmodeled passive structures (e.g., ligaments) and potential muscle weakness, and residual actuators apply the residual forces explained above. The weighting factor w_f is adjusted to make the reserves and residuals much more costly to use compared to the muscles; in OpenSim, this factor is the actuators' "optimal force" property. We simulated tasks with and without the assistive device to evaluate the muscle output from the given forces measured from the experiments. (5 subjects, 3 trials per condition).

3.9.1 Muscle force estimation.

Muscle forces were estimated using OpenSim (vers 4.0, OpenSim). The generic model of the upper limb was placed with virtual markers, which later will be scale to match the individual anatomical segment of the body part. Inverse kinematics tools were used to estimate the joint angles. Then, computed muscle control (CMC) tools were executed to obtain the muscle forces.

In the assisted simulations, the CMC algorithm controlled both the muscles and the device. As a result, the objective function included the torques applied by the single actuator of the device:

$$J_{\text{effort}} = \sum_{i \in M} a_i^2 + \left(\frac{\tau_{\text{left}}}{w_{\tau, \text{left}}} \right)^2 + \left(\frac{\tau_{\text{right}}}{w_{\tau, \text{right}}} \right)^2 . \#$$

To maximize the use of the device in place of muscles, we set the weighting factors w to a significant value (1000 N-m) so that using the device had a negligible penalty. The CMC optimization played the two roles of finding the optimal device behavior and predicting changes in muscle activity. The assisted simulations tracked the same kinematics as the no assistance simulations on which they were based, so the net joint moments throughout the motion were conserved for all degrees of freedom. With the aid of the device to achieve those same net joint moments, overall muscle coordination could change to arrive at a lower J_{effort} .

3.9.2 Validation of simulations.

The movement of reach forward motion has been conducted. This motion requires the subject to perform a right-hand movement from initial position to front reach motion. From the marker data and EMG data, the used model will be validated by comparing the EMG data and force output from the simulations.

3.9.3 Simulation workflow

This subsection resumes the simulation workflow that has been developed into an OpenSim simulation. These are the main steps :

- 1) Perform the Inverse Kinematics Tool on the upper limb model with the desired experimental marker data;
- 2) Perform the Inverse Dynamics Tool on the model with the motion generated by the IK;
- 3) Perform the Computed Muscle Control Tool to obtain the muscle activations
- 4) Compare the results of the muscle forces generated with EMG data.

Conclusion

This chapter presented the experimental procedure stage to acquire data for simulation purposes. It consists of motion capture data for specified upper limb tasks. In addition, the subject will be asked to wear the assistive device, and the upper right arm will be evaluated its muscle activity during the device's movement. EMG data has been recorded to compare with the simulation result later for further validation and evaluation. This chapter also consists of integrating the assistive device within a musculoskeletal OpenSim model of the upper limb. The integration modifies the upper limb model, adding assistive force components to emulate the behavior of assistive movement. The next chapter will discuss the validation results and results for specific tasks in upper limb motion.

Chapter 4

Result and Discussions

4.1 Introduction

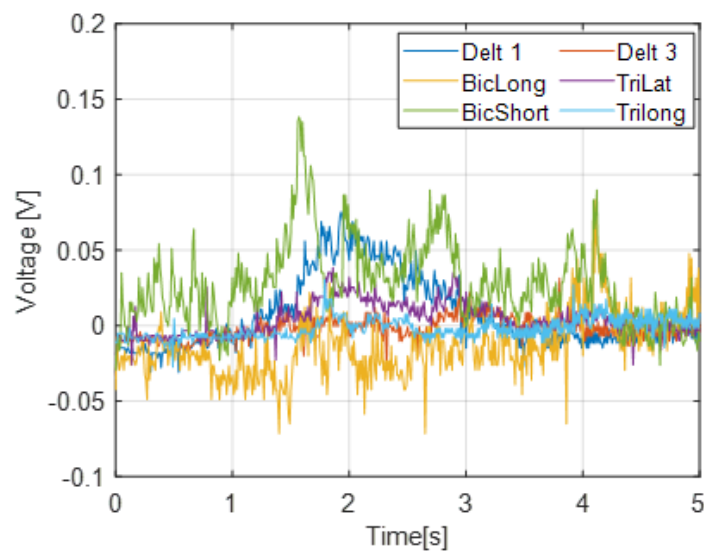
This section is devoted to reporting the results of the experimental and simulations that have been performed. Firstly, we perform the upper limb motion proposed in chapter 3, and the motion capture data taken has been used in OpenSim to perform scaling and inverse kinematic using the model. Then RRA and CMC were computed to obtain the muscle force. These muscle forces were then compared with the measured EMG data to validate the muscle activity measured. The result is discussed in this section.

4.2 Test cases evaluation for model validation

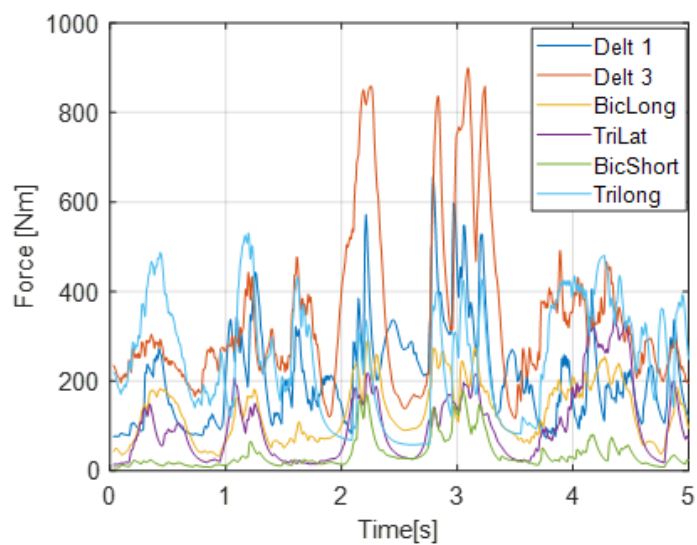
The validation of the model presented in chapter 3 will be done through a simulation of the upper limb model within the OpenSim framework. The motion data acquisition and simulation pipeline has been described in the previous chapter. Briefly, the marker data are firstly used to scale the upper limb model (without the device). Then the motion data are used to compute the inverse kinematics to gain the kinematics data such as joint angle. Then, the CMC tools are run to estimate the muscle force for the specified kinematics data. The estimated muscle force results were compared to recorded EMG data measured during the experimental procedures.

4.2.1 Simulation results

Firstly, this study utilizes the CMC to validate the OpenSim model. The dynamic motion of the upper limb, which is a reach-forward motion, has been conducted. The approach obtains the muscle force from the interested muscle, which will be compared with the measured EMG data. The figure below shows the measured EMG data for the 6 muscles of interest mentioned earlier and the muscle forces estimated using the musculoskeletal model in OpenSim. The result was only analyzed for one subject.



(a) Filtered EMG data for 6 muscles model



(b) Estimated muscles force using upper limb

Figure 30: EMG data and estimated muscle forces for the same reach forward motion.

As mention in section 3, we selected the deltoid anterior part (Delt 1), deltoid posterior part (Delt 3), the short head of biceps (BicShort), long head of biceps (BicLong), long head of triceps (TriLong), and lateral head of triceps (TriLat) as 6 muscles of interests. Figure 30 (a) shows the processed EMG data for the muscles taken during the experiment and estimated muscle forces shown in figure 30 (b) from the simulation of the musculoskeletal model.

The side-by-side comparison with the same muscle cluster is shown in figure 31 below. By adopting a neural mapping method [50], we assumed that BicShort has the same activation as BicLong and the other two heads of triceps have the same activation. In both experimental EMG data and estimated muscle forces from simulation, we can see that the Biceps muscles are working during the motion and present the main activity. On the other hand, the triceps muscle does not show big activity due to its minor role in joint motion. We can also see that the pattern of most muscle forces (Biceps and Triceps) is similar to the recorded EMG pattern. The similarity agreement between the recorded EMG data and the estimated muscle forces for the same motion shows that this model is acceptable to predict muscle activity for upper limb right-hand motion.

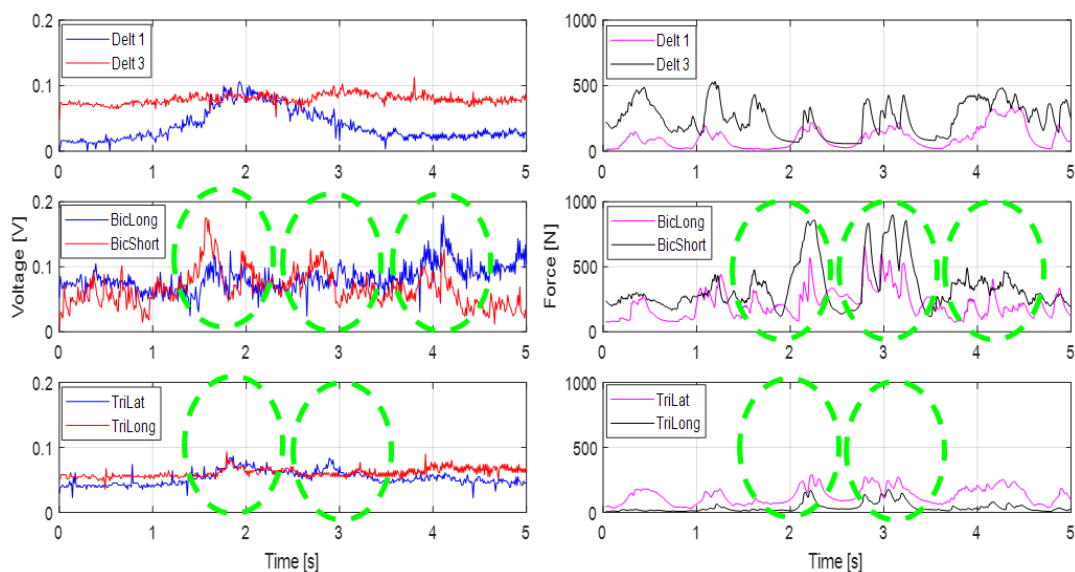


Figure 31: Comparison of muscle activity for the same muscle cluster

4.3 Simulation with an assistive device

The schematic of this simulation of an integrated model with an assistive device is shown in the figure below. From the input mentioned in section 3, the simulation of closed-loop control of a human-device system is performed. For this motion, 3 target muscles, the brachioradialis, biceps, and triceps muscles, are investigated for muscle activity.

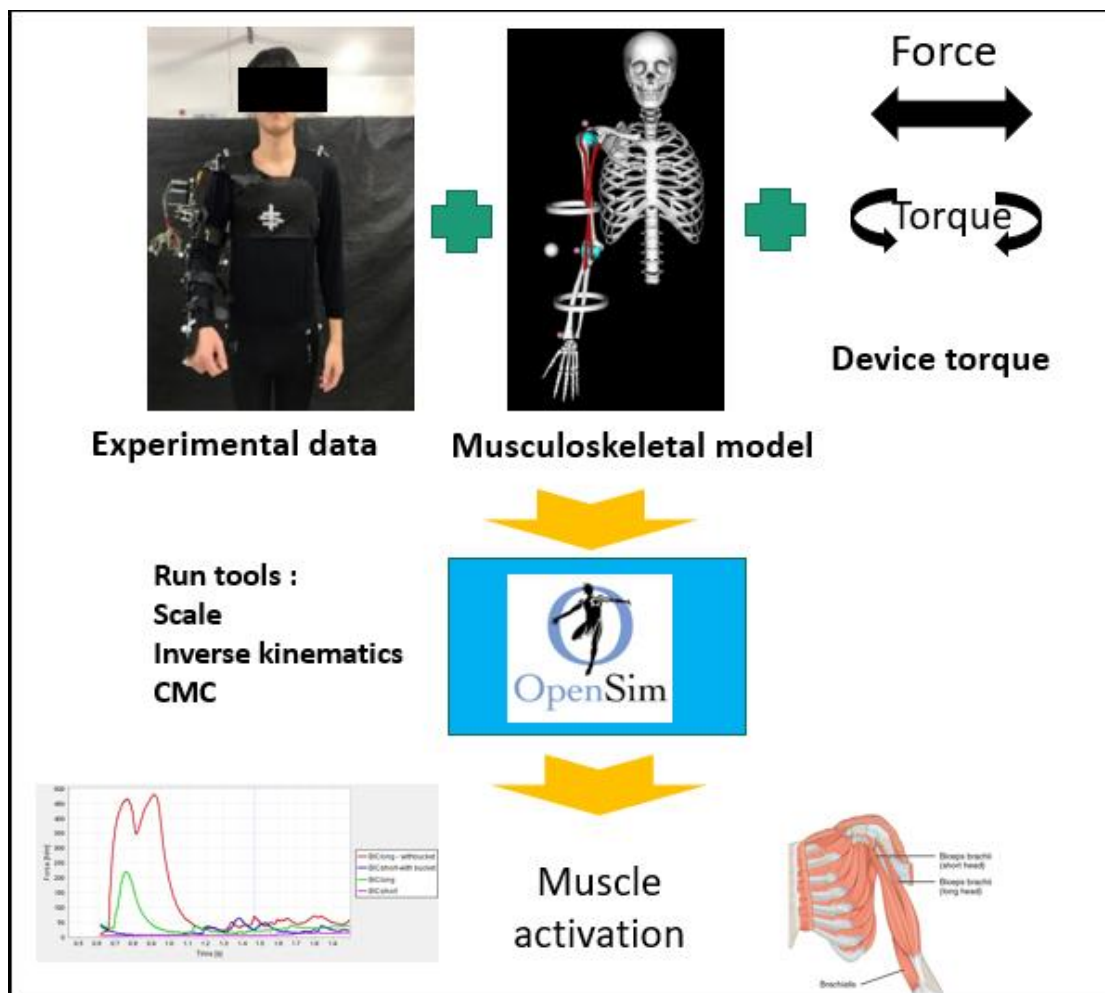


Figure 32: The required data for closed-loop simulation of a human-device system

The muscle estimation was evaluated by simulating the musculoskeletal model using the motion data provided through the experiment of the subject wearing and without wearing the developed assistive device. The muscles of interest in this study are shown in figure 33 below.



Figure 33: Three predominant muscles activating the elbow DoFs were selected to be the test's muscle: biceps, triceps, and brachioradialis muscle.

4.3.1 Upper limb motion – 90-degree elbow flexion and extension

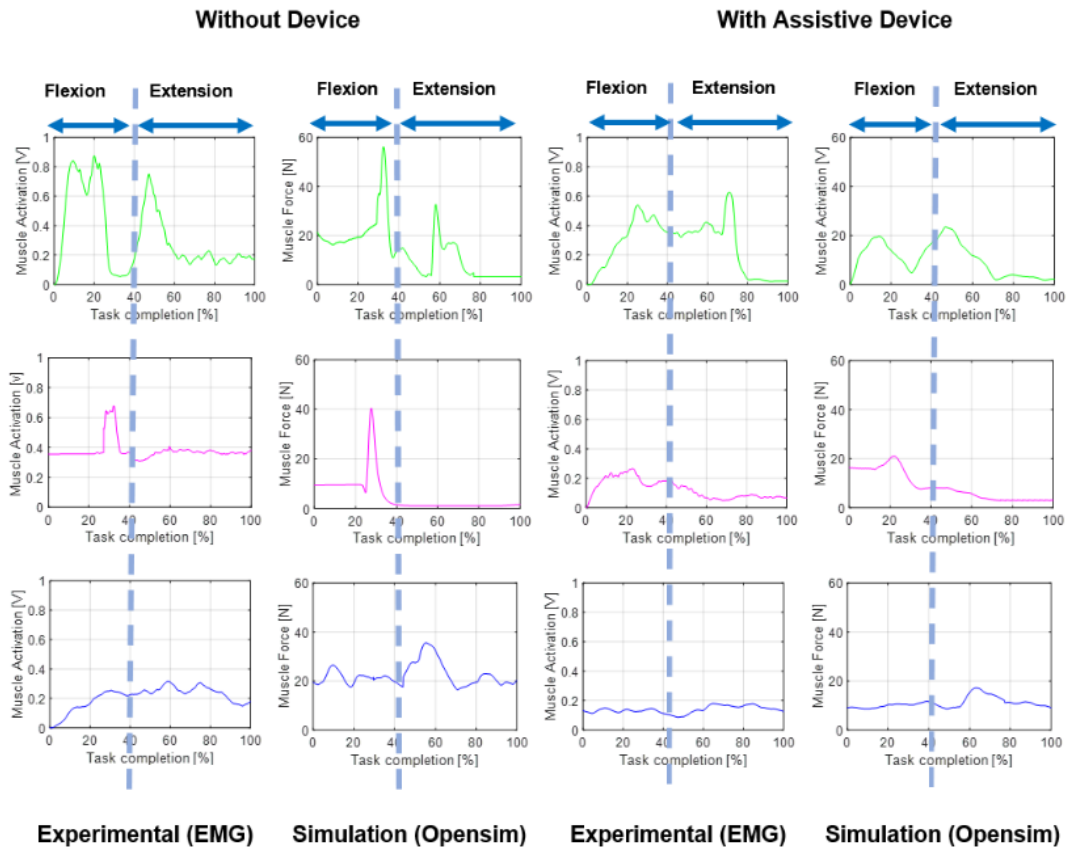


Figure 34: Comparison of EMG from experimental and muscle activations computed from Opensim resulting three muscle force brachioradialis (green), biceps (magenta), and triceps(blue) for 90-degree elbow flexion and extension motion with and without the assistive device.

The result of the experiments and simulations are presented. Figure 7.2, figure 7.3, and figure 7.4 compare 3 interested muscles for the upper limb movement with and without wearing the assistive device. Experiments on the upper arm device had shown that muscle activations could be significantly reduced when assistive force was enabled during upper limb movements. Overall, the results show that each of the muscles activated reduced thanks to the presence of the assistive device. In Figure 7.2 above, the most significant activated muscle would be Brachioradialis (green), which can be observed in EMG measured and simulation data from force produced. The initial peaks are mainly visible during the elbow's flexion (within the first 40% of movement) both in experimental and simulation for brachioradialis and biceps

muscle. As reported in [27,28,34], the primary activated muscle for elbow flexion movement would be in Brachioradialis and Biceps muscle, and the result from the EMG could confirm the reported article. However, we can see the visible peak when the arm is in extension motion (the last 50% of the movement) for the brachioradialis muscle. This is because the muscle was trying to sustain the movement because of the 1kg weight worn by the subject on the wrist.

On the other hand, we could observe the significant tricep muscle peak during the extension motion in musculoskeletal simulation with and without wearing the device. The tricep muscle is an extensor muscle of the upper extremity. Positioning and EMG sensor attachment probably cause minimal detection for the tricep muscle area during the experiment.

4.3.2 Upper limb motion – Maximum shoulder flexion and extension

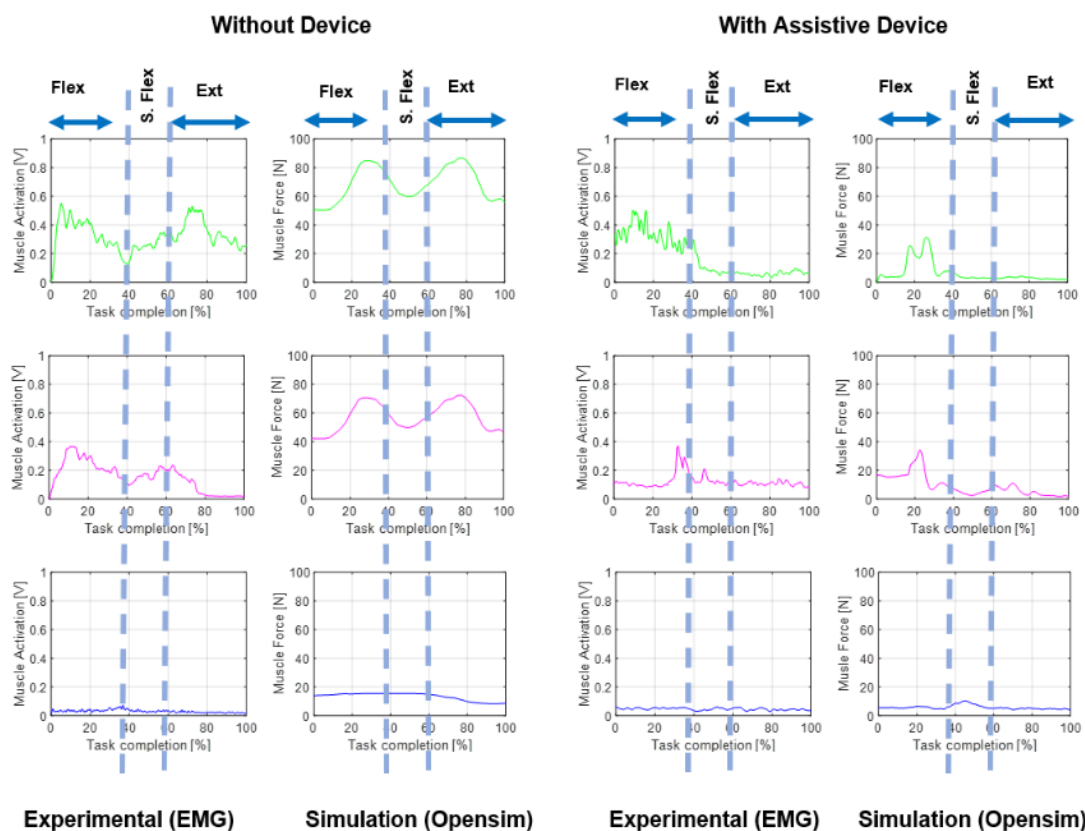


Figure 35: Comparison of EMG from experimental and muscle activations computed from Opensim resulting three muscle force brachioradialis (green), biceps (magenta), and triceps(blue) for maximum shoulder flexion and extension motion with and without the assistive device.

The result in Figure 35 shows a similar group of muscles activated during the arm's flexion, which peaks in the Brachioradialis and Biceps muscle can be observed in both experiment and simulation data for the first 40% of the movement. Then, these muscles also have another activation during the shoulder flexion. Although commonly, the muscle involved during elbow flexion mainly at the shoulder, the subject's weight could cause the muscle to do extra work to sustain the shoulder and arm during the shoulder flexion. When the subject wearing the device, only the initial peak for both muscles can be observed. Due to the assisted movement by the device, the elbow and shoulder are well supported during the shoulder flexion, and extension movement causes no muscle activated during the motions. For triceps data in both experimental, low detection would probably be from the poor sensor attachment and the excessive fat region.

4.3.3 Upper limb motion – Inward elbow flexion and extension

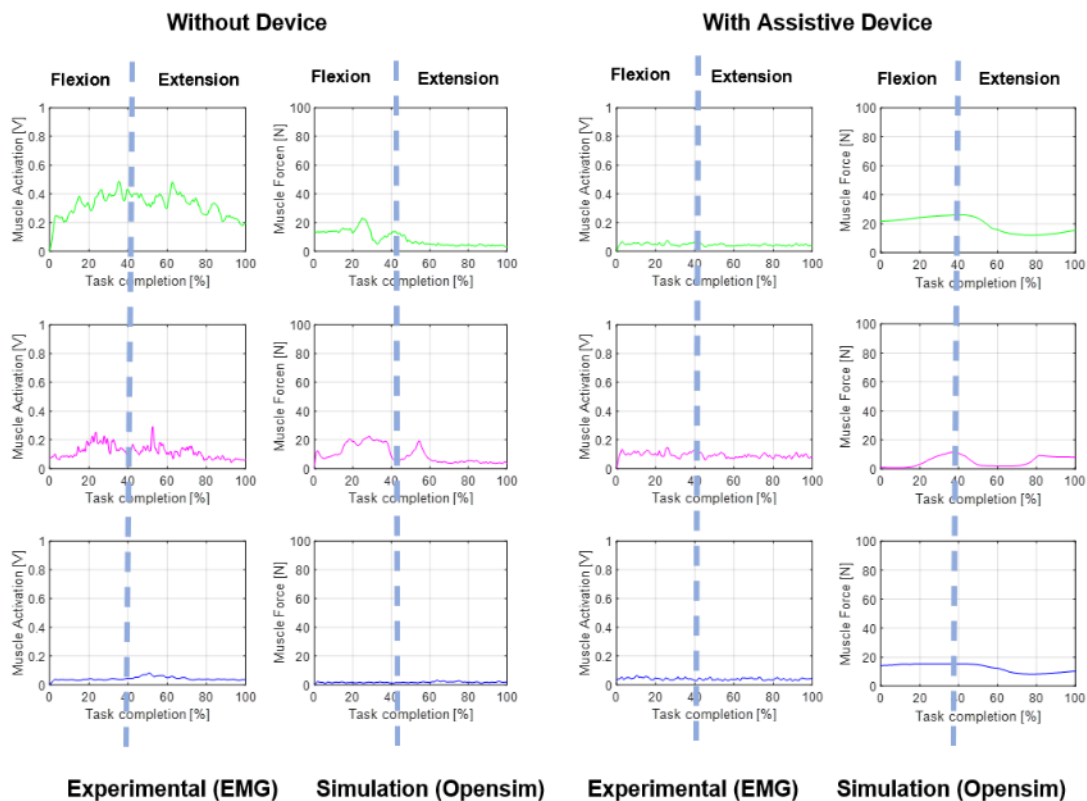


Figure 36: Comparison of EMG from experimental and muscle activations computed from Opensim resulting three muscle force brachioradialis (green), biceps (magenta), and triceps (blue) for inner elbow flexion and extension motion with and without the assistive device.

For inner elbow flexion and extension, the shoulder muscle would be most anticipated during these movements according to the muscle anatomy of the upper limb human movement. However, since this is a preliminary evaluation, we only focus on three muscles for all the motions for comparison, and none of the shoulder muscles are evaluated. Overall results in Figure 7.4 show that a shallow peak of muscle activated across the muscles. This visible activated muscle maybe because of the muscle trying to hold or sustain the arm with the weight during the motion.

4.4 Statistical Analysis

Since the data tested were not to be normally distributed, non-parametric tests were used throughout the analysis. In this study, the Wilcoxon test, or Wilcoxon signed-rank test is used to check whether two dependent samples differ significantly from each other. Since the Wilcoxon test is a nonparametric test, the data do not have to be normally distributed. However, to calculate a Wilcoxon test, the samples must be dependent. For this purpose, the non-parametric Wilcoxon signed-rank test was performed with the alpha value set at $p < .05$. This allowed the comparison of the normalized EMG data for experimental conditions and muscle force from simulations with and without device conditions, respectively.

4.4.1 Wilcoxon signed-rank test (Task 1 : 90 degree elbow flexion and extension)

For task 1, all tested muscles in both subject wearing and without wearing device conditions, the mean and standard deviation EMG and muscle force data are presented in Table 4 and Table 5 below.

Table 4: Mean (\pm SD) normalized EMG and Muscle Force for all tested muscles with and without device condition (**Flexion**).

	Brachioradialis		Biceps		Triceps	
	M(\pm SD) EXP	M(\pm SD) Sim	M(\pm SD) EXP	M(\pm SD) Sim	M(\pm SD) EXP	M(\pm SD) Sim
Without device	0.19	8.7	0.19	6.35	0.15	2.5
With device	0.11	5.26	0.08	2.23	0.13	2.1

Table 5: Mean (\pm SD) normalized EMG and Muscle Force for all tested muscles with and without device condition (**Extension**).

	Brachioradialis		Biceps		Triceps	
	M(\pm SD) EXP	M(\pm SD) Sim	M(\pm SD) EXP	M(\pm SD) Sim	M(\pm SD) EXP	M(\pm SD) Sim
Without device	0.16	4.9	0.3	0.98	0.25	5.95
With device	0.08	3.76	0.06	1.89	0.21	2.1

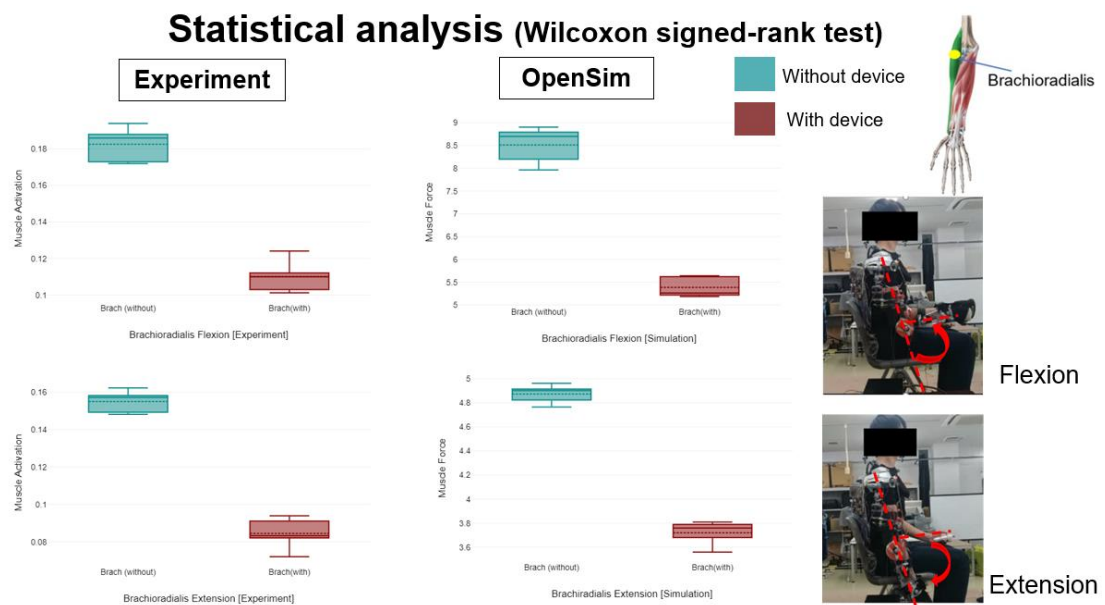


Figure 37 : Mean and STD (error bars) plot of the muscle activation (brachioradialis) for subject performing 90 deg elbow flexion and extension with assist and without assistive device conditions.

The Brachioradialis (without device) data had higher values (Mean = 0.19) than the Brachioradialis (with device) data (Mean = 0.11) in flexion and also during the extension motion which (without device) group data had higher values (Mean = 0.16) than the Brachioradialis (with device) group (Mean = 0.08). Wilcoxon Test showed that this difference was statistically significant for both motions measured, $p = .043$. This results in a p-value below the specified significance level of 0.05. The result of the Wilcoxon test is therefore significant for the present data and it is assumed that both samples show differences in measured data.

Statistical analysis (Wilcoxon signed-rank test)

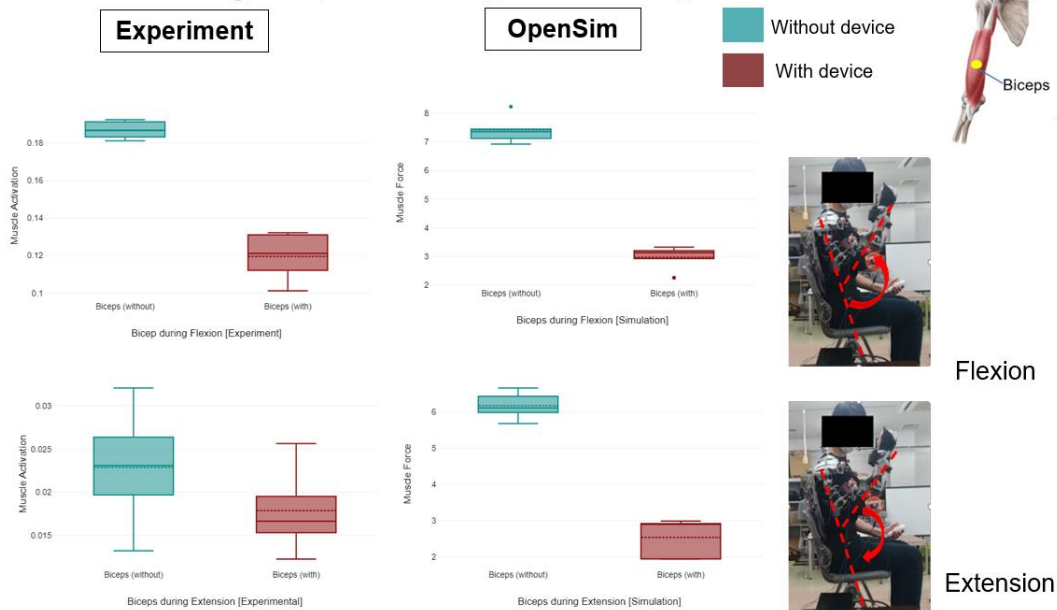


Figure 38: Mean and STD (error bars) plot of the muscle activation (biceps) for subject performing 90 deg elbow flexion and extension with assist and without assistive device conditions.

The Biceps (without device) data had higher values (Mean = 0.19) than the Biceps (with device) data (Mean = 0.08) in flexion and also during the extension motion which (without device) group data had higher values (Mean = 0.3) than the Biceps (with device) group (Mean = 0.06). Wilcoxon Test showed that this difference was statistically significant for both motions measured, $p = .043$ and $p = 0.042$. This results in a p-value below the specified significance level of 0.05. The result of the Wilcoxon test is therefore significant for the present data and the null hypothesis is rejected. Therefore, it is assumed that both samples show differences in measured data.

4.4.2 Wilcoxon signed-rank test (Task 2 : Maximum shoulder flexion and extension)

For task 2, all tested muscles in both subject wearing and without wearing device conditions, the mean and standard deviation EMG and muscle force data are presented in Table 6 and Table 7 below.

Table 6: Mean (\pm SD) normalized EMG and Muscle Force for all tested muscles with and without device condition (**Flexion**).

	Brachioradialis		Biceps		Triceps	
	M(\pm SD) EXP	M(\pm SD) Sim	M(\pm SD) EXP	M(\pm SD) Sim	M(\pm SD) EXP	M(\pm SD) Sim
Without device	0.17	8.35	0.19	7.35	0.12	2.23
With device	0.16	4.13	0.12	3.13	0.11	1.92

Table 7: Mean (\pm SD) normalized EMG and Muscle Force for all tested muscles with and without device condition (**Extension**).

	Brachioradialis		Biceps		Triceps	
	M(\pm SD) EXP	M(\pm SD) Sim	M(\pm SD) EXP	M(\pm SD) Sim	M(\pm SD) EXP	M(\pm SD) Sim
Without device	0.18	5.11	0.17	6.11	0.25	4.6
With device	0.05	1.9	0.02	2.9	0.19	2.1

Statistical analysis (Wilcoxon signed-rank test)

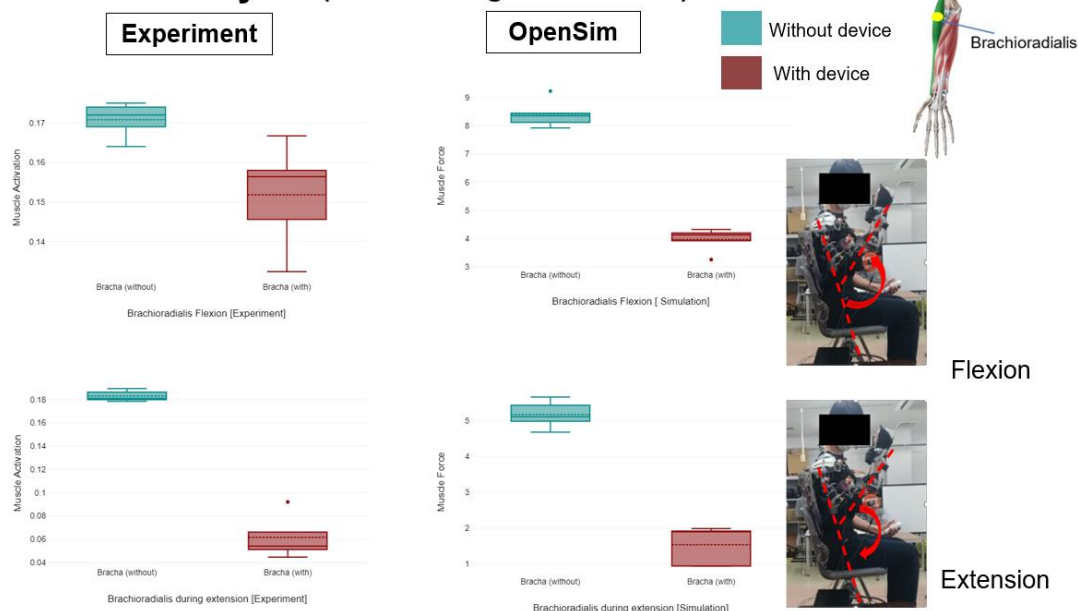


Figure 39 : Mean and STD (error bars) plot of the muscle activation (brachioradialis) for subject performing maximum shoulder flexion and extension with assist and without assistive device conditions.

For experimental data, the Bracha (without device) group had higher values (Mean = 0.17) than the Bracha (with device) group (Mean = 0.16). However, A Wilcoxon Test showed that this difference was not statistically significant, $p = .08$. This results in a p-value of .08 , which is above the specified significance level of 0.05. The result of the Wilcoxon test is therefore not significant for the present data and the null hypothesis is retained. During the extension, The Bracha (without device) group had higher values (Mean = 0.18) than the Bracha (with device) group (Mean = 0.05). A Wilcoxon Test showed that this difference was statistically significant, $p = .043$. This results in a p-value of .042 , which is below the specified significance level of 0.05. The result of the Wilcoxon test is therefore significant for the present data and the null hypothesis is rejected. Therefore, it is assumed that both samples show differences in measured data. While simulation data shows The Brachioradialis (without device) data had higher values (Mean = 8.35) than the Brachioradialis (with device) data (Mean = 4.13) in flexion and also during the extension motion which (without device) group data had higher values (Mean = 5.11) than the Brachioradialis (with device) group (Mean = 1.9). Wilcoxon Test showed that this difference was statistically significant for both motions measured, $p = .043$. This results in a p-value below the specified significance level of 0.05. The result of the Wilcoxon test is therefore significant for the present data and the null hypothesis is rejected. Therefore, it is assumed that both samples show differences in measured data.

Statistical analysis (Wilcoxon signed-rank test)

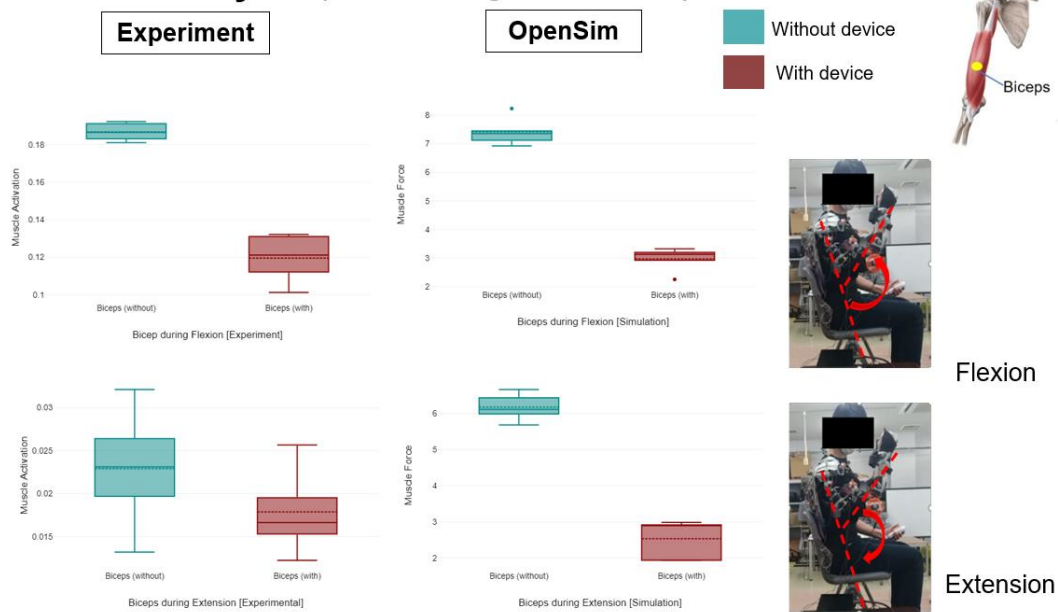


Figure 40: Mean and STD (error bars) plot of the muscle activation (biceps) for subject performing maximum shoulder flexion and extension with assist and without assistive device conditions.

For experimental data, The Biceps (without device) group had higher values (Mean = 0.19) than the Biceps (with device) group (Mean = 0.12). A Wilcoxon Test showed that this difference was statistically significant, $p = .043$. This results in a p-value of .043 , which is below the specified significance level of 0.05. The result of the Wilcoxon test is therefore significant for the present data and the null hypothesis is rejected. Therefore, it is assumed that both samples show differences in measured data. During extension, The Biceps (without device) group had higher values (Mean = 0.02) than the Biceps (with device) group (Mean = 0.02). However, A Wilcoxon Test showed that this difference was not statistically significant, $p = .08$. This results in a p-value of .08 , which is above the specified significance level of 0.05. The result of the Wilcoxon test is therefore not significant for the present data and the null hypothesis is retained. Therefore, it is assumed that both samples show no differences in measured data.

While simulation data shows, The Biceps (without device) data had higher values (Mean = 7.35) than the Biceps (with device) data (Mean = 3.13) in flexion and also during the extension motion which (without device) group data had higher values (Mean = 6.11) than the Brachioradialis (with device) group (Mean = 2.9). Wilcoxon Test showed that this difference was statistically significant for both motions

measured, $p = .043$. This results in a p-value below the specified significance level of 0.05. The result of the Wilcoxon test is therefore significant for the present data and the null hypothesis is rejected. Therefore, it is assumed that both samples show differences in measured data.

4.5 Discussion

Wearable assistive devices can potentially offset a substantial amount of arm loading during upper limb movement tasks. This study compared the functionality of the assistive device developed in this study for upper arm dynamic movements and its effect on the muscle output. Together with the experimental condition, two computer-based musculoskeletal models with and without device parameters have been set up. Specifically, we used measured tension forces during the device motion as input to compare differences in force and activation in the right arm muscles (Brachioradialis, biceps, and triceps) activity.

Results showed that a musculoskeletal model with and without an integrated assistive device could produce muscle activation patterns more similar to the EMG measured for all muscles of interest during the simulated upper dynamic tasks. Comparison of measured EMG muscle data and human-device models revealed that, although the model did not fully incorporate similar muscle physiology completely, muscle force was generated throughout the arm comparable with measured muscle activity from the experimental. The integrated human-device model produced encouraging results such that muscle force values for 2 primary muscles (Biceps and Brachioradialis) were reduced during the simulated task when wearing the assistive device. These results are congruent with expectations, with the assistive device that manages to support the upper limb movement, providing practical assistance. Furthermore, Wilcoxon signed rank test analysis shows significant difference could be found when comparing the muscle activation data with and without device condition during the motion.

Our study has several assumptions and limitations. Firstly, only healthy subjects were tested and modeled in this study, and the findings may not reflect those of an affected upper limb due to the stroke disease. Secondly, differences in kinematics between the assistive device joints and the anatomical upper limb joints may have

influenced model calculation during the simulation. However, they are unlikely to have influenced the main finding in this study of evaluation on significantly reduced muscle output when wearing the assistive device. Even though our simulation results are based on our developed assistive device design, our main findings are generalizable to other wearable devices, including cable-driven ones.

We only simulated 3 specific upper extremity movements in the present study that capture a small subset of possible upper arm movements. A more significant number of movements representing the wide variety of daily living tasks should be evaluated in the future to determine the effect of the assistive device more comprehensively on user biomechanics. In addition, we constrained all simulations and conditions to the same experimental kinematics from the healthy subject who was not impaired and did not use the device in regular daily life. Someone using an assistive device regularly may adapt their movement, as shown for other passive devices [34].

Our developed assistive device's primary function is to help ADL tasks for patients who cannot move one arm. However, the capability of the assistive device to assist the arm movement and its effect on muscle activity has not been studied to date. This study demonstrated that upper limb movement assisted by the wearable assistive device could reduce peak muscle force confirming the study hypothesis.

Chapter Conclusion

This chapter presented the validation method that has been adopted for the proposed method using biomechanical software to estimate muscle forces. It consists of an integration of the assistive device within a musculoskeletal OpenSim model of the human upper limbs. The integration modifies the upper limb model, adding a torque actuators component for them to emulate the behavior of the assisting movement. Then, Section 4.2 described the validation of the upper limb model specified to the experimental data. Section 4.3,4.4 and 4.5 shows the result and discussion regarding the comparison muscle activities of the subjects when using and without using the assistive device in both experimental and simulations.

Chapter 5

Conclusion and Future Recommendation

This work proposed an approach to use a musculoskeletal model of the upper right arm to predict individual muscle activation during the motion of elbow flexion when the subject is using the assistive device. The model is first validated dynamically by comparing the simulation of the movement and experimental EMG data, which shows agreement in the pattern. The validated model is later used to assess the upper limb target muscle when the subject is using the assistive device.

To successfully translate wearable assistive technology to upper limb disability patient during rehabilitation training, it is critical to understand its effectiveness, usability, and biomechanical interaction with humans. As a first step toward accomplishing this goal, we quantitatively evaluated our developed assistive device's mechanical and biomechanical performance. Our results showed that the device could reduce the muscle activity of several muscles crossing the upper arm. However, our mechanical evaluation revealed aspects of the design that limit the assistive device's assistance. In our future work, we will explore different assistance levels and identify a range of assistance that most enhance arm motor function and biomechanics. More comprehensive biomechanical studies will be performed to assess the device for more biomechanical parameters (e.g., joint kinematics), more participants (both able-bodied subjects and people with upper arm disability), and more movements that typify activities of daily living. Finally, several design refinements need to be made, especially those that reduce friction and add a motion range to the system.

The method's limitations suggest that if the interest is focused on muscle forces, EMG data can only provide a preliminary assessment of muscle activation patterns and does not provide information on how muscle forces change within specific tasks

due to the nonlinear relationship between EMG and muscle forces[42]. The ideal way for comparing results of a musculoskeletal model and actual internal structure forces would be to measure joint reaction forces during the movement of interest (in this case, inclined walking) and relate them to the calculated joint reaction forces. This type of validation is limited to impaired participants, who might not even complete all tasks.

Furthermore, the musculoskeletal models were not adjusted participant-specifically in the current study, further explaining the differences between the model predictions and the EMG measurements. However, it can be assumed that the participant-specific differences based on the available treatment are substantially averaged out over the five participants. Moreover, the goal was to assess whether this human-device integrated model can be used in future research for evaluating muscle output during rehabilitation training when using the assistive device. To conclude, this study showed that the integrated human-device musculoskeletal model yielded good agreement between the measured and estimated muscle activity for most conditions and muscles. Therefore, it can be used for further analysis in similar groups of participants.

References

- [1] Population Division, DESA, United Nations. (2009, Feb. 18). Magnitude and Speed of Population Ageing. *World Population Ageing 1950-2050*. [Online]. Available: www.un.org/esa/population/publications/worldageing19502050/
- [2] Population Division, DESA, United Nations. (2009, Feb. 18). Demographic Determinants of Population Ageing. *World Population Ageing 1950-2050*. [Online]. Available: www.un.org/esa/population/publications/worldageing19502050/
- [3] National Institute of Population and Social Security Research. (2009, Feb. 18). Trend of the Proportion of Three Major Age Groups. *Summary of the Japanese Population Projection*. [Online]. Available: <http://www.ipss.go.jp/index-e.html>
- [4] DESA, United Nations.(2009, March 02). World Programme of Action Concerning Disabled Persons. *Mandates of the Secretariat for the Convention on the Rights of Persons with Disabilities*. [Online]. Available: <http://www.un.org/disabilities/default.asp?id=23>
- [5] D. J. Reinkensmeyer, L. E. Kahn, M. Averbuch, A. McKenna-Cole, B. D. Schmit, and W. Z. Rymer, "Understanding and Treating Arm Movement Impairment after Chronic Brain Injury: Progress with the Arm Guide," *Journal of Rehabilitation Research and Development*, vol. 37, no. 6, pp. 653-662, 2000.
- [6] R. S. Mosher and B. Wendel, "Force-Reflecting Electrohydraulic Servomanipulator," *Electro-Tech.*, vol. 66, pp. 138-141, 1960.
- [7] W. Cloud, "Man Amplifiers: Machines that Let You Carry a Ton," *Popular Science*, vol. 187, no. 5, pp. 70-73, 1965.
- [8] R. S. Mosher, "Handyman to Hardiman," *Society of Automotive Engineers Publication*, SAE 670088, 1967.
- [9] V. L. Nickel, A. Karchak Jr., and J. R. Allen, "Electrically Powered Orthotic Systems," *Journal of Bone Joint Surgery Am.*, vol. 51, pp. 343-351, 1969.
- [10] G. Schmeisser and W. Seamone, "An Upper Limb Prosthesis-Orthosis Power and Control System with Multi-Level Potential," *Journal of Bone Joint Surgery Am.*, vol. 55, pp. 1493-1501, 1973.
- [11] M. Vukobratovic, "Legged Locomotion Robots and Anthropomorphic Mechanisms," *Mihailo Pupin Institute*, Belgrade, 1975.
- [12] N. Benjuya and S. B. Kenney, "Hybrid Arm Orthosis," *Journal of Prosthetics Orthotics*, vol. 2, no. 2, pp. 155-163, 1990.
- [13] G. Burdea, E. Roskos, D. Silver, R. Stone, and D. Dipaolo, "Diagnostic/Rehabilitation System using Force Measuring and Force Feedback Dexterous Masters," in *Proc. of Fifth Medicine Meets Virtual Reality Conference*, San Diego, CA, USA, 1992, pp. 18-10.

- [14] G. Burdea, J. Zhuang, E. Roskos, D. Silver, and N. Langrana, "A Portable Dexterous Master with Force Feedback," *Teleoperators and Virtual Environments*, vol. 1, no. 1, pp. 18-28, 1992.
- [15] D. Gomez, G. Burdea, and N. Langrana, "The Second Generation Rutgers Master- RMII," in *Proc. of Automation Conference*, Taipei, Taiwan, 1994, pp. 7-10.
- [16] H. Kazerooni and S. L. Mahoney, "Dynamics and Control of Robotic Systems Worn by Humans," *ASME Journal of Dynamic System, Measurement Control*, vol. 113, no. 3, pp. 379-387, 1991.
- [17] F. H. Martini, M. J. Timmons, and R. B. Tallitsch, *Human Anatomy*, Prentice Hall, Pearson Education, Inc, 2003, ch. 8.
- [18] V.M. Zatsiorsky, *Kinematics of Human Motion*, Human Kinetics, 1998, ch 5.
- [19] K. N. An and E. Y. Chao, "Kinematic Analysis of Human Movement," *Annals Biomedical Engineering*, vol. 12, pp. 585-597, 1984.
- [20] E. Engin, "On the Biomechanics of the Shoulder Complex," *Journal of Biomechanics*, vol. 13, pp. 575-590, 1980.
- [21] J. T. London, "Kinematics of the Elbow," *Journal of Bone and Joint Surgery*, vol. 63-A, pp. 529-535, 1981.
- [22] J. G. Andrews and Y. Youm, "A Biomedical Investigation of Wrist Kinematics," *Journal of Biomechanics*, vol. 12, pp. 83-93, 1979.
- [23] C. P. Neu, J. J. Crisco, and S. W. Wolfe, "In Vivo Kinematic Behavior of the Radio-Capitate Joint during Wrist Flexion-Extension and Radio-Ulnar Deviation," *Journal of Biomechanics*, vol. 34, pp. 1429-1438, 2001.
- [24] Y. Youm, R. Y. McMurthy, A. E. Flatt, and T. E. Gillespie, "Kinematics of the Wrist.
I. An Experimental Study of Radial-Ulnar Deviation and Flexion-Extension," *Journal of Bone and Joint Surgery*, vol. 60, pp. 423-431, 1978.
- [25] B. D. Ferris, J. Stanton, and J. Zamora, "Kinematics of the Wrist-Evidence for two Types of Movement," *Journal of Bone and Joint Surgery (Br)*, vol. 82-B, no. 2, pp. 242-245, 2000.
- [26] Y. Youm, "Design of a Total Wrist Prosthesis," *Annals of Biomedical Engineering*, vol. 12, pp. 247-262, 1984.
- [27] B. Buchholz, T. J. Armstrong, and S. A. Goldstein, "Anthropometric Data for Describing the Kinematics of the Human Hand," *Ergonomics*, vol. 35, pp. 261-273, 1992.
- [28] J. M. F. Landsmeer, "Anatomical and Functional Investigations on the Articulation of the Human Fingers," *Acta Anatomica*, vol. 25, pp. 1-69, 1955.
- [29] J. T. Barmakian, "Anatomy of the Joints of the Thumb," *Hand Clinics*, vol. 8, pp. 683-691, 1992.
- [30] A. M. Hollister, W. L. Buford, L. M. Myers, D. J. Giurintano, and A. Novick, "The Axes of Rotation of the Thumb Carpometacarpal Joint," *Journal of Orthopedics Research*, vol. 10-B, pp. 454-460, 1992.

- [31] K. Kiguchi, K. Iwami, M. Yasuda, K. Watanabe, and T. Fukuda, "An Exoskeletal Robot for Human Shoulder Joint Motion Assist," *IEEE/ASME Transaction on Mechatronics*, vol. 8, no. 1, pp. 125-135, 2003.
- [32] K. Kiguchi, S. Kariya, K. Watanabe, K. Izumi, and T. Fukuda, "An Exoskeletal Robot for Human Elbow Motion Support-Sensor Fusion, Adaptation, and Control," *IEEE Transaction on System Man Cybernetics. B*, vol. 31, no. 3, pp. 353-361, 2001.
- [33] K. Kiguchi, R. Esaki, and T. Fukuda, "Development of a Wearable Exoskeleton for Daily Forearm Motion Assist," *Advanced Robotics*, vol. 19, no. 7, pp. 751-771, 2005.
- [34] K. Kiguchi, "Active Exoskeletons for Upper-Limb Motion Assist," *Journal of Humanoid Robotics*, vol. 4, no. 3, pp. 607-624, 2007.
- [35] K. Kiguchi, T. Yamaguchi, and M. Sasaki, "Development of a 4DOF Exoskeleton Robot for Upper-Limb Motion Assist," in *Proc. of ASME/JSME Joint Conference on Micromechatronics for Information and Precision Equipment*, Santa Clara, USA, 2005, S10 03.
- [36] K. Kiguchi, M. H. Rahman, M. Sasaki, and K. Teramoto, "Development of a 3DOF Mobile Exoskeleton Robot for Human Upper Limb Motion Assist," *Robotics and Autonomous Systems*, vol. 56, no. 8, pp. 678-691, 2008.
- [37] R. A. R. C. Gopura and K. Kiguchi, "Development of a 6DOF Exoskeleton Robot for Human Upper-Limb Motion Assist," in *Proc. of IEEE International Conference on Information and Automation for Sustainability*, Colombo, Sri Lanka, 2008, pp. 13-18.
- [38] E. Papadopoulos and G. Patsianis, "Design of an Exoskeleton Mechanism for the Shoulder Joint," in *Proc. of Twelfth World Congress in Mechanism and Machine Science*, Besancon, France, 2007. pp. 1-6.
- [39] M. Mulas, M. Folgheraiter, and G. Gini, "An EMG-Controlled Exoskeleton for Hand Rehabilitation," in *Proc. of International Conference on Rehabilitation Robotics*, 2005, pp. 371-374.
- [40] L. Lucas, M. DiCicco, and Y. Matsuoka, "An EMG-Controlled Hand Exoskeleton for Natural Pinching," *Journal of Robotics and Mechatronics*, vol. 16-B, no 5, pp. 482-488, 2004.
- [41] D. Sasaki, T. Noritsugu, and M. Takaiwa, "Development of Active Support Splint Driven by Pneumatic Soft Actuator (ASSIST)," *Journal Robotics and Mechatronics*, vol. 16, pp. 497-502, 2004.
- [42] T. Noritsugu, D. Sasaki, H. Yamamoto, and M. Takaiwa, "Wearable Power Assist Device for Hand Grasping Using Pneumatic Artificial Rubber Muscle," in *Proc. SICE Annual Conference in Sapporo*, Hokkaido, Japan, 2004, pp. 420-425.
- [43] N. G. Tsagarakis and D. C. Caldwell, "Development and Control of a 'Soft-Actuated' Exoskeleton for Use in Physiotherapy and Training," *Journal of Autonomous Robots*, vol. 15, pp. 21-33, 2003.
- [44] J. C. Perry and J. Rosen, "Upper-Limb Powered Exoskeleton," *Journal of Humanoid Robotics*, vol. 4, no. 3, pp. 529-548, 2007.

- [45] J. C. Perry, J. Rosen, and S. Burns, "Upper-Limb Powered Exoskeleton Design," *IEEE/ASME Transaction on Mechatronics*, vol. 12, no. 4, pp. 408-417, 2007.
- [46] H. Kawasaki, S. Ito, Y. Ishigure, Y. Nishimoto, T. Aoki, T. Mouri, H. Sakaeda, and M. Abe, "Development of a Hand Motion Assist Robot for Rehabilitation Therapy by Patient Self-Motion Control," in *Proc. IEEE International Conference on Rehabilitation Robotics*, Noordwijk, The Netherlands, 2007, pp. 234-240.
- [47] M. Mistry, P. Mohajerian, and S. Schaal, "An Exoskeleton Robot for Human Arm Movement Study," in *Proc. of IEEE/RSJ International Conference on Intelligent Robots and Systems*, Alberto, Canada, 2005, pp. 4071- 4076.
- [48] S. Lee, S. Park, M. Kim, and C. W. Lee, "Design of a Force Reflecting Master Arm and Master Hand using Pneumatic Actuators," in *Proc. of IEEE International Conference on Robotics and Automation*, Leuven, Belgium, 1998, pp.2574-2579.
- [49] J. Rosen, N. Brand, M. B. Fuchs, and M. Arcan, "A Myosignal-Based Powered Ex- oskeleton System," *IEEE Transaction on System Man Cybernetics A*, vol. 31, no. 3, pp. 210-222, 2001.
- [50] A. Gupta and M. K. O'Malley, "Design of a haptic arm exoskeleton for training and rehabilitation," *IEEE/ASME Transaction Mechatronics*, vol. 11, pp. 280-289, 2006.
- [51] A. Sledd and M. K. O'Malley, "Performance Enhancement of a Haptic Arm Ex- oskeleton," in *Proc. of IEEE Symposium on Haptic Interfaces for Virtual Environ- ment and Teleoperator Systems*, Virginia, USA, 2006, pp. 375-381.
- [52] A. Frisoli, F. Rocchi, S. Marcheschi, A. Dettori, F. Salsedo, and M. Bergamasco, "A New Force-Feedback Arm Exoskeleton for Haptic Interaction in Virtual Envi- ronments," in *Proc. of First Eurohaptics Conference and Symposium on Haptic In- terfaces for Virtual Environment and Teleoperator Systems*, Pisa, Italy, 2005, pp. 195-201.
- [53] A. Frisoli, L. Borelli, A. Montagner, S. Marcheschi, C. Procopio, F. Salsedo, M. Bergamasco, M. C. Carboncini, M. Tolaini, and B. Rossi, "Arm rehabilitation with a robotic exoskeleton in Virtual Reality," in *Proc. of International Conference on Rehabilitation Robotics*, Noordwijk, The Netherlands, 2007, pp. 631-642.
- [54] T. Nef, M. Mihelj, G. Colombo, and R. Riener, "ARMin-Robot for Rehabilitation of the Upper Extremities," in *Proc. of IEEE International Conference on Robotics and Automation*, Orlando, USA, 2006, pp. 3152-3157.
- [55] T. Nef and R. Riener, "ARMin-Design of a Novel Arm Rehabilitation Robot," in *Proc. of IEEE International Conference on Rehabilitation Robotics*, Chicago, USA, 2005, pp. 57-60.

- [56] M. Mihelj, T. Nef, and R. Riener, "ARMin II-7 DOF Rehabilitation Robot: Mechanism and Kinematics," in *Proc. of IEEE International Conference on Robotics and Automation*, Roma, Italy, 2007, pp. 4120-4125.
- [57] J. L. Pons, E. Rocon, A. F. Ruiz, and J. C. Moreno, "Upper-Limb Robotic Rehabilitation Exoskeleton: Tremor Suppression," *Rehabilitation Robotics*, Book edited by S. S. Kommu, pp. 453-470, 2007.
- [58] A. F. Ruiz, A. Forner-Codrero, E. Rocon, and J. L. Pons, "Exoskeleton for Rehabilitation and Motor Control," in *Proc. of IEEE International Conference on Biorobotics and Biomechanics*, Pisa, Italy, 2006, pp. 601-606.
- [59] G. R. Johnson, D. A. Carus, G. Parrini, S. Scattareggia Marchese and R. Valeggi, "The Design of a Five-Degree-of-Freedom Powered Orthosis for the Upper Limb," in *Proc. of the Institution of Mechanical Engineers Part H-Journal of Engineering in Medicine*, vol. 215, no. 3, pp. 276-284, 2001.
- [60] I. Sarakoglou, N. G. Tsagarakis, and D. G. Caldwell, "Occupational and Physical Therapy Using A Hand Exoskeleton Based Exerciser," in *Proc. of IEEE International Conference on Intelligent Robots and Systems*, Sendai, Japan, 2004, pp. 2973-2978.
- [61] C. D. Takahashi, L. Der-Yeghiaian, V. Le, R. R. Motiwala, and S. C. Cramer, "Robot-Based Hand Motor Therapy after Stroke," *Brain*, vol. 131, no. 2, pp. 425-437, 2008.
- [62] A. Wege and G. Hommel, "Development and Control of a Hand Exoskeleton for Rehabilitation of Hand Injuries," in *Proc. of IEEE/RSJ International Conference on Intelligent Robots and Systems*, Alberto, Canada, 2005, pp. 3046-3051.
- [63] I. Kawabuchi, "A Designing of Humanoid Robot Hands in Endo skeleton and Exoskeleton Styles," *Humanoid Robots, New Developments*, Book edited by Armando Carlos de Pina Filho, pp. 401-426, 2007.
- [64] J. He, E. J. Koeneman, R. S. Schultz, H. Huang, J. Wanberg, D. E. Herring, T. Sugar, R. Herman, and J. B. Koeneman, "Design of a Robotic Upper Extremity Repetitive Therapy Device," in *Proc. of IEEE International Conference on Rehabilitation Robotics*, Chicago, USA, 2005, pp. 95-98.
- [65] C. Carignan, M. Liszka, and S. Roderick, "Design of an Arm Exoskeleton with Scapula Motion for Shoulder Rehabilitation," in *Proc. of International Conference on Advanced Robotics*, Seattle, USA, 2005, pp. 524-531.
- [66] S. J. Ball, I. E. Brown, and S. H. Scott, "A planar 3DOF robotic exoskeleton for rehabilitation and assessment," in *Proc. of IEEE International Conference on Engineering in Medicine and Biology Society*, Lyon, France, 2007, pp. 4024-4027.
- [67] S. J. Ball, I. E. Brown, and S. H. Scott, "MEDARM: A rehabilitation robot with 5DOF at the shoulder complex," in *Proc. of IEEE/ASME International Conference on Advanced Intelligent Mechatronics*, Zurich, Switzerland, 2007, pp. 1-6.
- [68] S. J. Ball, I. E. Brown, and S. H. Scott, "Designing a robotic exoskeleton for shoulder complex rehabilitation," in *Proc. of Canadian Medical and Biological Engineering Conference*, Toronto, Canada, 2007.

- [69] H. Kobayashi and K. Hiramatsu, "Development of Muscle Suit for Upper Limb," in *Proc. of IEEE International Conference on Robotics and Automation*, New Orleans, USA, 2004, pp. 2480-2485.
- [70] T. G. Sugar, J. He, E. J. Koeneman, J. B. Koeneman, R. Herman, H. Huang, R. S. Schultz, D. E. Herring, J. Wanberg, S. Balasubramanian, P. Swenson, and J. A. Ward, "Design and Control of RUPERT: A Device for Robotic Upper Extremity Repetitive Therapy," *IEEE Transaction on Neural Systems and Rehabilitation Engineering*, vol. 15, Issue 3, pp. 336-346, 2007.
- [71] J. He, E. J. Koeneman, R. S. Schultz, D. E. Herring, J. Wanberg, H. Huang, T. Sugar, R. Herman, and J. B. Koeneman, "RUPERT: a Device for Robotic Upper Extremity Repetitive Therapy," in *Proc. of IEEE/EMBS International Conference of Engineering in Medicine and Biology Society*, Shanghai, China 2005, pp. 6844-6847.
- [72] W. Chou, T. Wang, and J. Xiao, "Haptic Interaction with Virtual Environment using an Arm type Exoskeleton Device," in *Proc. of IEEE International Conference on Robotics and Automation*, New Orleans, USA, 2004, pp. 243-247.
- [73] G. Yang, H. L. Ho, W. Chen, W. Lin, S. H. Yeo, and M. S. Kurbanhusen, "A Haptic Device Wearable on a Human Arm," in *Proc. of IEEE Conference on Robotics, Automation and Mechatronics*, Singapore, 2004, pp. 243-247.
- [74] M. Bouzit, G. Popescu, G. Burdea, and R. Boian, "The Rutgers Master II-ND Force Feedback Glove," in *Proc. of VR Haptics Symposium*, Orlando, USA, 2002, pp. 145-152.
- [75] S. Adamovich, A. Merians, R. Boian, M. Tremaine, G. Burdea, M. Recce, and H. Poizner, "A Virtual Reality Based Exercise System for Hand Rehabilitation Post-Stroke," *Special Issue on Virtual Rehabilitation*, vol. 14, no. 2, pp. 161-174, 2005.
- [76] D. Jack, R. Boian, A. S. Merians, M. Tremaine, G. C. Burdea, S. V. Adamovich, M. Recce, and H. Poizner, "Virtual Reality-Enhanced Stroke Rehabilitation," *IEEE Transaction on Neural Systems and Rehabilitation Engineering*, vol. 9, no. 3, pp. 308-318, 2001.
- [77] K. Nagai, I. Nakanishi, H. Hanafusa, S. Kawamura, M. Makikawa, and N. Tejima, "Development of an 8DOF Robotic Orthosis for Assisting Human Upper Limb Motion," in *Proc. of IEEE International Conference on Robotics and Automation*, Leuven, Belgium, 1998, pp. 4386-4391.
- [78] A. Nakai, T. Ohashi, and H. Hashimoto, "7DOF Arm Type Haptic Interface for Teleoperation and Virtual Reality Systems," in *Proc. of IEEE/RSJ International Conference on Intelligent Robots and Systems*, Victoria, Canada, 1998, pp. 1266-1271.
- [79] (2009, Feb. 05). Hand Mentor. [Online]. Available: <http://www.handmentor.com/index.php?id=32>
- [80] E. Rocon, A. F. Ruiz, J. L. Pons, J. M. Belda-Lois, and J. J. Sanchez-Lacuesta, "Rehabilitation Robotics: A Wearable Exoskeleton for Tremor Assessment and Suppression," in *Proc. of IEEE International Conference on Robotics and Automation*, Barcelona, Spain, 2005, pp. 241-246.

- [81] I. Sardellitti, E. Cattin, S. Roccella, F. Vecchi, M. C. Carrozza, P. Dario, P. K. Artemiadis, and K. J. Kyriakopoulos, "Description, Characterization and Assessment of a BioInspired Shoulder Joint-First Link Robot for NeuroRobotic Applications," *IEEE/RAS-EMBS International Conference on Biomedical Robotics and Biomechanics*, Pisa, Italy, 2006, pp. 112-117.
- [82] E. Guizzo and H. Goldstein, "The rise of the body bots," *IEEE Spectrum*, vol. 42, no. 10, pp. 42-48, 2005.
- [83] C. J. Yang, J. F. Zang, Y. Chen, Y. M. Dong, and Y. Zhang, "A Review of Exoskeleton-Type Systems and Their Key Technologies," *Journal of Mechanical Engineering Science C*, vol. 222, pp. 1599-1612, 2008.
- [84] K. A. Farry, I. D. Walker, and R.G. Baraniuk, "Myoelectric Teleoperation of a Complex Robotic Hand," *IEEE Transaction on Robotics and Automation*, vol. 12, no. 5, pp.775-788, 1996.
- [85] O. Fukuda, T. Tsuji, A. Ohtsuka, and M. Kaneko, "EMG based Human-Robot Interface for Rehabilitation Aid," in *Proc. of IEEE International Conference on Robotics and Automation*, Leuven, Belgium, 1998, pp. 3942-3947.
- [86] D. Nishikawa, W. Yu, H. Yokoi, and Y. Kakazu, "EMG Prosthetic Hand Controller using Real-time Learning Method," in *Proc. of IEEE International Conference on Systems, Man, and Cybernetics*, Tokyo, Japan, 1999, pp.I-153-158.
- [87] K. Kiguchi, M. H. Rahaman, and M. Sasaki, "Neuro-Fuzzy based Motion Control of a Robotic Exoskeleton: Considering End-effector Force Vectors," in *Proc. of IEEE International Conference on Robotics and Automation*, Orlando, USA, 2006, pp. 3146-3151.
- [88] K. Kiguchi, T. Tanaka, and T. Fukuda, "Neuro-Fuzzy Control of a Robotic Exoskeleton with EMG Signals," *IEEE Transaction on Fuzzy System*, vol. 12, no. 4, pp. 481- 490, 2004.
- [89] K. Kiguchi, Y. Imada, and M. Liyanage, "EMG-Based Neuro-Fuzzy Control of a 4DOF Upper-Limb Power-Assist Exoskeleton," in *Proc. of International Conference of the IEEE Engineering in Medicine and Biology Society*, Lyon, France, 2007, pp. 3040-3043.
- [90] K. Kiguchi, S. Kariya, K. Watanabe, and T. Fukuda, "Application of Multiple Neuro-Fuzzy Controllers of an Exoskeletal Robot for Human Elbow Motion Support," *Transaction on Control, Automation and System Engineering*, vol. 4, no. 1, pp. 49-55, 2002.
- [91] K. Kiguchi and T. Fukuda, "A 3DOF Exoskeleton for Upper-Limb Motion - Consideration of the Effect of Bi-Articular Muscles," in *Proc. of International Conference of the IEEE Engineering in Medicine and Biology Society*, New Orleans, LA, USA, 2004, pp. 2424-2429.
- [92] K. Kiguchi and Q. Quan, "Muscle-Model-Oriented EMG-Based Control of an Upper-limb Power-Assist Exoskeleton with a Neuro-Fuzzy Modifier," in *Proc. of IEEE World Congress of Computational Intelligence*, Hong Kong, 2008, pp. 1179- 1184.

- [93] D. S. Andreasen, S. K. Allen, and D. A. Backus, "Exoskeleton with EMG Based Active Assistance for Rehabilitation," in *Proc. of IEEE International Conference on Rehabilitation Robotics*, Chicago, IL, USA, 2005, pp. 333-336.
- [94] E. Cavallaro, J. Rosen, J. C. Perry, and S. Burns, "Real-Time Myoprocessors for a Neural Controlled Powered Exoskeleton Arm," *IEEE Transactions on Biomedical Engineering*, vol. 53, no. 11, pp. 2387-2396, 2006.
- [95] M. A. Oskoei and H. Hu, "Myoelectric Control Systems-A Survey," *Biomedical Signal Processing and Control*, vol. 2, pp. 275-294, 2007. M. A. Oskoei and H. Hu, "Myoelectric Control Systems-A Survey," *Biomedical Signal Processing and Control*, vol. 2, pp. 275-294, 2007.
- [96] S. Lee and Y. Sankai, "Virtual Impedance Adjustment in Unconstrained Motion for an Exoskeletal Robot Assisting the Lower limb," *Advanced Robotics*, vol. 19, no. 7, pp. 773-795, 2005.
- [97] H. Kawamoto and Y. Sankai, "Power Assist Method Based on Phase Sequence and Muscle Force Condition for HAL," *Advanced Robotics*, vol. 19, no. 7, pp. 717-734, 2005.
- [98] H. Kazerooni, J. L. Racinea, L. Huang, and R. Steger, "On the Control of the Berkley Lower Extremity Exoskeleton (BLEEX)," in *Proc. of IEEE International Conference on Robotics and Automation*, Barcelona, Spain, 2005, pp. 4353-4360.
- [99] H. Kawamoto, S. Lee, S. Kanbe, and Y. Sankai, "Power Assist Method for HAL-3 Using EMG-Based Feedback Controller," in *Proc. of IEEE International Conference on Systems, Man and Cybernetics*, Washington, DC, USA, 2003, pp. 1648-1653.

APPENDIX

(PUBLICATION)

PAPER • OPEN ACCESS

Preliminary Study on Muscle Force Estimation using Musculoskeletal Model for Upper Limb Rehabilitation with Assistive Device for Home Setting

To cite this article: Muhamad Fadzli *et al* 2019 *J. Phys.: Conf. Ser.* **1372** 012023

View the [article online](#) for updates and enhancements.

You may also like

- [Muscle Activity and Gait Analysis of Assistive Device for Rehabilitation Gait Abnormalities Patient](#)
Ruzy Haryati Hambali, Suriati Akmal and Nurul Hamizan Komaruddin
- [A biarticular passive exosuit to support balance control can reduce metabolic cost of walking](#)
Hamid Barazesh and Maziar Ahmad Sharbafi
- [From a biological template model to gait assistance with an exosuit](#)
Vahid Firouzi, Ayoob Davoodi, Fariba Bahrami et al.



ECS The Electrochemical Society
Advancing solid state & electrochemical science & technology

242nd ECS Meeting

Oct 9 – 13, 2022 • Atlanta, GA, US

Early hotel & registration pricing ends September 12

Presenting more than 2,400 technical abstracts in 50 symposia

The meeting for industry & researchers in
BATTERIES
ENERGY TECHNOLOGY
SENSORS AND MORE!

 Register now!

  **ECS Plenary Lecture featuring M. Stanley Whittingham,**
Binghamton University
Nobel Laureate –
2019 Nobel Prize in Chemistry



Preliminary Study on Muscle Force Estimation using Musculoskeletal Model for Upper Limb Rehabilitation with Assistive Device for Home Setting.

Muhamad Fadzli⁽¹⁾, Akihiko Hanafusa⁽¹⁾, Yuji Kubota⁽¹⁾ and Daigo Nishimori⁽¹⁾

¹ Department of Bio-science and Engineering, Shibaura Institute of Technology, 307 Fukasaku, Minuma-ku, Saitama 337-8570, Japan

nb18110@shibaura-it.ac.jp

Abstract. Post-stroke rehabilitation using assistive device has the potential to cover the need for improvement of the upper limb functionality. Moreover, using a biomechanical model to estimate the muscle activity during the rehabilitation training could improve the training module as well as help understand the target muscle during the motion of body part while using the assistive device. In this study, the author has focused on using a musculoskeletal model of the right arm to estimate the individual muscle force by simulating the movement of the right arm while using the developed assistive device. A developed upper limb assistive device has been investigated for its potential as a rehabilitation device for persons with physical disability of upper limb motion. The muscle force estimation is based on an inverse dynamic method, improved with additional constraints of the joints in order to obtain the muscle's activity from motion capture data. The acquired muscle force data could be used to improve the arm assistive device in rehabilitation training for home setting purpose.

1. Introduction

The number of stroke survivors in this world is quite large, and most of these survivors experience impairment impact on the upper limb function [1]. Patients who suffer from the upper limb impairment usually have difficulty performing daily activities that require using the upper limb, such as feeding, washing, etc. Some patients may recover some functionality of the upper limb function following the rehabilitation. However, most of the high technology assistive device are placed at the rehabilitation centre and must be operated with the help and observation of the therapists. Recently, wearable assistive devices have also started to play an important role as a rehabilitation device [2–4]. The needs of the assistive device and its cost effective and user friendly nature could help patients with rehabilitation training at home. The lack of the need for a therapist number is an added advantage, thus demanding the assistive device to be robust and easy to handle. The development and improvement of the assistive device need to come together with an understanding of the muscle force and muscle activation of the target muscle during the rehabilitation training.

Presently, three main approaches i.e., assessment scales, movement evaluation, and surface electromyography (sEMG) analysis are widely applied to evaluate the upper extremities. As these assessments are mainly viewed and scored by the therapist, the evaluation results are often subjective and general. The movement evaluation method using the motion capture systems can provide data on the physical movement of the upper limb, which can then be used for monitoring the progress of the



rehabilitation. However, this method cannot account for muscle characteristics in patients, and the neurological mechanism used to overcome the problems associated with their pathology is also still unknown. Although all these methods are useful in the assessment of upper limb function, they are still inadequate for quantitative evaluation due to the lack of deep muscle's activation information and noise contamination from the movement artefact. Moreover, a direct interaction with the subject is needed in order to gain the information, and this could be a limitation based on the patient's condition, time consumed to setup the system and the cost for the actual test involving many equipment and subjects.

Given this, this study presents a method using a musculoskeletal model focusing on the upper limb to predict muscle force during the elbow flexion with the assistive device. Individual muscle force was investigated during the movement of the elbow flexion with the healthy subject using the assistive device and the results were compared with those of the one not using any assistive device. Through this approach, the specific functional muscle involved during the movement can be known, making it possible to conduct improvement in the assistive device for rehabilitation training purpose. A brief flowchart of the proposed muscle force estimation is shown in figure 1.

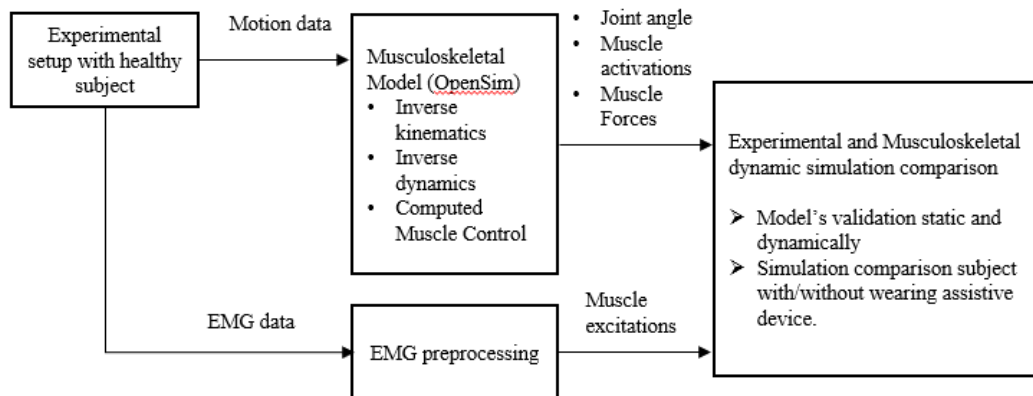


Figure 1: Flowchart of proposed muscle force prediction using musculoskeletal model.

2. Method

In order to study the muscle force based on the given motion data, a musculoskeletal model from the musculoskeletal software, OpenSim [7] was utilized. A suitable pre-existing musculoskeletal model has been used and scaled to match the marker data. Then the model is validated dynamically by comparing the muscle force estimated from simulation and EMG data from the experiment. Finally, an experiment is performed on a healthy subject with assistive device and the result is compared with the simulation data for the same motion.

2.1. Data Acquisition and Experimental Setup for Musculoskeletal Model Validation

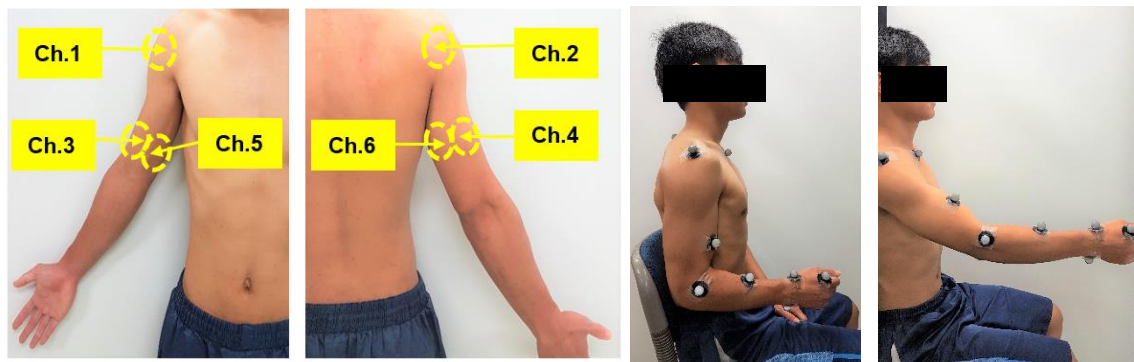
2.1.1. Electromyogram (EMG) & Motion Capture Data Recording.

A healthy subject volunteered for this investigation and gave their informed, written consent. The project was approved by the Human Research Ethics committee at the Shibaura Institute of Technology (SIT), Japan. The subject was quietly seated in the chair with their torso kept upright and their right hand keeping at close to a 90-degree elbow flexion. The reach forward motion is designed to obtain motion of the right upper limb. The motion simulated the elbow flexion from 90 degree to forward reaching and return to initial position. The same motion was repeated three times to get three sets of data. The configuration of the EMG recording and marker placement for motion capture system is shown in figure 2. Motion data was acquired using the Mac3D system available in our laboratory. This equipment consists of 10 infrared cameras that are able to capture the 3D position of the different markers over

time. During the motion recording, 10 markers were used at specific positions together with marker clusters according to the recommendation on definitions of joint coordinate systems [6].

Six predominant muscles at upper arm activating elbow DoFs were selected to be the muscle of test, as shown in figure 2 (a) and (b). Six channels of bipolar differential amplifier were carefully placed on these muscles based on both the anatomy and hand touch experience. The active EMG electrodes of each channel were positioned at the muscle belly. The skin underneath the electrodes was cleaned with alcohol patch to reduce the resistance between the skin and the electrodes. The motion recording was sampled at 200 Hz and synchronized with the EMG recording through the motion capture system.

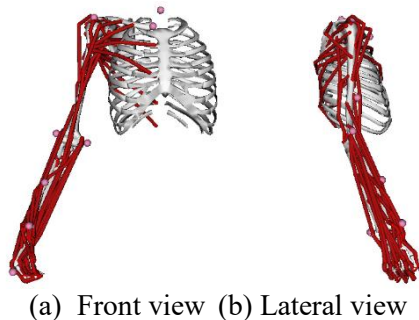
Ch.1: Deltoid (anterior part) Ch.4: Triceps (lateral head)
 Ch.2: Deltoid (posterior part) Ch.5: Biceps (short head)
 Ch.3: Biceps (long head) Ch.6: Triceps (long head)



(a) 3 channels (front) (b) 3 channels (back) (c) initial position (d) reach forward motion
Figure 2: The configuration of 6 channels EMG electrodes for upper arm (a) and (b), and a healthy subject performing the reach forward movement is shown in (c) and (d).

2.1.2. Joint angle estimation, Joint torque, and Muscle Force Estimation using OpenSim

Delp et al. [5] have developed an open source platform called OpenSim. This platform allows the dynamic simulation on the musculoskeletal system using provided motion capture data. These simulations use inverse kinematics method to obtain kinematics data such as joint angle of each joint during the movement, which is later used in inverse dynamic simulations to obtain the joint moments. Then, an original algorithm, called Computed Muscle Control (CMC), based on inverse dynamics method is used to compute the muscle forces allowed to obtain the muscle excitation. An upper limb model for the right hand is available in this platform. It has realistic movements and precise muscular topology for the joints. This study utilizes the CMC to validate the OpenSim Model. Then the same approach is used to study the active muscle in the human musculoskeletal model during the motion of the upper arm.



(a) Front view (b) Lateral view
Figure 3: OpenSim upper limb musculoskeletal model. This model was developed by Saul KR [7]. It consists of 7 body segments and 32 muscles across the shoulder, elbow, forearm, and wrist.

2.1.3. Validation Result

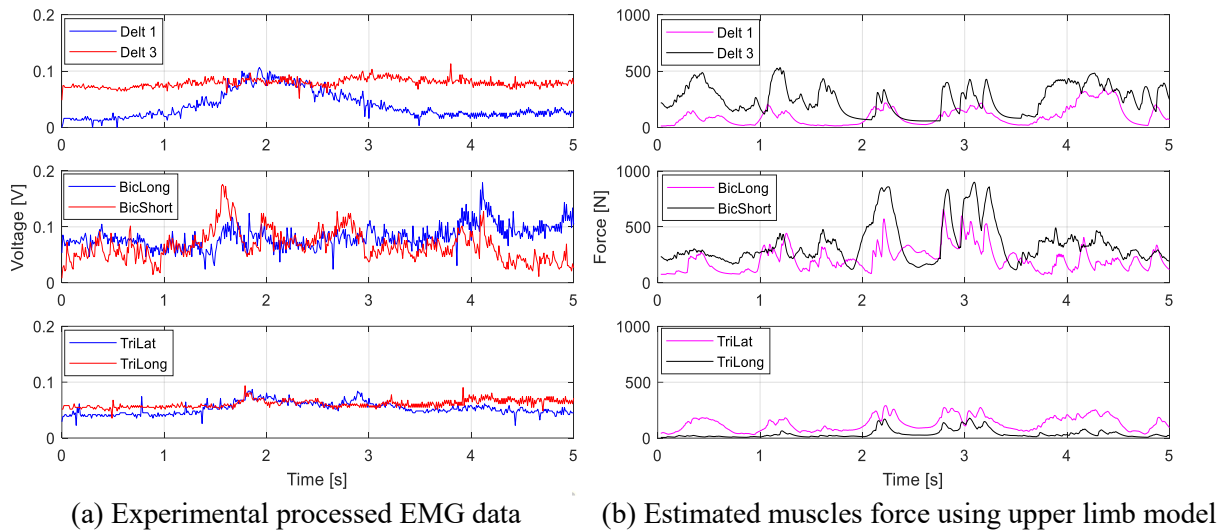


Figure 4: Experimental muscle excitation and estimated muscle forces for the same reach forward motion.

As mention in section 2.1.1, we selected deltoid anterior part (Delt 1), deltoid posterior part (Delt 3), short head of biceps (BicShort), long head of biceps (BicLong), long head of triceps (TriLong), and lateral head of triceps (TriLat) as 6 muscles of interests. Figure 4 (a) shows the processed EMG data for the muscles taken during the experiment and estimated muscle forces shown in figure 4 (b) from the simulation of the musculoskeletal model. By adopting a neural mapping method [10], we assumed that BicShort has the same activation as BicLong and other two heads of triceps have the same activation. We can see in both experimental EMG data and estimated muscle forces from simulation shows that the Biceps muscles are working during the motion and presents the main activity. On the other hand, the triceps muscle does not show big activity due to its minor role in joint motion. We also can see that the pattern of the most muscle forces (Biceps and Triceps) shows similarity with the recorded EMG pattern. The similarity agreement between the recorded EMG data and the estimated muscle forces for the same motion shows that this model is acceptable to predict muscle activity for upper limb right hand motion.

2.2. Experiment with Assistive Device and Simulation with Musculoskeletal Model

2.2.1. Assistive Device, Experiment & Simulation Protocol

A lightweight assistive device [8], which is wire-driven by 2 servo motors was developed. The device can generate the motions of elbow flexion/extension movement and internal/external rotation movement, performed by pulling the wire hung on a pulley connected to the wrist part. During the experiment, the subjects were standing with their torso kept upright and their right hand kept relaxed. One motion designed had the elbow flexion from the natural position to close to a 100 degree. Two separate motions have been designed where the subject performed the motions with and without the assistive device. Then the same motion was simulated using the musculoskeletal model in OpenSim. The marker data taken is produced using the Motion Capture 3D system available in our laboratory. A torque of 4Nm is applied to the musculoskeletal model, simulating the model with assistive device to achieve the same flexion motion close to 90 degree. A target muscle, which is the bicep (short), is investigated for muscle activity.

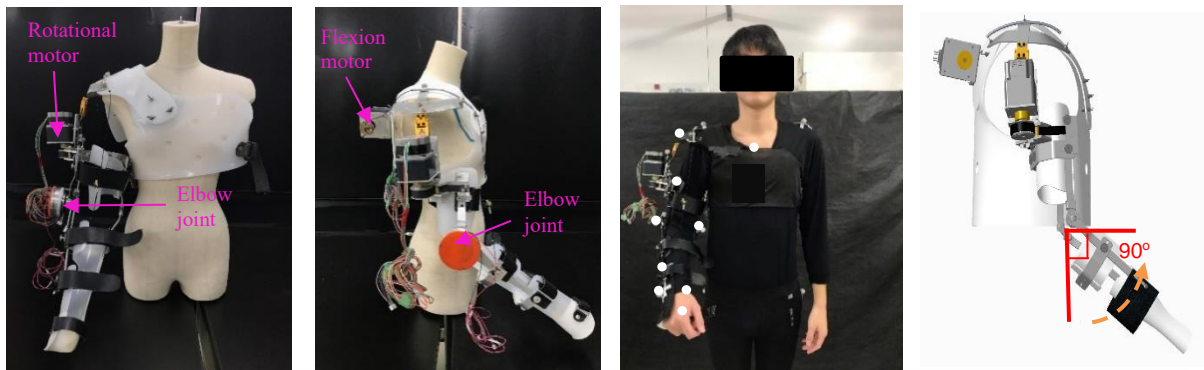


Figure 5: Upper limb right hand assistive device and subject wearing the device performing motion of elbow flexion close to 90 degree.

3. Results and Discussion

The purpose of the current work is to study the muscle activation estimation method via musculoskeletal model when using upper limb assistive device. The muscle estimation was evaluated by simulating the musculoskeletal model using the motion data provided through the experiment of the subject wearing and without wearing the developed assistive device. Figure 6 (a) shows the measured EMG data signal processed with 1Hz cut off low pass filter and figure 6 (b) shows the estimation of the muscle force of the target muscle during the elbow flexion of one subject using and without using the assistive device.

As can be seen from figure 6, the pattern of the muscle force estimation using the musculoskeletal model shows good agreement with the experimental muscle excitation (EMG) pattern. The most significant difference can be observed by magnitude of the muscle activation without device, which is slightly higher when compared to the muscle with assistive movement. Even though it is normal for the assistive part to produce less muscle activities, our proposed estimation method proven can be used and it will be possible for us to get a deeper understanding of the human dynamic movement mechanism while using an assistive device for rehabilitation purpose.

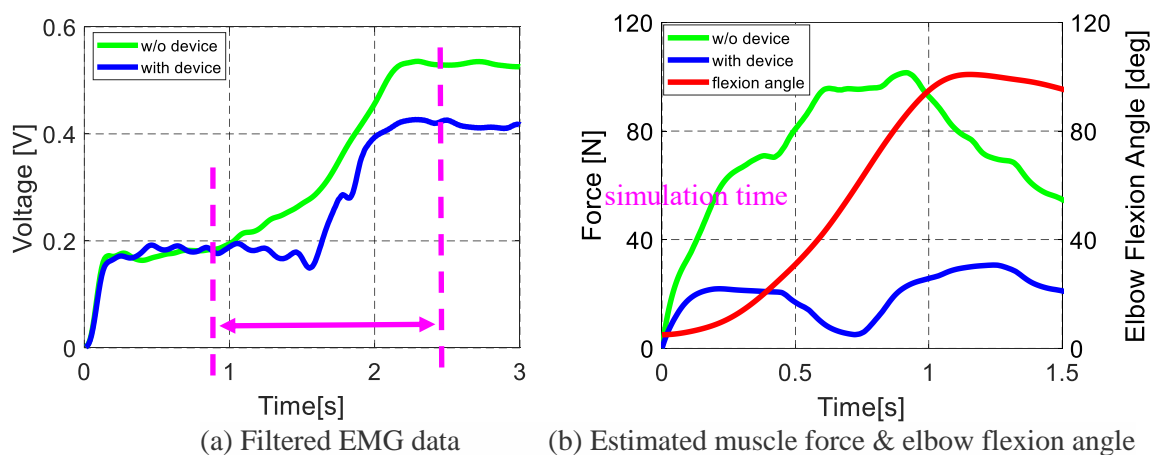


Figure 6: EMG data from experimental and estimated muscle force from simulation for the subject wearing/without wearing the assistive device.

Several limitations of our study should be noted. Firstly, the musculoskeletal model used in OpenSim is only scaled based on the marker data from the 3D motion capture system. The best practice in building the musculoskeletal model, the MRI data from the subject should be used to construct the model from

scratch. However, the procedures are very difficult and require a lot of time to construct and validate a musculoskeletal model for simulation purpose. Second, the choice of muscles should be investigated carefully. As there may be more muscles wrapping around the elbow, each muscle mechanical function should be first figured out and the main action muscles chosen then as the flexors and extensors as muscles of interest. Lastly, as we only collected one subject's motion and EMG data for one movement, a generalizable criterion cannot be established. Nevertheless, the scaling and validation process make the musculoskeletal model make it suitable to be used for the tasks. This could allow the performance of a variety of movement imitated rehabilitation training while using the assistive device in the future.

4. Conclusion

This work proposed an approach to use a musculoskeletal model of the upper right arm to predict individual muscle activation during the motion of elbow flexion when the subject is using the assistive device. The model is first validated dynamically by comparing the simulation of the movement and experimental EMG data, which shows agreement in the pattern. The validated model is later used to assess the upper limb target muscle when the subject is using the assistive device. This method has great potential to be explored and is reliable to determine the muscle activation that could provide us with deeper understanding of the muscle characteristics during the rehabilitation training when using the device. Future improvement of the mechanical design and movement of assistive device can also be considered aligned with the human dynamic movement data achieved from simulations results.

References

- [1] Mozaffarian D, Benjamin E J, Go A S et al. 2015 Heart disease and stroke statistics—2015 update: a report from the American Heart Association *Circulation* **131** 4 pp. e29–e322,.
- [2] Jung Y and Bae J 2015 Kinematic analysis of a 5-DOF upper-limb exoskeleton with a tilted and vertically translating shoulder joint *IEEE Trans. on Industrial Mechatronics* **20** 3 pp. 1643–1648.
- [3] Perry J C, Rosen J and Burns S 2007 Upper-limb powered exoskeleton design *IEEE Trans. on Industrial Mechatronics* **12** 4 pp. 408–17.
- [4] Nishimura M, Hyodo K, Kawanishi M and Narikiyo T 2015 Proof of concept for robot-aided upper limb rehabilitation using disturbance observers *IEEE Trans. on Human-Machine Systems* **45** 1 pp. 110–18.
- [5] Delp S L, Anderson F C, Arnold A S, Loan P, Habib A and John C T 2007 Guendelman, E., Thelan, D.G. OpenSim: Open-source software to create and analyze dynamic simulations of movement *IEEE Transactions on Biomedical Engineering* **55** pp 1940–50.
- [6] Wu G, F C T van der Helm, H E J, (DirkJan), Veeger M, Makhsous, Van Roy P, Anglin C, Nagels J, Karduna A R, McQuade K and Wang X 2005 ISB recommendation on definitions of joint coordinate systems of various joints for the reporting of human joint motion. Part II. Shoulder, elbow, wrist and hand *J. Biomech* **38** pp. 981–92.
- [7] Saul K R, Hu X, Goehler C M, Daly M, Vidt M E, Velisar A and Murray W M 2015 Benchmarking of dynamic simulation predictions in two software platforms using an upper limb musculoskeletal model *Computer Methods in Biomechanics and Biomedical Engineering*. **18** pp.1445–58. 10.1080/10255842.2014.916698.
- [8] Hanafusa A, Shiki F, Ishii H, Nagura M, Kubota Y, Ohnishi K and Shibata Y 2018 Development of an active upper limb orthosis controlled by EMG with upper arm rotation. In *Intelligent Human Systems Integration – Proc. 1st Int Conf on Intelligent Human Systems Integration IHSI 2018*.
- [9] Shahrol M, Annisa J, Ana S, Zainal A, Mohd S J, Noor A M, Muhamad F A and Helmy H 2015 Development of Upper Limb Rehabilitation Robot Device for Home Setting *Proc 2015 IEEE Int Symp on Robotics and Intelligent Sensors*, pp. 376–80.
- [10] Pizzolato, C.; Lloyd, D.G.; Sartori, M.; Ceseracciu, E.; Besier, T.F.; Fregly, B.J. 2015 CEINMS: A toolbox to investigate the influence of different neural control solutions on the prediction of muscle excitation and joint moments during dynamic motor tasks. *J. Biomech.*, **48**, 3929-3936.

2019 Joint Conference

icomms'19

ICADME 2019

2019
ICoBE

CERTIFICATE OF PARTICIPATION

This is to clarify that

**MUHAMAD FADZLI
(PRESENTER)**

has participated in

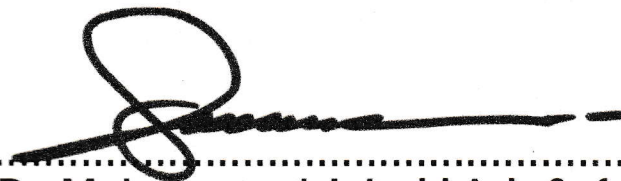
**5th JOINT INTERNATIONAL CONFERENCE ON MECHATRONIC,
MECHANICAL AND BIOMEDICAL ENGINEERING
(JICOMMBE 2019)**

26th – 27th August 2019

Rainbow Paradise Beach Resort, Penang, Malaysia

Organized by

**School of Mechatronic Engineering
Universiti Malaysia Perlis.**


.....
Dr. Muhammad Juhairi Aziz Safar
General Chair



UNIVERSITI
MALAYSIA
PERLIS

Simulation of A Human-device Biomechanical Model to Estimate Muscle Activities for Upper Limb Dynamic Movement.

Muhamad Fadzli¹, Akihiko Hanafusa¹ and Shahrol Mohamaddan¹

¹Department of Bioscience and Engineering, Shibaura Institute of Technology, Saitama, Japan.
Correspondence author: nb18110@shibaura-it.ac.jp.

Abstract. The recovery of arm movements is one of the most important goals during stroke rehabilitation to avoid long-term disability that may restrict daily living activities (ADL). With recent advanced technologies, there is a lot of interest in using robots and wearable devices for rehabilitation purposes. However, this technology also offers numerous challenges to its design, and evaluations including discovering the effect of its assistive technology on human muscle behavior. Experimental testing has provided the necessary direct evaluation of muscle output for many developed wearable devices. However, experiments are resource-intensive and require enormous time, especially in the early design or improvement of the device. Therefore, computational simulations play an essential role in solving these challenges. This study has developed a human-device model for a wearable upper limb assistive device. It can determine the range of motion angles of the human arm joints and the muscle output during the arm motion. Assisting movement by the wearable device was evaluated by measuring muscle activation in with-assist and without-assist conditions. Validation of our developed model shows good agreement (muscle force activation pattern has similarity with 1 standard deviation of EMG) with experimental data for dynamic upper limb motion. The results of this study highlight the importance of evaluating muscle output using the biomechanical simulation, which could reduce the resource-intensive and time consumed with the experimental testing, could be achieved.

1. Introduction

The number of adult patients with functional impairment of the upper limbs caused by stroke has increased rapidly in recent years. [1,2]. It could reduce the patients' quality of life, restricting activity daily living (ADL) and bringing enormous pain to their psychology and physiology in general.

Many patients reported could achieve recovery, and usually, arm motor skills restoration is often incomplete. In order to regain the function of motor skills, many rehabilitation approaches are proven and are being used widely, such as locomotor training and repetitive training observed by therapist experts.

With recent advanced technologies, there is a lot of interest in using robots and wearable devices for rehabilitation purposes. An assistive device that applies forces to the body to assist with motor tasks is one approach that may assist people with upper limb disorder or prevent injury. Recent studies also show that these assistive devices could affect the muscle output during the tasks to help with rehabilitation, especially for the upper limb. When providing practical assistance, it is expected that these passive wearable devices can reduce muscle output (e.g., muscle activations) during motor tasks. Many of these wearable passive devices are designed to support and assist the upper arm movement for the static task. However, the effect of the assistive force on muscle output was not widely investigated. It is unclear whether this device built for static tasks would suit supporting dynamic arm movements, including daily living activities [3] and rehabilitation exercises [4].

Experimental testing has provided the necessary direct evaluation of muscle output for many developed exoskeletons [4-6]. However, experiments are resource-intensive and require enormous time, especially in early design or the device's improvement. Computational musculoskeletal modeling and simulation tools have offered a cost-effective, alternative approach to experimental testing for exoskeletons. Musculoskeletal simulations are usually developed to track experimental measurements and then used to estimate difficult or impossible parameters to measure experimentally [7-8]. For example, simulation-based estimates of muscle forces have revealed which muscles are responsible for bodyweight support and forward progression during level walking and running [9-11]. Thus, in the study, we used computational modeling and simulation to evaluate muscle output during dynamic upper limb movements for an assistive device developed in our laboratory.

The first stage of this study involves developing a human-device model according to our developed wearable assistive device. Then, OpenSim software was used to simulate the effect of the assistive device on the muscle output during the motion. At this stage, the model's validation has taken place by comparing the simulation result with the experimental data. And finally, after the model has been validated and is suitable for further simulation, two daily living activities (ADL) tasks have been designed and carried out to evaluate the model by comparing the muscle activities when the subject is wearing and without wearing the assistive device.

2. Methods

2.1 Modeling a human-device model

In order to investigate further the effect of a wearable assistive device on the upper limb using the computational method approach, the first stage will involve editing the human model to create a human-device model. Figure 1 below shows a wearable assistive device with a combination of servo motor and cable mechanism developed in our laboratory that has been used in this study. This device can generate elbow flexion and extension movement motions by pulling the cable hung on a pulley connected to the forearm part. Also shown in the figure, the position of a load cell to measure the tension force generated from the cable from the power transmission during the motions. This data will later be used as an assistive force in the simulation procedure. The device's mechanism and details can be referred to in this paper [12].

The mechanical parts of the assistive device were designed using 3d drawing software which is CREO Software. The device is then separated into 3 main parts: trunk, upper arm, and lower arm. Then this model will further edit its axis of orientation and position to be exported to the format of biomechanical software OpenSim. Then this model should be exported to a file in STL geometry file format. These files later will be added to the geometry of the human body in the OpenSim model.

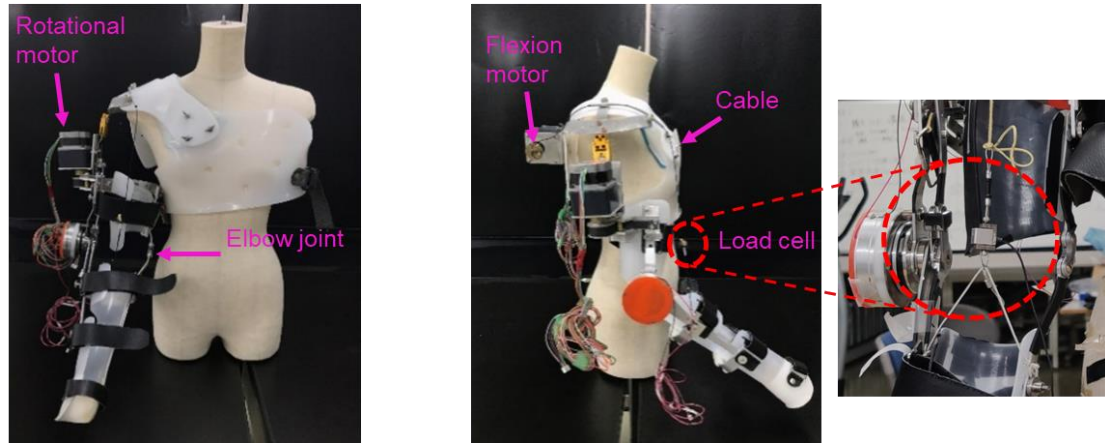


Figure 1. The developed wearable assistive device [12] and the load cell position for tension force measurement.

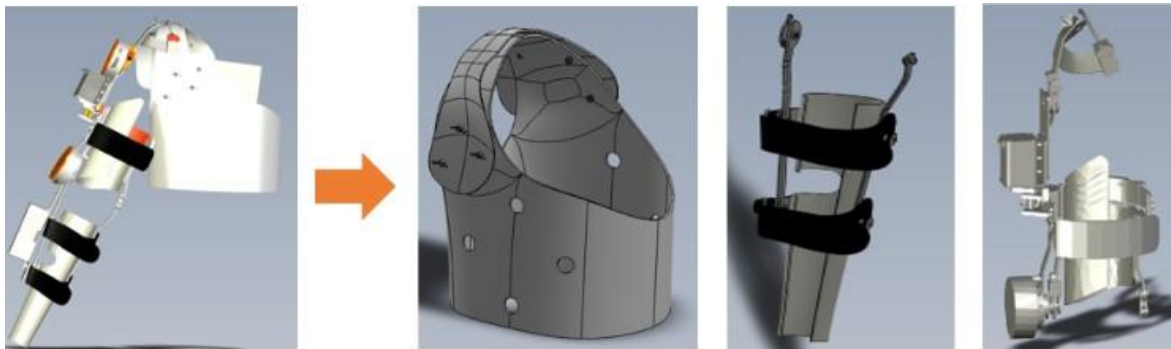


Figure 2. The mechanical parts of the device are separated into 3 main parts using the CREO Software.

There are a good number of models available in biomechanical software, Opensim. Since this study focuses on a wearable assistive device for the upper limbs, the related musculoskeletal model is chosen and used. The dynamic upper extremity musculoskeletal model [13], as shown in Figure 3 below, has been chosen in this study. The model had four rigid segments representing the rib cage and right humerus, radius, and hand.

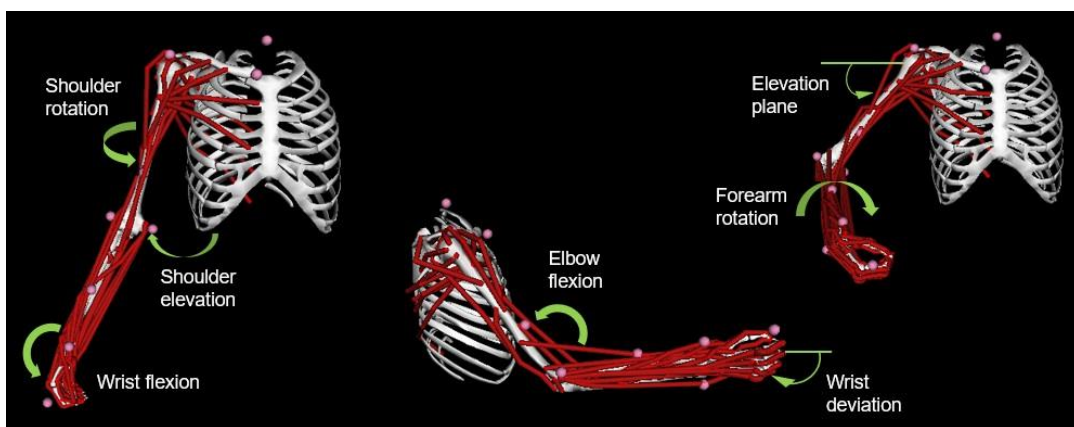


Figure 3. Dynamic Musculoskeletal model of the upper limb. The dynamic model incorporates 7 degrees of freedom, including shoulder rotation and elevation and wrist flexion, wrist deviation and elbow flexion, and elevation plane of the shoulder and forearm rotation [13].

The set of rigid bodies representing the wearable device system are added to the Opensim upper limb model by editing the human-based model file from the Opensim documentation [14]. After adding the device bodies, the relationship between these bodies, such as joint definitions, is further defined. In

addition, the inertial properties of the imported rigid bodies file need to be defined carefully, such as the mass of the body, center of mass, and tensor of inertia. For example, the new integrated model (trunk body) mass properties calculation is shown below in Figure 4. The completed integration of the wearable device bodies and the dynamic model is shown in Figure 5.

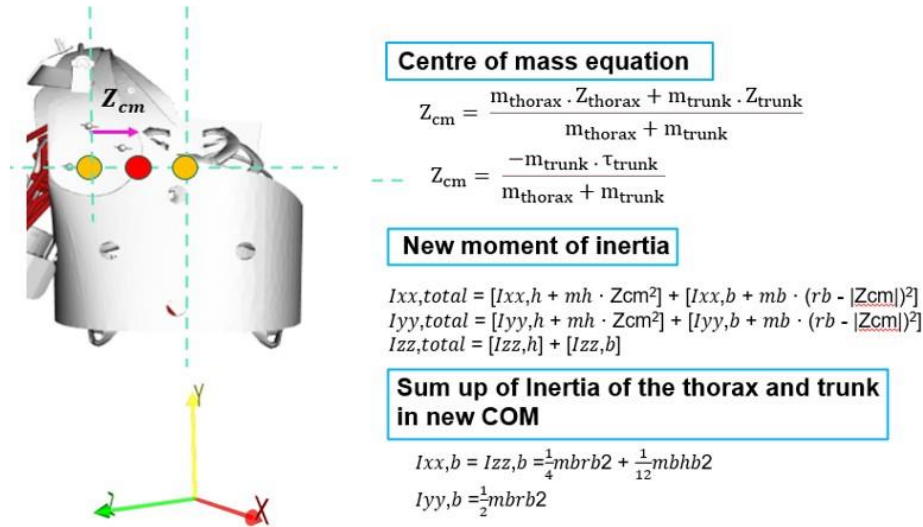


Figure 4. Inertial parameters calculation of the bodies of the integration model and device part (trunk).

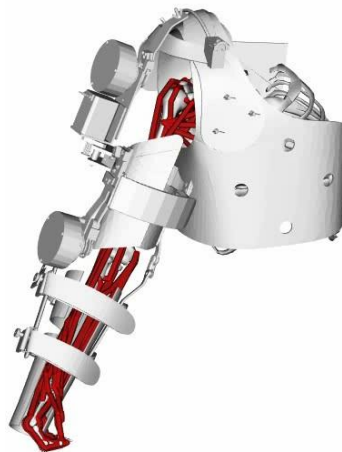


Figure 5. Integrated human-device model for upper limb dynamic simulation.

2.2 Data Acquisition and Experimental Setup for human-device Model Validation

Once the human-device musculoskeletal model development stage is complete, the model was validated by estimating muscle activities during the upper limb motion conducted in two different conditions. We compare the interested muscle activities in simulation with an experimental procedure when a healthy subject wears the assistive device. These initial steps are essential to understand better the kinematic and dynamic behavior of the musculoskeletal model that interfaced with our assistive device.

2.2.1 Acquisition of the kinematic data and Electromyogram (EMG)

One male subject (22 years old) in good physical condition performed an upper limb motion task. The performed task is presented in Figure 6 below. During the execution of the task, the body segments' motion was acquired with the motion capture system. 10 passive markers were placed on the section in specific sites following the International Society of Biomechanics (ISB) recommendations

based on body landmarks. The markers trajectories in the 3D space were analyzed and exported as .trc files and then loaded into Opensim software to scale the initial model kinematics. Figure 6 (b) shows measured elbow and shoulder flexion-extension angles together with measured tension force.

Surface EMG signals were acquired by a commercial EMG acquisition system (P-EMG plus, Oisaka.co.jp, Japan). In this experimental setup, the configuration of the EMG recording is shown in Figure 7 below. Three predominant muscles activating the elbow DoFs were selected as the test's muscle: biceps, triceps, and brachioradialis muscle. The active EMG electrodes of each channel were positioned at the muscle belly according to the SENIAM guide, and the ground electrode was attached to the elbow bone. The subjects were weighted with a 1kg load strapping on the right wrist for every motion. EMG signals were recorded in each posture at 1 kHz that was digitally filtered using a bandpass filter (20 to 500 Hz) in addition to a notch filter. The raw EMG was rectified, and the RMS EMG was computed for the test's most stable region. The configuration setup of the EMG of the muscles of interest is shown in Figure 7.

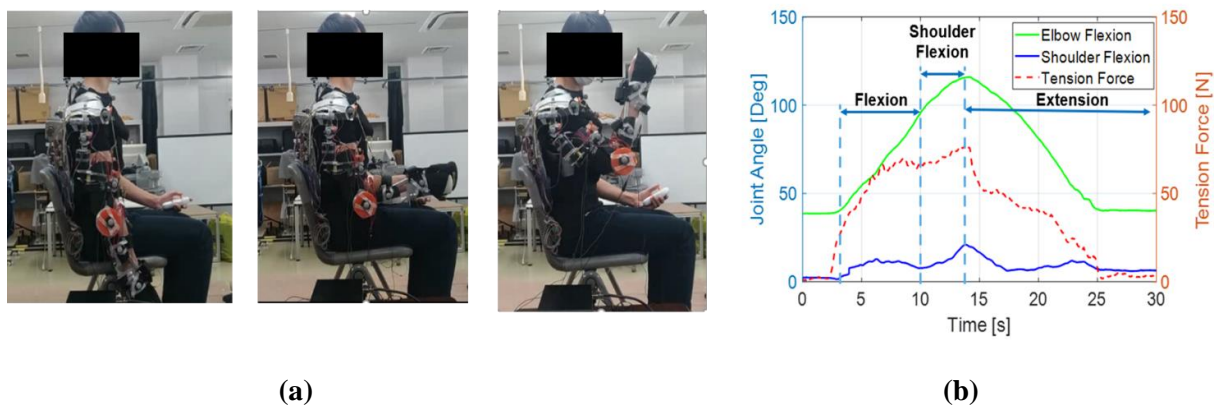


Figure 6. Subject wearing an assistive device performing maximum shoulder flexion and extension. This movement acquires the subject to flex the elbow to the close 90 deg, and then the upper arm will be brought to the upper limit of the arm's reachable motion and then return to the initial position. Data (b) shows measured elbow flexion angle, shoulder flexion angle, and tension force versus time.

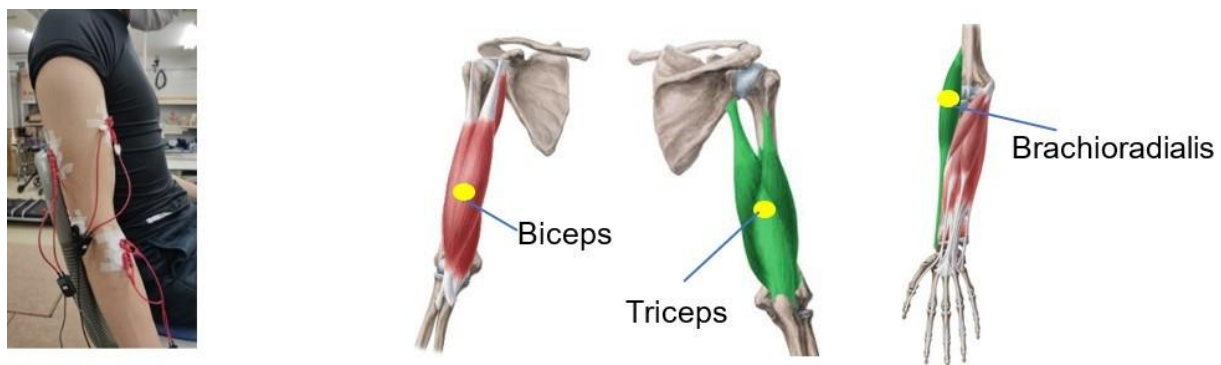


Figure 7. EMG signals were recorded from sets of electrodes attached to the muscles of interest (biceps, triceps, and brachioradialis).

2.3 Analysis of the effect of the assistive force on muscle activation using biomechanical simulations.

2.3.1 Human-device model validation

The behavior of the developed human-device model under kinematic and dynamic input has been evaluated. To simulate the motion tasks, measured assistive force is applied to assist the motion. The first step in the analysis of experimental data in Opensim is scaling. The developed human-device model matches a particular subject as closely as possible when the scale tool alters the anthropometry of the model. Then, the inverse kinematic (IK) tool is run. The IK tool tries to find the joint angles of the model best reproduce the experimental kinematics of a particular subject based on experimental marker

positions. Lastly, the CMC tool executed can compute a set of muscle excitations that could drive a dynamic musculoskeletal model to track the desired kinematics in the presence of applied external forces. The assistive device applies assistive force to the upper limb and assists in the arm's flexion and extension. For model validation purposes, muscle output from the simulated tasks will be compared to the experimental EMG muscles data. The validation result will be explained further in the result and discussion sections.

2.3.2 Estimation of muscle activity during ADL tasks

During the motor tasks, dynamic motion of the upper limb caused various muscle activities, especially shoulder muscle, to be activated. Specific ADL tasks that involve vertical shoulder flexion and internal rotation would activate muscles, as shown in Table 1 below. As previously mentioned in our main objective, the muscle behavior during the ADL tasks will be investigated further through computational simulation using a developed human-device musculoskeletal model. In this study, two tasks most anticipated for the upper limb, such as nose touching and moving objects, have been designed and evaluated.

Table 1

Motion	Activated Muscles
Shoulder vertical flexion	Deltoid (anterior), Pectoralis major
Shoulder vertical extension	Deltoid (posterior)
Shoulder internal rotation	Deltoid (anterior), Teres major

3. Results and Discussion

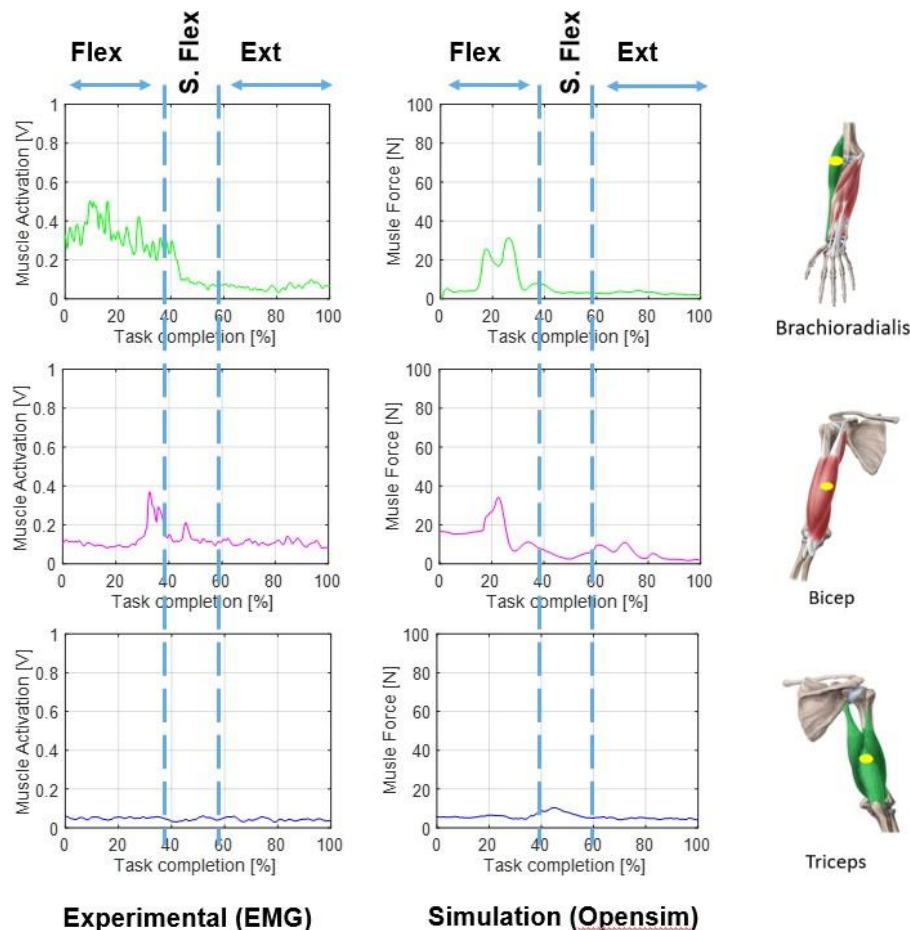


Figure 8. Comparison of EMG from experimental and muscle activations computed from Opensim resulting three muscle force brachioradialis (green), biceps (magenta), and triceps (blue) for maximum

shoulder flexion and extension motion with the subject wearing the assistive device.

Firstly, to validate the developed human-device model, muscle activities (EMG) during upper limb motion were evaluated experimentally and compared to the muscle force generated in the same simulated task. Figure 8 compares three interested muscles for the upper limb movement when the subject performs tasks while wearing the assistive device. The most significant activated muscle would be Brachioradialis (green) and Biceps (magenta) observed in EMG measured and simulation muscle force data. The initial peaks are mainly visible during the elbow's flexion (within the first 40% of movement) both in experimental and simulation for Brachioradialis and Biceps muscle. As reported in [8,9,10], the primary activated muscle for elbow flexion movement would be these stated muscles, and the EMG result confirmed the reported articles. The triceps muscle is an extensor muscle usually activated during the extension of the arm. However, poor positioning and attachment caused minimal detection during the experiment. Overall, the similarity agreement observed between the recorded EMG data and the estimated muscle forces for the motion shows that this developed human-device model is acceptable to estimate muscle activity for upper limb right-hand motion with the wearable assistive device.

After validating the developed model's simulation results, the computational simulation has been carried out to investigate the model performance by evaluating the muscle activities. Computational simulation is conducted in two conditions by comparing the activated muscle output from the model with the wearable assistive device and the one without it. Results (Figure 9) showed that muscle activations (deltoid anterior, pectoralis major, teres major) could be significantly reduced thanks to the presence of the assistive device. This could explain with the assisted movement by the device; the elbow and shoulder are well supported during upper arm movement. In this simulation also, we could observe that the primary activated muscle during the tasks could be measured.

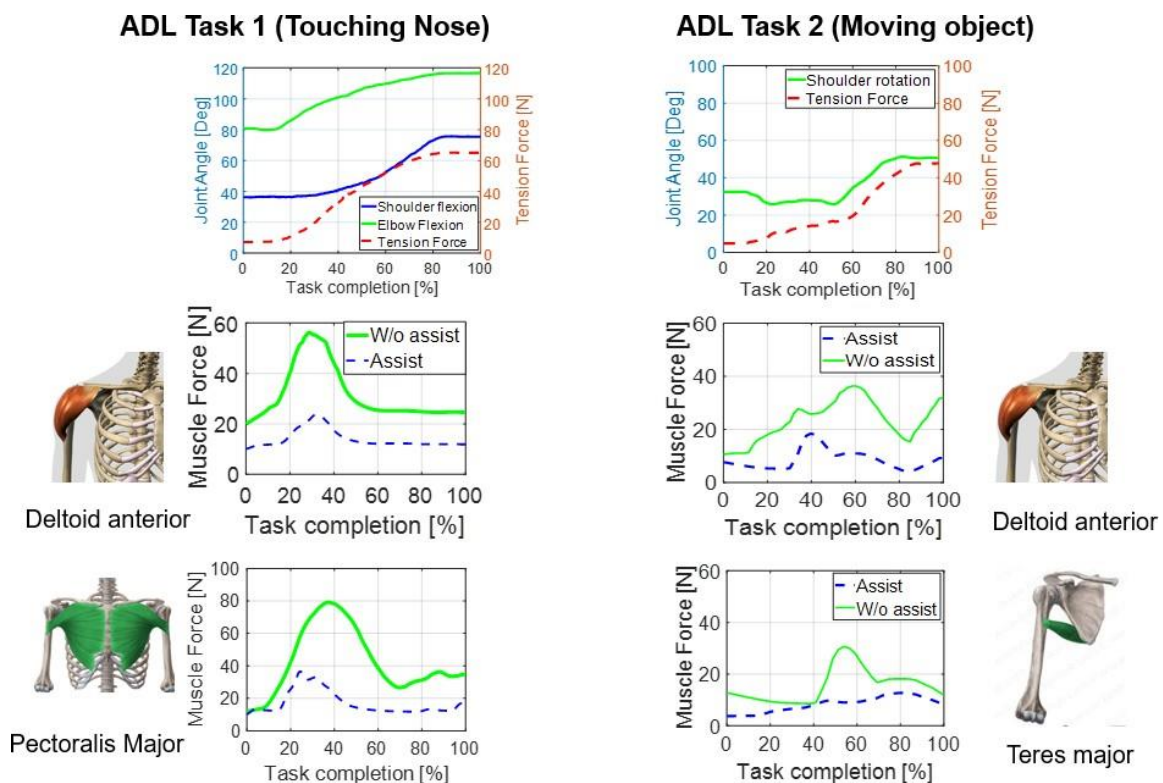


Figure 9. Muscle activations computed from Opensim resulting estimation muscle output of the developed human-device model from two different ADL tasks.

This study compared the functionality of the assistive device for upper arm dynamic movements and its effect on the muscle output. Two computer-based musculoskeletal models with and without device parameters have been set up and validated. After completing developing the human-device model, a comparison of measured EMG muscle data and human-device models revealed that, although the model did not fully incorporate similar muscle physiology completely, muscle force was generated

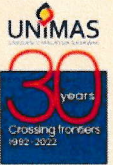
throughout the arm comparable with measured muscle activity from the experimental. This result shows that our developed model has good agreement to be used for further simulation tasks. Results showed that a musculoskeletal model with and without an integrated assistive device could produce muscle activation patterns for all muscles of interest during the simulated upper dynamic tasks. The integrated human- device model produced encouraging results such that muscle force values for all primary muscles were reduced during the simulated task when wearing the assistive device. These results are congruent with expectations, with the assistive device that manages to support the upper limb movement, providing practical assistance.

4. Conclusion

We quantitatively evaluated our developed assistive device's mechanical and biomechanical performance in this study. Our results showed that the device could reduce the muscle activity of several muscles crossing the upper arm. After several validating procedures, the agreement with the experimental shows that our model can be used in the computational study for further biomechanical analysis. Different assistance levels and identifying a range of assistance that most enhances arm motor function and biomechanics will be explored further in our future work.

References

- [1] URL <http://www.who.int/mediacentre/factsheets/fs352/en/>
- [2] R W Teasell and L Kalra. "Whats new in stroke rehabilitation". *Stroke*, vol. 35, 383–385, 2004.
- [3] Saul KR, Hu X, Goehler CM, Daly M, Vidt ME, Velisar A, Murray WM. Benchmarking of dynamic simulation predictions in two software platforms using an upper limb musculoskeletal model. *Computer Methods in Biomechanics and Biomedical Engineering*. 2015; 18:1445-58. 10.1080/10255842.2014.916698 (2015).
- [4] J C Perry, J Rosen and S Burns. "Upper-Limb Powered Exoskeleton Design". *Mechatronics IEEE/ASME Transactions on*, vol. 12, 408–417, 2007.
- [5] H I Krebs, S P Buerger, K A Jugenheimer, D Williams and N Hogan. "3-D extension for MIT-MANUS: a robot-aided neuro-rehabilitation workstation". *ASME 2000 IDETC/CIE DETC2000/MECH-14151 Baltimore*, 2000.
- [6] A Seth, J L Hicks, T K Uchida et al. "OpenSim: Simulating musculoskeletal dynamics and neuromuscular control to study human and animal movement". *PLoS Comput Biol*, vol. 14, no. 7, 1006223–1006223, 2018.
- [7] P Agarwal, M S Narayanan, Leng-Feng Lee, F Mendel and V N Krovi. "Simulation- Based Design of Exoskeletons Using Musculoskeletal Analysis". *Proceedings of the ASME Design Engineering Technical Conference*, 2010.
- [8] Zhou Lelai, Li Yibin and Bai Shaoping. "A human-centered design optimization approach for robotic exoskeletons through biomechanical simulation". *Robotics, and Autonomous Systems*, vol. 91, 337–347, 2017.
- [9] D Pujals. *Simulation of the Assistance of an Exoskeleton on Lower Limbs Joints Using OpenSim*. Barcelona, 2017.
- [10] P Agarwal, Pei-Hsin Kuo, R R Neptune and A D Deshpande. "A Novel Framework for Virtual Prototyping of Rehabilitation Exoskeletons". In *IEEE International Conference on Rehabilitation Robotics*, 2013.
- [11] H S Lo and S Q Xie. "Exoskeleton robots for upper-limb rehabilitation: State of the art and future prospects". *Medical engineering & physics*, vol. 34, 261–268, 2012.
- [12] W U Tzong-Ming and Chen Dar-Zen. *Design and preliminary evaluation of an exoskeleton for upper limb resistance training*. Higher Education Press and Springer-Verlag, Berlin Heidelberg, 2012.
- [13] A Hanafusa, F Shiki, H Ishii et al. "Development of an active upper limb orthosis controlled by EMG with upper arm rotation". *Intelligent Human Systems Integration - Proceedings of the 1st International Conference on Intelligent Human Systems Integration IHSI: Integrating People and Intelligent Systems*, pages 163–169, 2018.
- [14] URL <https://simtk-confluence.stanford.edu:8443/display/OpenSim/Documentation>.
- [15] D Copaci, E Cano, L Moreno and D Blanco. "New design of a soft robotics wearable elbow exoskeleton based on shape memory alloy wire actuators". *Appl Bionics Biomech*, vol. 2017, 1–11, 2017.



CERTIFICATE OF PARTICIPATION

This is to certify that

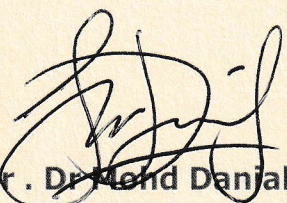
MUHAMAD FADZLI BIN ASHARI

Have participated and presented at

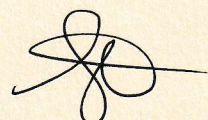
ENCON
2022

14th International UNIMAS Engineering Conference 2022

23 - 24 February 2022


A P. Ir. Dr. Mend Danjal Ibrahim

EnCon 2022 Chairman
Faculty of Engineering, UNIMAS


Prof. Ir. Dr. Siti Noor Linda Taib

Dean
Faculty of Engineering, UNIMAS

Research Article

Evaluation of Upper Limb Muscle Activation Using Musculoskeletal Model with Wearable Assistive Device

M. F. Ashari , A. Hanafusa, and S. Mohamaddan 

Department of Bioscience and Engineering, Shibaura Institute of Technology, 337-8570 Saitama, Japan

Correspondence should be addressed to M. F. Ashari; nb18110@shibaura-it.ac.jp

Received 4 November 2021; Revised 5 May 2022; Accepted 21 May 2022; Published 6 July 2022

Academic Editor: Yanxin Zhang

Copyright © 2022 M. F. Ashari et al. This is an open access article distributed under the Creative Commons Attribution License, which permits unrestricted use, distribution, and reproduction in any medium, provided the original work is properly cited.

In recent years, wearable assistive device has been used to support upper arm movement training for rehabilitation purposes. A wearable assistive device could affect the muscle output during motor tasks to support upper limb disorder rehabilitation training. However, the investigation of muscle activity with the given assistive force is not widely investigated. In this study, the evaluation of upper limb muscle activities using musculoskeletal simulation systems with the developed wearable cable-driven assistive device has been carried out. An experimental protocol consisting of a series of motions was executed with five healthy subjects. Muscle activation on the brachioradialis, biceps, and triceps muscles was measured by using surface electromyography (EMG) and analyzed. The simulations with a musculoskeletal model to estimate muscle output with and without a wearable assistive device were performed for three tasks. An assistive upper arm device was integrated into the musculoskeletal model, and the desired assistive force is translated to the arm joint along with a tendon routing structure. Assisting movement by the wearable device was evaluated by measuring muscle activation with-assist and without-assist conditions. The results show that the use of the wearable assistive device can effectively assist in arm movement. Comparisons of measured EMG muscle data and the musculoskeletal model revealed that muscle force was generated throughout the arm. The integrated musculoskeletal model results show that muscle force values for two primary muscles (biceps and brachioradialis) were reduced during the simulated task when wearing the assistive device. These results are congruent with expectations, with the assistive device that supports the upper limb movement, providing practical assistance. The results highlight the importance of evaluating muscle output for the developed wearable assistive device to support the assistive movement. Lastly, the musculoskeletal simulation system could reduce the resource-intensive, and time consumed with the experimental testing could be achieved.

1. Introduction

In the past years, in many areas, assistive devices have been developed to support humans in performing different types of tasks and support activity of daily life. Assistive devices have also been developed in the medical or rehabilitation field. These devices treat or support patients in case of loss of function caused by diseases, especially stroke patients.

Stroke often causes permanent and complex long-term disability in adults, reducing the patients' quality of life and bringing enormous pain to their physiology and psychology and burdening families in general [1, 2]. In literature, upper limb hemiparesis is widely reported as one of the primary impairments after stroke. While many patients

recover ambulatory function after dense hemiplegia, arm motor skills restoration is often incomplete. More than 60% of patients cannot use their paretic hands in functional activities [3]. The recovery of arm movements is one of the most important goals during stroke rehabilitation to avoid long-term disability that may restrict activities of daily living (ADL) and social and occupational activities and lead to depression.

Effective rehabilitation training can improve patients' nerve function and maintain the degree of joint activity to help the patient gain their upper limb function capability. Traditional rehabilitation training is a one-to-one auxiliary exercise for patients by therapists. This method is challenging to develop an effective treatment plan, and it is tough

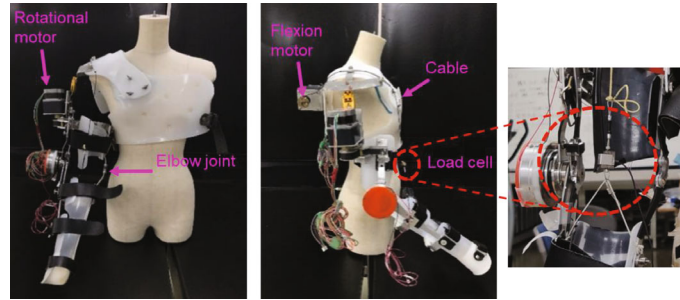


FIGURE 1: The overview of the developed wearable assistive device [22] and the load cell position for tension force measurement.

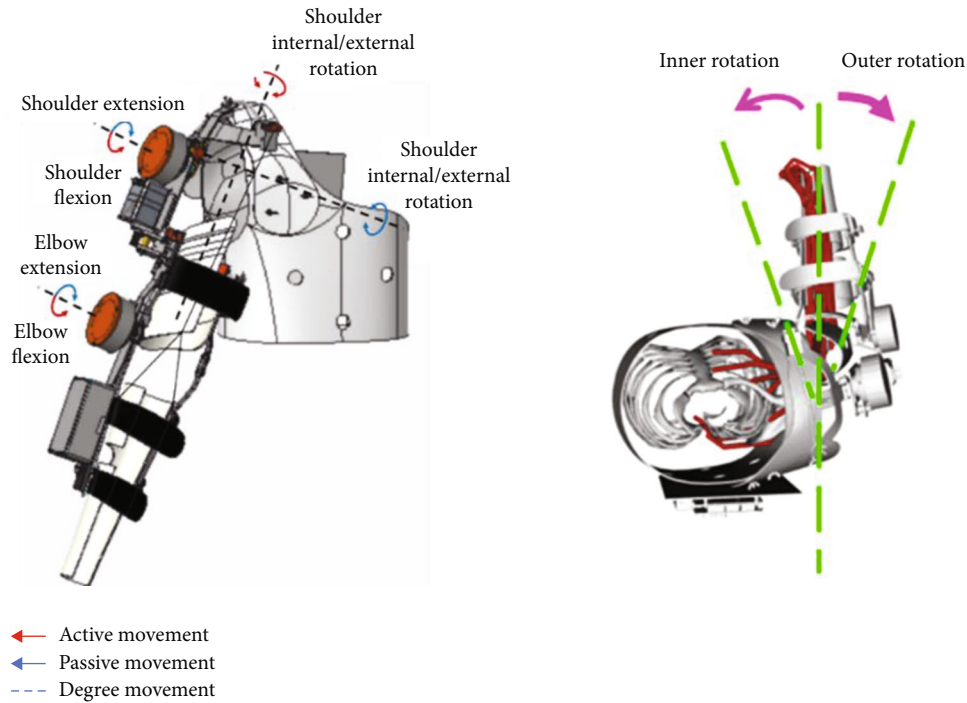


FIGURE 2: Assistive device motion range according to its degree of motion.

to control accurately [4]. The traditional treatment methods, which are based on the therapist's clinical experience, also have significant staff consumption problems, long rehabilitation cycles, limited rehabilitation effects, and so on. With rehabilitation assistive technology and medicine development, the rehabilitation device has become a novel assistive rehabilitation treatment technology. It is essential to utilize technology for rehabilitation training to recover stroke patients' limb function [5]. The research and application of rehabilitation device systems are expected to effectively alleviate the contradiction between the supply and demand of rehabilitation medical resources and improve the quality of life of stroke patients [5, 6].

The wearable assistive device that applies forces to the body to assist with motor tasks is one approach that may assist people during the rehabilitation of upper limb disorder. For example, exoskeletons could improve task economy [7], enhance strength and functional ability [8, 9], lower biomechanical loads and associated injury risks [10], or protect

healing musculoskeletal tissues during recovery from trauma surgery. At present, a variety of exoskeleton rehabilitation robots are developed, e.g., a dynamic exoskeleton system ADEN-7 robot with 7 degrees of freedom [11] and ARMIN robot with six degrees of freedom (four active and two passive) semiexoskeleton structure [12], an ARMEO robot providing arm weight reduction support system for training, enhancing performance feedback and evaluation tools [13]. Currently, it is a relatively safe and efficient rehabilitation robot structure. However, most of these high-technology devices are placed at the rehab center and need to be operated on by specialists and the patient to come regularly. Therefore, it is crucial to investigate the potential of adapting this technology which is potentially lighter, more affordable, and more convenient to use (e.g., basic operating manual) than high technology exoskeletons. These attributes make the assistive device more wearable and suitable for continuous use at the home, workplace, and community.

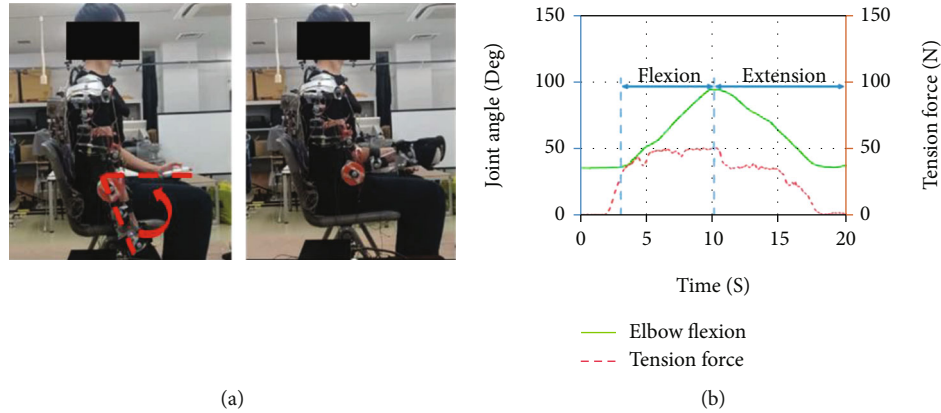


FIGURE 3: Subjects wearing an assistive device were asked to flex their elbow close to 90 degrees and return to the initial position. Data (b) shows measured elbow flexion angle and tension force versus time.

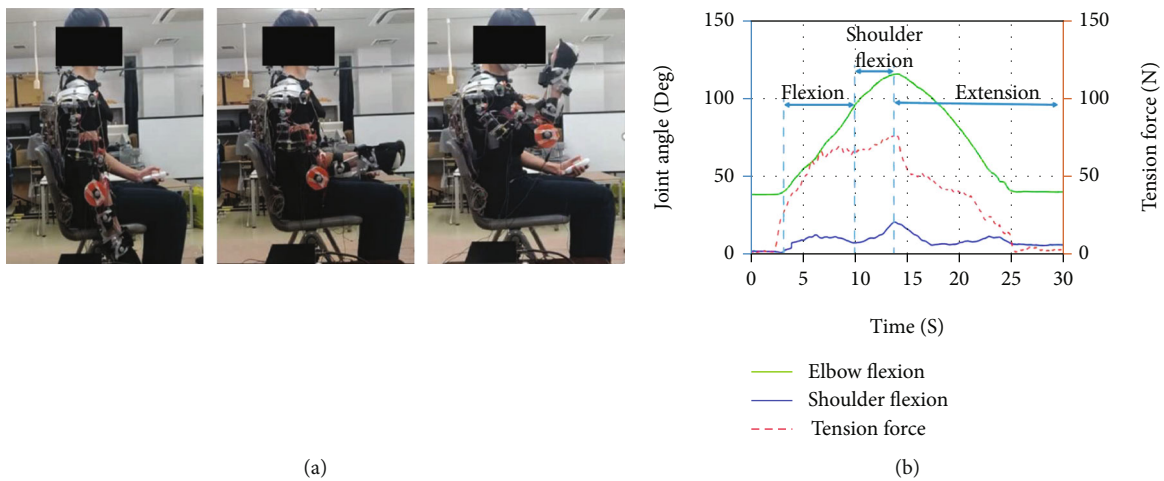


FIGURE 4: Subject wearing an assistive device performing maximum shoulder flexion and extension. This movement acquires the subject to flex the elbow to the close to 90 deg, and then the upper arm will be brought to the upper limit of the arm's reachable motion and then return to the initial position. Data (b) shows measured elbow flexion angle, shoulder flexion angle, and tension force versus time.

When providing effective assistance, it is expected that wearable assistive devices can reduce muscle output (e.g., muscle activations) during motor tasks. Experimental testing has provided a necessary direct evaluation of muscle output for powered [9, 14] and passive [9, 15–17] exoskeletons. However, experiments are resource-intensive and possibly require several iterations of physical prototypes. Especially in the early design of human-machine interfaces, computational musculoskeletal modeling and simulation tools have offered a cost-effective, alternative approach to experimental testing for both upper extremities [18, 19] and lower extremity exoskeletons [20]. Thus, in the proposed study, we used computational modeling and simulation to evaluate muscle output during dynamic right upper limb movements for a wearable assistive device we have developed to assist with right upper limb movement. Our study's primary goal was to quantify muscle output with and without our wearable assistive device during three simulated tasks involving dynamic right upper limb movement. We hypothesized that the resulting exoskeleton output force would cause muscle

output to be lower for some muscles with the assistive device than without wearing the device.

2. Materials and Methods

2.1. Assistive Device. Owing to the anatomy theory, motion mechanism, and range of human upper limbs for rehabilitation training, a wearable assistive device with a combination of servo motor and cable mechanism was developed. This device can generate elbow flexion and extension movement motions by pulling the cable hung on a pulley connected to the forearm part. A cable-driven motor is rear-mounted to achieve long-distance transmission and reduce the drive inertia of the end joints. The mechanism and details of the device can be referred to in this paper [21]. The shoulder joint internal/external rotation mechanism's transmission mechanism is an active gear with belt transmission, where both ends of the maximum reachable range are provided with a limiter switch. Once it exceeds the rehabilitation range, the passive gear will be blocked. It cannot continue

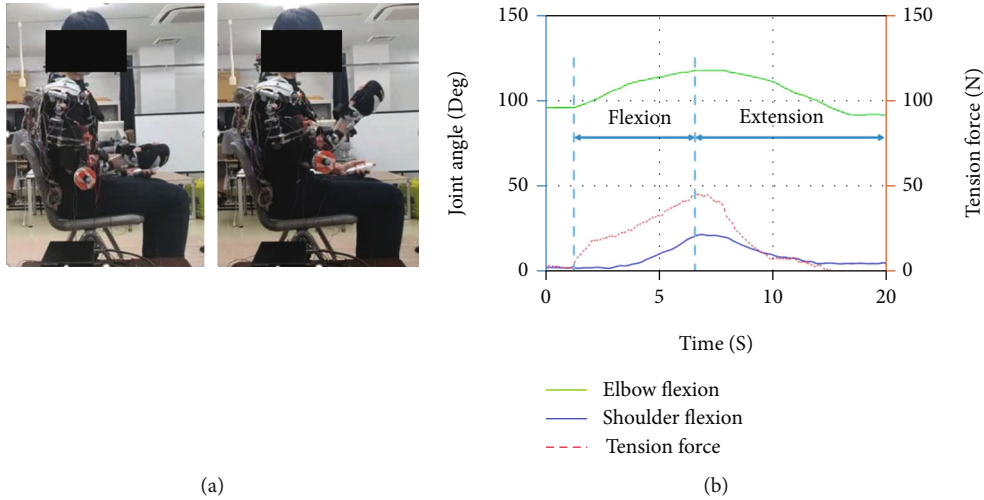


FIGURE 5: Subject wearing an assistive device performing maximum shoulder flexion and extension to the initial position. The arm's initial position was kept in front of the inner side of the frontal body of the subject. The elbow was flexed to the maximum and returned to the initial position. Data (b) shows measured elbow flexion angle, shoulder flexion angle, and tension force versus time.

to move, ensuring the subject's safety and avoiding secondary injuries to the subject.

As illustrated in Figure 1 above, the elbow motion mechanism is constructed by a two-way winding coil structure. The driven part of the elbow joint movement mechanism is mounted on the forearm. The two-way driven pulley of the motor transmits the power to the elbow through the cable; thus, it completes the elbow flexion/extension motion. The wearable device's range of motion and its operational degree of freedom is shown in Figure 2.

As mentioned in this study's objective, the relationship between the assistive force given by the assistive device and its relationship to the muscle output will be investigated further. Therefore, an experimental procedure has been conducted to measure the assistive force during the device's upper limb motion. Three specified tasks—elbow flexion and extension, shoulder flexion and extension, and inner rotation with shoulder flexion and extension—have been designed according to the device's capability and also associated with the training in rehabilitation upper limb movements. A load cell (TCS-20L, NEC company, Japan) has been used to measure the tension force generated from the cable during the power transmission for the movements. The measurement setting is connected to the motion capture system so that every activity with the subject is recorded simultaneously.

3. Experimental Protocol

An experimental protocol was approved by the Shibaura Institute of Technology (SIT) Review Board. All subjects were told the aim of the experiments and provided written consent to participate in this study, and this consent procedure was approved by SIT. The individual in this manuscript has given written informed consent to publish these case details. In this study, five right-handed able-bodied subjects (all males, ages ranging 23-30-year old; weight 58.2 ± 6.8 kg; height 167 ± 6.2 cm) participated. The subjects did not

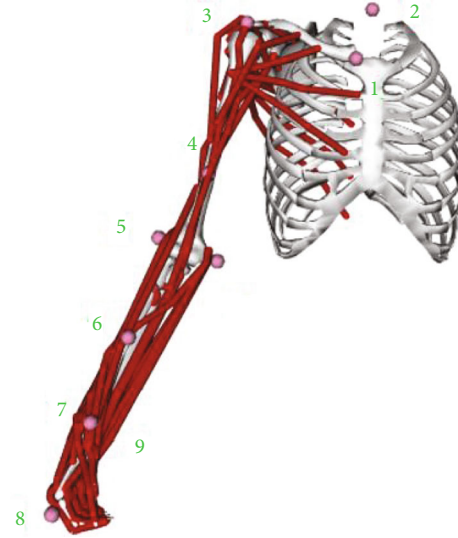


FIGURE 6: Ten marker locations following the International Society of Biomechanics (ISB).

TABLE 1: Markers corresponding names.

Marker number	Names
1	R. Clavicle
2	C7
3	R. Shoulder
4	R. Bicep
5	E. Elbow lateral
6	R. Forearm
7	R. Radius
8	R. Hand
9	R. Ulna
10	R. Elbow medial

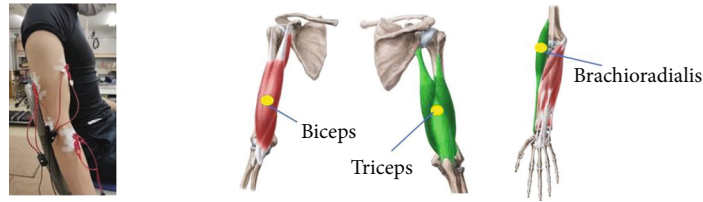


FIGURE 7: EMG signals were recorded from sets of electrodes attached to the muscles of interest (biceps, triceps, and brachioradialis), while the subjects were weighted with a load on the wrist.

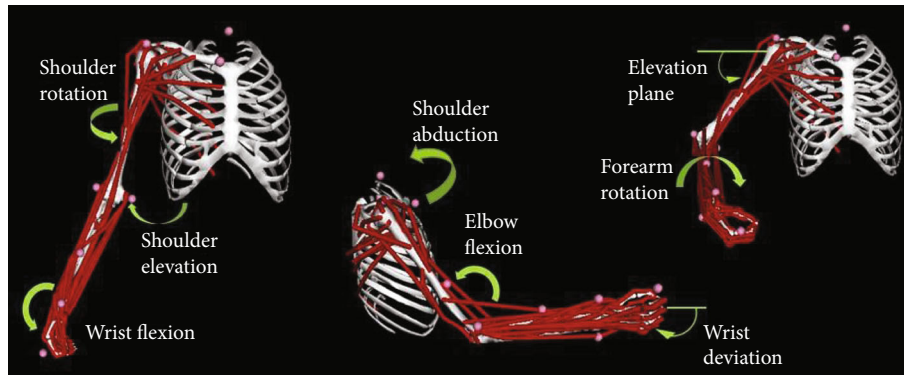


FIGURE 8: Dynamic musculoskeletal model of the upper limb. The dynamic model incorporates 7 degrees of freedom, including shoulder rotation and elevation and wrist flexion, wrist deviation and elbow flexion, and elevation plane of the shoulder and forearm rotation.



(a) 3D model and its 3 main parts modeled in CAD Creo software (b) Integrated model

FIGURE 9: Wearable device model components and their position and orientation in the model. The modeled components shown in (a) were designed using the CAD Creo Software and later been imported into the OpenSim software to produce a human-device integrated model (b) that will later be used in simulation in the OpenSim software.

have any skeletal or muscular diseases that could affect their muscle activity. The protocol involved performing three motions with two conditions which were with and without wearing the assistive device. The assistive device was applied to the subjects in the right arm. The arm movement speed is naturally moved according to the subjects without the device. When using the device, the speed of the movement liaises with the speed of the motor used.

During the experiment, the subjects were quietly seated in the chair with their torso keeping upright and their right hand keeping relaxing. Three motions shown in Figures 3–5 are designed to obtain the motion of the right upper limb. The traces in every figure indicated the movement trajectory from the initial position to the destination position in a single trip of each motion and returned to the initial position. These arm movements are freely repeated to capture the commonality and the EMG and motion properties' variability.

4. Experimental Setup

4.1. Motion Recording. Data were acquired in the Shibaura Institute of Technology (SIT) laboratory using the 3D Motion Capture System. This equipment consists of infrared cameras, which can capture the 3D position of the different markers over time. Ten markers are placed in the subject to capture the different motions analyzed. The markers' numbers and locations were selected following the International Society of Biomechanics (ISB) recommendations based on body landmarks to place the markers. Finally, since only the motion of the right arm is studied, the markers are only set in the right part of the body, and the device was also applied to the subjects at the right shoulder. The markers setup is shown in Figure 6, with the corresponding names in Table 1.

4.2. Electromyography (EMG) Measurement. Surface EMG signals were acquired by a commercial EMG acquisition

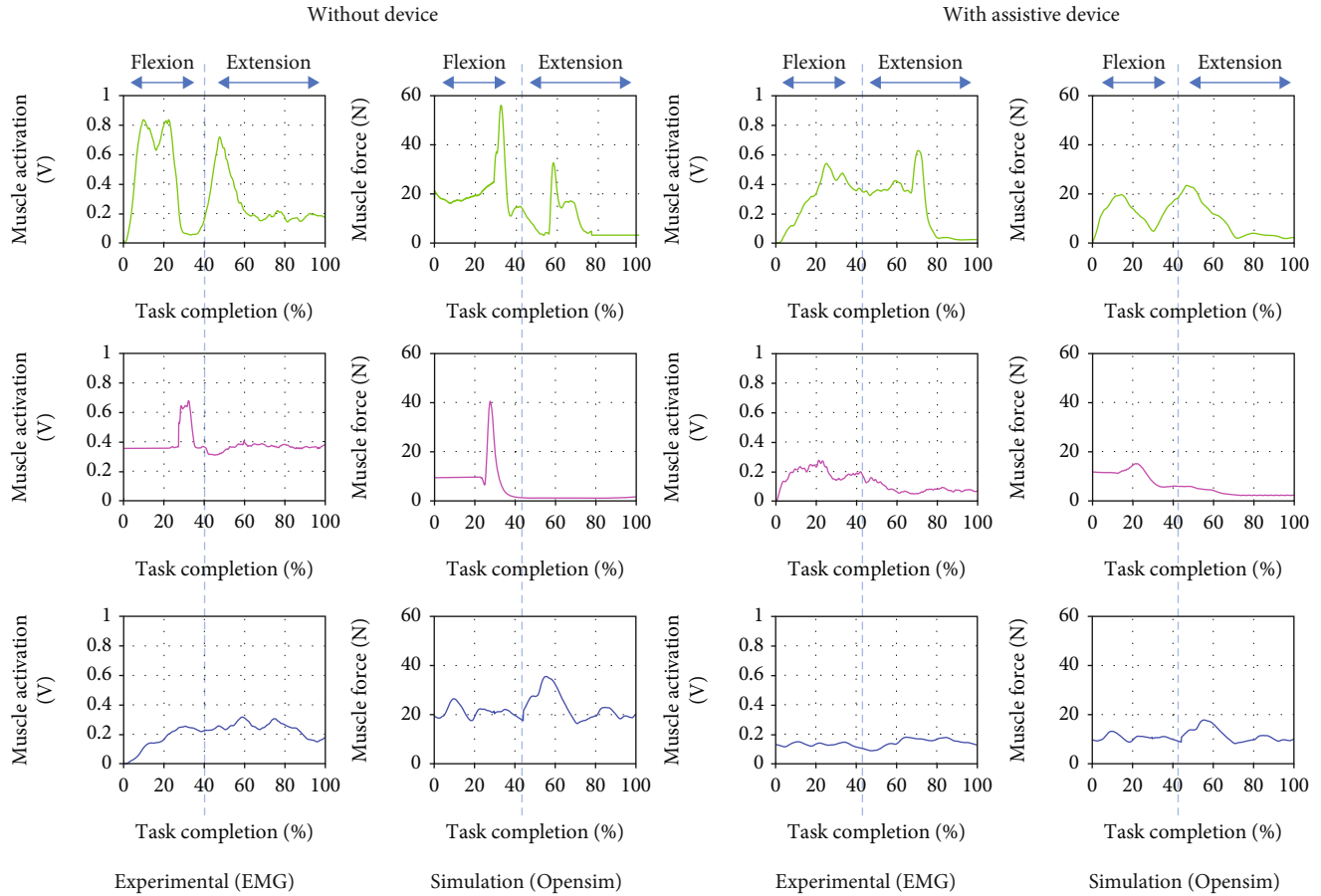


FIGURE 10: Comparison of EMG from experimental and muscle activations computed from OpenSim resulting in three muscle force brachioradialis (green), biceps (magenta), and triceps (blue) for 90-degree elbow flexion and extension motion with and without the assistive device.

system (P-EMG plus, <http://oisaka.co.jp>, Japan). In this experimental setup, the configuration of the EMG recording is shown in Figure 7. Three predominant muscles activating the elbow DoFs were selected to be the test's muscles: biceps, triceps, and brachioradialis muscle. Eight channels (only three channels were used) of the bipolar differential amplifier were carefully placed on these muscles according to the anatomy and hand touch experience according to the SENIAM guide. The skin underneath the electrodes was cleaned with an alcohol patch to reduce the skin's and sensors' resistance. The active EMG electrodes of each channel were positioned at the muscle belly along the muscle fiber direction with the reference electrode orthogonal to the active electrodes' midline. The ground electrode was attached to the elbow bone. The subjects were weighted with a 1 kg load strapping on the right wrist for every motion. EMG signals were recorded in each posture at 1 kHz that were digitally filtered using a bandpass filter (20 to 500 Hz) in addition to a notch filter. The raw EMG was rectified, and the RMS EMG was computed for the test's most stable region.

4.3. Musculoskeletal Model. The dynamic upper extremity musculoskeletal model [23], as shown in Figure 8, had four

rigid segments representing the rib cage and right humerus, radius, and hand. The model was modified to include only 32 Hill-type muscle-tendon actuators. For our simulations, we limited the dynamic model to 4 degrees of freedom: shoulder elevation, elevation plane angle of the shoulder, axial shoulder rotation, and elbow flexion. The other upper extremity degrees of freedom, such as wrist flexion, wrist deviation, and forearm rotation, were held constant at an angle of 0°. The fingers' movement and the wrist are not studied for two reasons: the considered arm support will not articulate the fingers, and those are the last part affected by the disease.

4.4. Upper Arm-Device Integrated Model. The model of the device was created previously using CREO software. These 3-dimensional elements representing the 3 main parts of the device, the trunk, upper arm, and lower arm, as shown in Figure 9(a), were added to the musculoskeletal model in OpenSim. The mass of each component was defined according to the materials for developing the device. The moments of inertia were estimated from the computer-aided design model according to the defined materials. During this integration to build a human-device model, the new weight consists of body

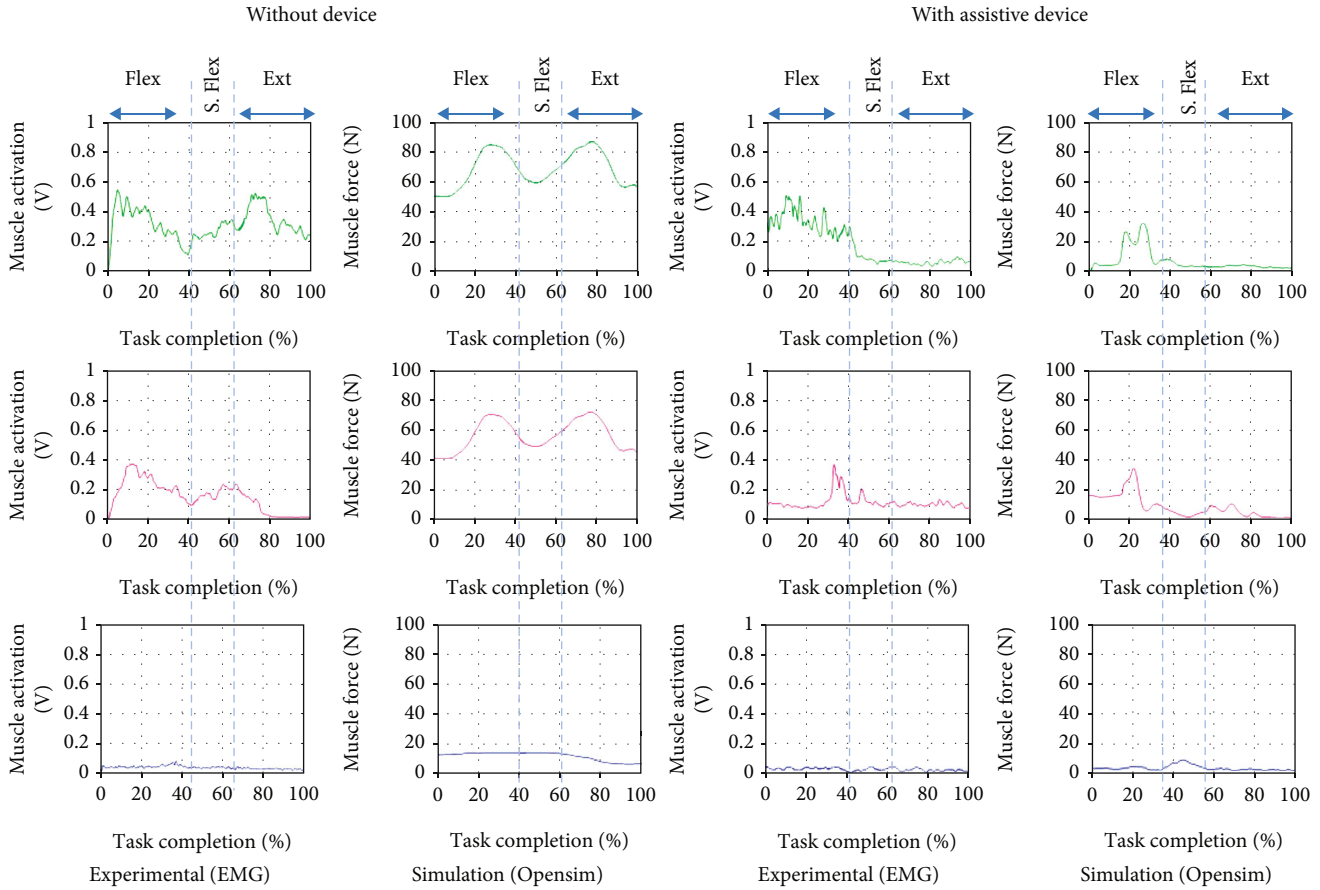


FIGURE 11: Comparison of EMG from experimental and muscle activations computed from OpenSim resulting in three muscle force brachioradialis (green), biceps (magenta), and triceps (blue) for maximum shoulder flexion and extension motion with and without the assistive device. ** (Flex: flexion; S. Flex: shoulder flexion; Ext: extension).

and device weight, calculation center of mass, and inertial parameters are already considered, and the effect is realized during the simulation.

4.5. *Analysis of the Effect of the Assistive Force on Muscle Activation Using Biomechanical Simulations.* We simulated tasks with and without the assistive device to evaluate the muscle output from the given force measured in the experiments. As explained previously, joint kinematics were defined from the experimentally measured healthy upper limb movement subjects. To carry out muscle analysis, the Computed Muscle Control (CMC) Tool was solved to compute a set of muscle activations required for the dynamic model to track the desired kinematics by minimizing the sum of muscle activations [16]. In this study, the effect of the assistive force on the muscle output was evaluated. The acquired assistive force from the experimental was defined in OpenSim and applied to the integrated human-device model system to acquire the interested muscle activations to support the arm movement.

5. Results

We compared the steady-state muscle activations between simulations with and without the assistive device for the

simulated static task. For each of the three simulated dynamic upper limb movements, we computed an outcome measure of the muscle activity for each muscle of interest (brachioradialis, biceps, and triceps). The muscles' location is shown previously in Figure 7.

5.1. *Upper Limb Motion: 90-Degree Elbow Flexion and Extension.* The result of the experiments and simulations are presented. Figures 10–12 compare three interested muscles for the upper limb movement with and without wearing the assistive device. Experiments on the upper arm device had shown that muscle activations could be significantly reduced when assistive force was enabled during upper limb movements. Overall, the results show that each of the muscles activated reduced thanks to the presence of the assistive device. In Figure 10 above, the most significant activated muscle would be brachioradialis (green), which can be observed in EMG measured and simulation data from force produced. The initial peaks are mainly visible during the elbow's flexion (within the first 40% of movement) both in experimental and simulation for brachioradialis and biceps muscle. As reported in [24–26], the primary activated muscle for elbow flexion movement would be in brachioradialis and biceps muscles, and the result from the EMG could confirm the reported article. However, we can see the visible peak when

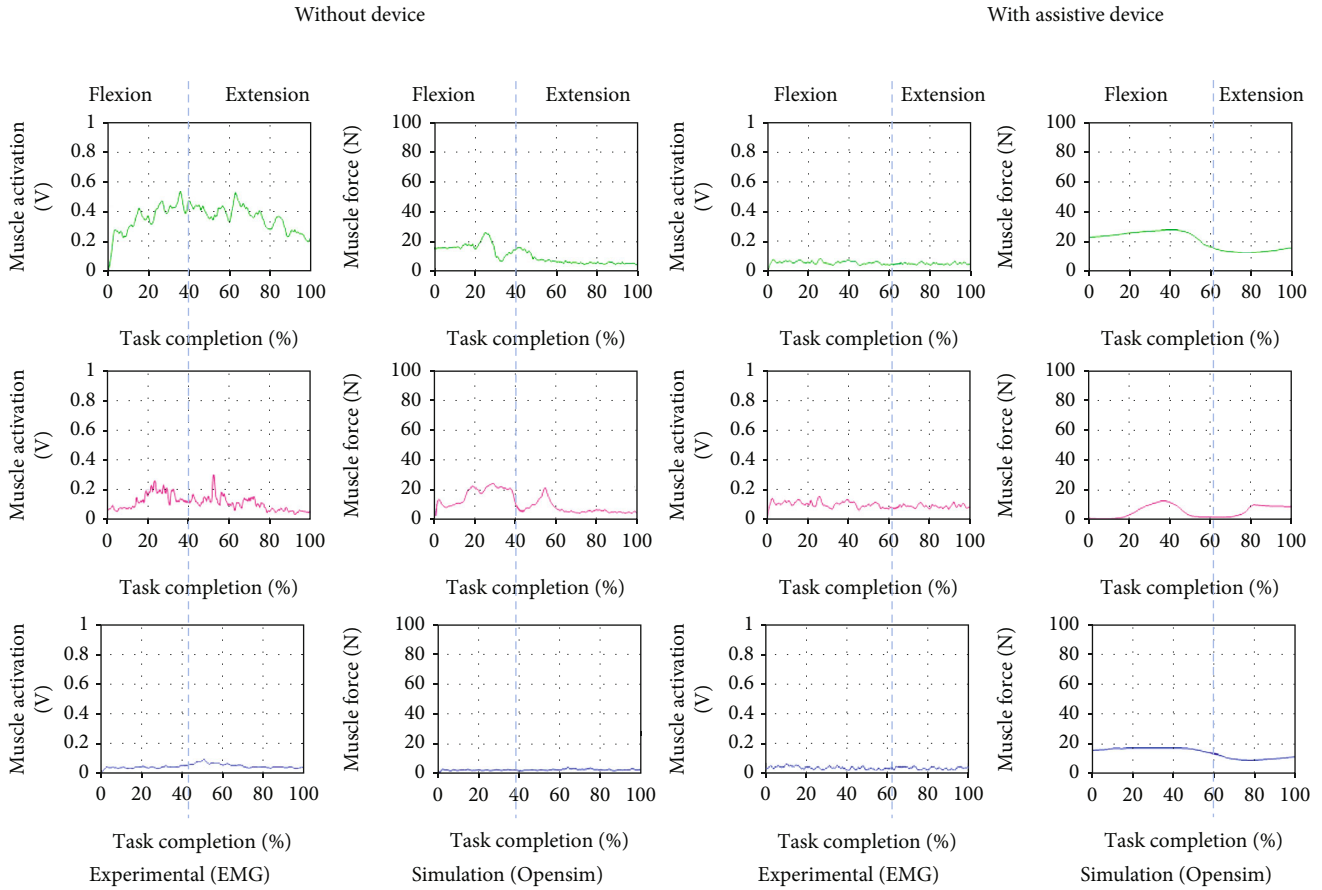


FIGURE 12: Comparison of EMG from experimental and muscle activations computed from OpenSim resulting in three muscle force brachioradialis (green), biceps (magenta), and triceps (blue) for inner elbow flexion and extension motion with and without the assistive device.

the arm is in extension motion (the last 50% of the movement) for the brachioradialis muscle. This is because the muscle was trying to sustain the movement because of the 1 kg weight worn by the subject on the wrist. On the other hand, we could observe the significant triceps muscle peak during the extension motion in musculoskeletal simulation with and without wearing the device. The triceps muscle is an extensor muscle of the upper extremity. Positioning and EMG sensor attachment probably cause minimal detection for the triceps muscle area during the experiment.

5.2. Upper Limb Motion: Maximum Shoulder Flexion and Extension. The result in Figure 11 shows a similar group of muscles activated during the arm's flexion, which peaks in the brachioradialis, and biceps muscles can be observed in both experiment and simulation data for the first 40% of the movement. Then, these muscles also have another activation during the shoulder flexion. Although commonly, the muscle involved during elbow flexion is mainly at the shoulder, the weight in the subject's arm could cause the muscle to do extra work to sustain the shoulder and arm during the shoulder flexion. Only the initial peak for both muscles can be observed when the subject wears the device. Due to the assisted movement by the device, the elbow and shoulder are well supported during the shoulder flexion, and extension movement causes no muscle activated during the motions. In both experiments,

low detection would probably be from the poor sensor attachment and the excessive fat region for triceps muscle data.

5.3. Upper Limb Motion: Inner Elbow Flexion and Extension.

For inner elbow flexion and extension, the shoulder muscle would be the most anticipated during these movements according to the muscle anatomy of the upper limb human movement. However, since this is a preliminary evaluation, we only focus on three muscles for all the motions for comparison, and none of the shoulder muscles is evaluated. Overall results in Figure 12 show that a shallow muscle peak is activated across the muscles. This visible activated muscle may be because of the muscle trying to hold or sustain the arm with the weight during the motion.

6. Discussion

Wearable assistive devices can potentially offset substantial arm loading during upper limb movement tasks. This study compared the functionality of the assistive device developed in this study for upper arm dynamic movements and its effect on the muscle output. Together with the experimental condition, two computer-based musculoskeletal models with and without device parameters have been set up. Specifically, we used measured tension forces during the device motion as input to

compare differences in force and activation in the right arm muscles (Brachioradialis, biceps, and triceps) activity.

Results showed that a musculoskeletal model with and without an integrated assistive device could produce muscle activation patterns similar to the EMG measured for all muscles of interest during the simulated upper dynamic tasks. A comparison of measured EMG muscle data and human-device models revealed that, although the model did not fully incorporate similar muscle physiology completely, muscle force was generated throughout the arm comparable with measured muscle activity from the experimental. The integrated human-device model produced encouraging results such that muscle force values for 2 primary muscles (biceps and brachioradialis) were reduced during the simulated task when wearing the assistive device. These results are congruent with expectations, with the assistive device manages to support the upper limb movement, providing practical assistance.

Our study has several assumptions and limitations. Firstly, only healthy subjects were tested and modeled in this study, and the findings may not reflect those of an affected upper limb due to the stroke disease. Secondly, differences in kinematics between the assistive device joints and the anatomical upper limb joints may have influenced model calculation during the simulation. However, they are unlikely to have influenced the main finding in this study of evaluation of significantly reduced muscle output when wearing the assistive device. Even though our simulation results are based on our developed assistive device design, our main findings are generalizable to other wearable devices, including cable-driven ones.

We only simulated 3 specific upper extremity movements in the present study that capture a small subset of possible upper arm movements. A more significant number of movements representing the wide variety of daily living tasks should be evaluated in the future to determine the effect of the assistive device more comprehensively on user biomechanics. In addition, we constrained all simulations and conditions to the same experimental kinematics from the healthy subject who was not impaired and did not use the device in regular daily life. Someone using an assistive device regularly may adapt their movement, as shown for other passive devices [26].

Our developed assistive device's primary function is to help with ADL tasks for patients who cannot move one arm. However, the capability of the assistive device to assist the arm movement and its effect on muscle activity has not been studied to date. This study demonstrated that upper limb movement assisted by the wearable assistive device could reduce peak muscle force confirming the study hypothesis.

7. Conclusions

To successfully translate wearable assistive technology to upper limb disability patients during rehabilitation training, it is critical to understand its effectiveness, usability, and biomechanical interaction with humans. As a first step toward accomplishing this goal, we quantitatively evaluated our developed assistive device's mechanical and biomechanical performance. Our results showed that the

device could reduce the muscle activity of several muscles crossing the upper arm. However, our mechanical evaluation revealed aspects of the design that limit the assistive device's assistance. In our future work, different assistance levels and identifying a range of assistance that most enhances arm motor function and biomechanics will be explored further. More comprehensive biomechanical studies will be performed to assess the device for more biomechanical parameters (e.g., joint kinematics), more participants (both able-bodied subjects and people with upper arm disability), and more movements that typify activities of daily living. Finally, several design refinements need to be made, especially those that reduce friction and add a motion range to the system.

The method's limitations suggest that if the interest is focused on muscle forces, EMG data can only provide a preliminary assessment of muscle activation patterns and does not provide information on how muscle forces change within specific tasks due to the nonlinear relationship between EMG and muscle forces [27]. The ideal way to compare the results of a musculoskeletal model and actual internal structure forces would be to measure joint reaction forces during the movement of interest and relate them to the calculated joint reaction forces. This type of validation is limited to impaired participants, who might not even complete all tasks.

Furthermore, the musculoskeletal models were not adjusted participant specifically in the current study, further explaining the differences between the model predictions and the EMG measurements. However, it can be assumed that the participant-specific differences based on the available treatment are substantially averaged out over the five participants. Moreover, the goal was to assess whether this human-device integrated model can be used in future research for evaluating muscle output during rehabilitation training when using the assistive device. To conclude, this study showed that the integrated human-device musculoskeletal model yielded good agreement between the measured and estimated muscle activity for most conditions and muscles. Therefore, it can be used for further analysis in similar groups of participants.

Data Availability

The human-device integrated model data used to support the findings of this study have not been made available because the device was only available at our laboratory.

Ethical Approval

The study was conducted according to the guidelines approved by the Ethics Committee of the Shibaura Institute of Technology Review Board.

Consent

Informed consent was obtained from all subjects involved in the study.

Conflicts of Interest

The authors declare no conflict of interest.

Authors' Contributions

M.F.A. was the principal investigator and contributed to the analysis, data collection, and summarization. A.H.'s supervision and S.M. contributed to the review and methodology validation. All authors have agreed to the approval of the final manuscript.

References

- [1] <http://www.who.int/mediacentre/factsheets/fs352/en/>.
- [2] R. W. Teasell and L. Kalra, "What's new in stroke rehabilitation," *Stroke*, vol. 35, no. 2, pp. 383–385, 2004.
- [3] A. Seth, J. L. Hicks, T. K. Uchida et al., "OpenSim: simulating musculoskeletal dynamics and neuromuscular control to study human and animal movement," *PLoS Computational Biology*, vol. 14, no. 7, article e1006223, 2018.
- [4] P. Agarwal, M. S. Narayanan, L.-F. Lee, F. Mendel, and V. N. Krovi, "Simulation-based design of exoskeletons using musculoskeletal analysis," in *Proceedings of the ASME 2010 International Design Engineering Technical Conferences and Computers and Information in Engineering Conference of Volume 3: 30th Computers and Information in Engineering Conference, Parts A and B*, pp. 1357–1364, Montreal, Quebec, Canada, 2010.
- [5] Z. Lelai, L. Yibin, and B. Shaoping, "A human-centered design optimization approach for robotic exoskeletons through biomechanical simulation," *Robotics and Autonomous Systems*, vol. 91, pp. 337–347, 2017.
- [6] D. Pujals, *Simulation of the Assistance of an Exoskeleton on Lower Limbs Joints Using OpenSim*, [M.S. thesis], Universitat Politècnica de Catalunya, Barcelona, 2017.
- [7] K. Holzbaaur, W. M. Murray, and S. L. Delp, "A model of the upper extremity for simulating musculoskeletal surgery and analyzing neuromuscular control," *Annals of Biomedical Engineering*, vol. 33, no. 6, pp. 829–840, 2005.
- [8] K. R. Saul, X. Hu, C. M. Goehler et al., "Benchmarking of dynamic simulation predictions in two software platforms using an upper limb musculoskeletal model," *Computer Methods in Biomechanics and Biomedical Engineering*, vol. 18, no. 13, pp. 1445–1458, 2015.
- [9] J. Chand, S. Hammer, and J. Hicks, "Collecting Experimental Data," *OpenSim Documentation*, 2012, <http://simtkconfluence.stanford.edu:8080/display/OpenSim/Collecting+Experimental+Data>.
- [10] D. G. Thelen, F. C. Anderson, and S. L. Delp, "Generating dynamic simulations of movement using computed muscle control," *Journal of Biomechanics*, vol. 36, no. 3, pp. 321–328, 2003.
- [11] "Creo Software," <https://www.ptc.com/en/products/creo>.
- [12] E. Pirondini, M. Coscia, S. Marcheschi et al., "Evaluation of the effects of the arm light exoskeleton on movement execution and muscle activities: a pilot study on healthy subjects," *Journal of NeuroEngineering and Rehabilitation*, vol. 13, no. 1, 2016.
- [13] R. Gopura and K. Kiguchi, "Mechanical designs of active upper-limb exoskeleton robots: state-of-the-art and design difficulties," in *2009 IEEE International Conference on Rehabilitation Robotics*, pp. 178–187, Kyoto, Japan, 2009.
- [14] P. Agarwal, P.-H. Kuo, R. R. Neptune, and A. D. Deshpande, "A novel framework for virtual prototyping of rehabilitation exoskeletons," in *2013 IEEE 13th International Conference on Rehabilitation Robotics (ICORR)*, pp. 1–6, Seattle, WA, USA, 2013.
- [15] L. L. Menegaldo, A. De Toledo Fleury, and W. Hi, "A 'cheap' optimal control approach to estimate muscle forces in musculoskeletal systems," *Journal of Biomechanics*, vol. 39, no. 10, pp. 1787–1795, 2006.
- [16] H. I. Krebs, S. P. Buerger, K. A. Jugenheimer, D. Williams, and N. Hogan, "3-D extension for MIT-MANUS: a robot-aided neuro-rehabilitation workstation," in *Volume 7B: 26th Biennial Mechanisms and Robotics Conference*, Baltimore, Maryland, USA, 2000.
- [17] J. C. Perry, J. Rosen, and S. Burns, "Upper-limb powered exoskeleton design," *IEEE/ASME Transactions on Mechatronics*, vol. 12, no. 4, pp. 408–417, 2007.
- [18] P. S. Lum, C. G. Burgar, P. C. Shor, M. Majmundar, and M. Van Der Loos, "Robot-assisted movement training compared with conventional therapy techniques for the rehabilitation of upper-limb motor function after stroke," *Archives of Physical Medicine and Rehabilitation*, vol. 83, no. 7, pp. 952–959, 2002.
- [19] H. S. Lo and S. Q. Xie, "Exoskeleton robots for upper-limb rehabilitation: state of the art and future prospects," *Medical engineering & physics*, vol. 34, no. 3, pp. 261–268, 2012.
- [20] N. Jarrassé, T. Proietti, V. Crocher et al., "Robotic exoskeletons: a perspective for the rehabilitation of arm coordination in stroke patients," *Frontiers in Human Neuroscience*, vol. 8, pp. 947–947, 2014.
- [21] D. G. Magermans, E. Chadwick, H. E. J. Veeger, and F. C. T. van der Helm, "Requirements for upper extremity motions during activities of daily living," *Clinical Biomechanics*, vol. 20, no. 6, pp. 591–599, 2005.
- [22] A. Hanafusa, F. Shiki, H. Ishii et al., "Development of an active upper limb orthosis controlled by EMG with upper arm rotation," in *Intelligent Human Systems Integration-Proceedings of the 1st International Conference on Intelligent Human Systems Integration IHSI: Integrating People and Intelligent Systems*, pp. 163–169, Springer, 2018.
- [23] P. Maciejasz, J. Eschweiler, K. Gerlach-Hahn, A. Jansen-Troy, and S. Leonhardt, "A survey on robotic devices for upper limb rehabilitation," *Journal of neuroengineering and rehabilitation*, vol. 11, no. 1, 2014.
- [24] R. D. Crowninshield, "Use of optimization techniques to predict muscle forces," *Journal of Biomechanical Engineering*, vol. 100, no. 2, pp. 88–92, 1978.
- [25] K. N. An, K. R. Kaufman, and E. Chao, "Physiological considerations of muscle force through the elbow joint," *Journal of Biomechanics*, vol. 22, no. 11–12, pp. 1249–1256, 1989.
- [26] G. Kwakkel, B. J. Kollen, and H. I. Krebs, "Effects of robot-assisted therapy on upper limb recovery after stroke: a systematic review," *Neurorehabilitation and Neural Repair*, vol. 22, no. 2, pp. 111–121, 2008.
- [27] K. Luttgen and K. E. Wells, *Kinesiology: Scientific Basis of Human Movement*, Saunders, Philadelphia, 7th edition, 1982.

Muscle Force Estimation for Upper Limb Assistive Device for Home Setting

Muhamad Fadzli, Akihiko Hanafusa, Kubota Yuuji, Nishimori Daigo

Abstract— Stroke rehabilitation using assistive device has the potential to cover the need of improvement of upper limb functionality. Moreover, using biomechanical model to estimate the muscle activity during the rehabilitation training could improve the training module as well as improvement of the motion of the assistive device. In this study, the author has focused on using biomechanical model of right arm to estimate the muscle force by simulating the movement of the right arm while using assistive device developed in our laboratory.

I. INTRODUCTION

The number of stroke survivor are considerably huge numbers in this world and most of the survivor have impairment impact on upper limb function (1). Some patients may recover some functionality of the upper limb function following the rehabilitation. However, most of the high technology assistive device were placed at the rehabilitation center and must be operated with the therapist. Recently, the needs of the assistive device with cost effective and home user friendly could help the patients with the rehabilitation training at home.

The development and improvement of the assistive device need to come together with the understanding of the muscle activation of the target muscle during the rehabilitation training. Given this, this study presents a method using musculoskeletal model focusing on upper limb to predict muscle force during the elbow flexion with the assistive device. Through this approach, the specific functional muscle involve during the movement could be known, making it possible to conduct improvement in the assistive device for rehabilitation training purpose.

II. METHODS

Experimental Setup and Muscle Force Estimation using OpenSim.

A subject was seated in the chair with their torso keeping upright and their right hand keeping relaxing. One motion is designed where the elbow flexion from natural position to close to 90 degree. Two separate sessions have been conducted which the subject performing the motions with and without assistive device. During the motion recording, 10 markers were used to specific positions together with marker clusters according to the recommendation on definitions of joint coordinate systems. The most dominant muscle which is

bicep was selected to be the muscle of test and active EMG electrode is positioned accordingly. The motion recording was sampled at 200 Hz and synchronized with the EMG recording through the motion capture system.

Delp et al. (2) have developed an open source platform called OpenSim. This platform allows the dynamic simulation on musculoskeletal system with motion capture. An upper limb model for the right hand [3] is available in this platform. It has realistic movements and precise muscular topology for the joints.

III. RESULTS

Fig.1 shows that the model used could estimate the force generated by a single muscle during movement. The assistive movement (red) produced less muscle activities resulting the muscle force excitation lowered compare to non-assisting movement (blue).

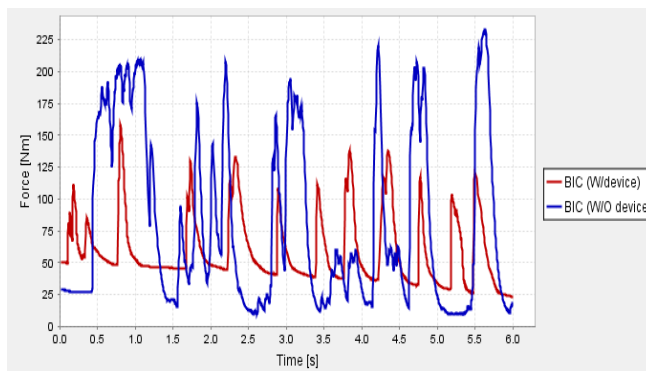


Figure 1. Estimation of bicep muscle force during elbow flexion

IV. DISCUSSION & CONCLUSION

The muscle force estimation method used could further the improvement of the assistive device. Few improvements to the model such as dynamic validation should be focused to have accurate muscle force result. The good agreement in EMG data taken and kinematics data proved that this approach could be used to identify muscle excitation during arm movement.

References

- [1] Ashford, S.; Slade, M.; Malaprade, F.; Turner-Stokes, L. "Evaluation of functional outcome measures for the hemiparetic upper limb: A systematic review." *J. Rehabil. Med.* 2008, 40, 787–795.
- [2] Delp, S.L., Anderson, F.C., Arnold, A.S., Loan, P., Habib, A., John, C.T., Guendelman, E., Thelan, D.G. OpenSim: Open-source software to create and analyze dynamic simulations of movement. *IEEE Transactions on Biomedical Engineering*, vol 55, pp 1940-1950. (2007).

Muscle Force Estimation for Upper Limb Assistive Device for Home Setting

Muhamad Fadzli Bin Ashari¹, Akihiko Hanafusa¹, Yuji Kubota¹, Daigo Nishimori¹

Department of Bio-science & Engineering,
Shibaura Institute of Technology, Japan



Introduction & Objective

The number of stroke survivor are considerably huge numbers in this world and most of the survivor have impairment impact on upper limb function. Some patients may recover some functionality of the upper limb function following the rehabilitation. However, most of the high technology assistive device were placed at the rehabilitation center and must be operated with the therapist. Recently, the needs of the assistive device with cost effective and home user friendly could help the patients with the rehabilitation training at home. The development and improvement of the assistive device need to come together with the understanding of the muscle activation of the target muscle during the rehabilitation training.

Objective:

This study presents a method using musculoskeletal model focusing on upper limb to predict muscle force during motion using the assistive device. Through this approach, the specific functional muscle involve during the movement could be known, making it possible to conduct improvement in the assistive device for rehabilitation training purpose.

Methodology

Assistive Device

As shown in Fig.1 below, a light weight assistive device which is driven by 2 servo motors has been developed. Flexion motor pulls up wire that is connected to wrist part. The device can generate the motions of elbow flexion/extension and internal /external rotation.

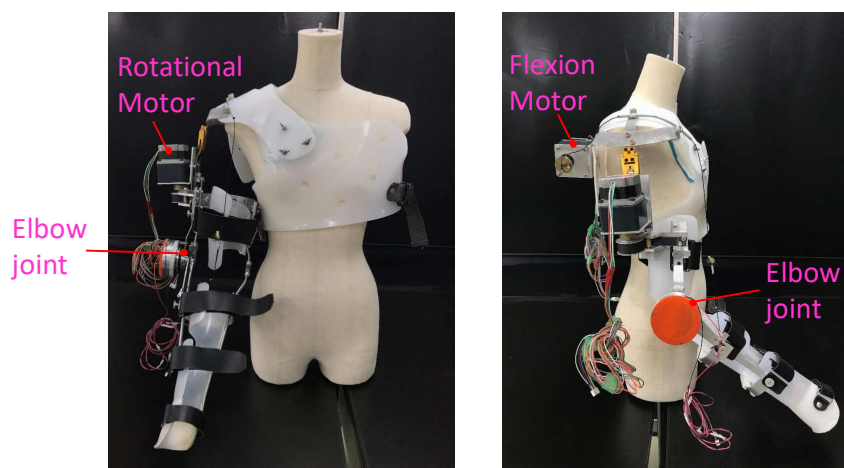


Figure 1. Upper limb right hand assistive device specifications

Experimental Setup

One motion is designed where the elbow flexion from natural position to close to 90 degree. Two separate sessions have been conducted which the subject performing the motions with and without assistive device. During the motion recording, 10 markers were used and active EMG electrode was positioned on bicep.

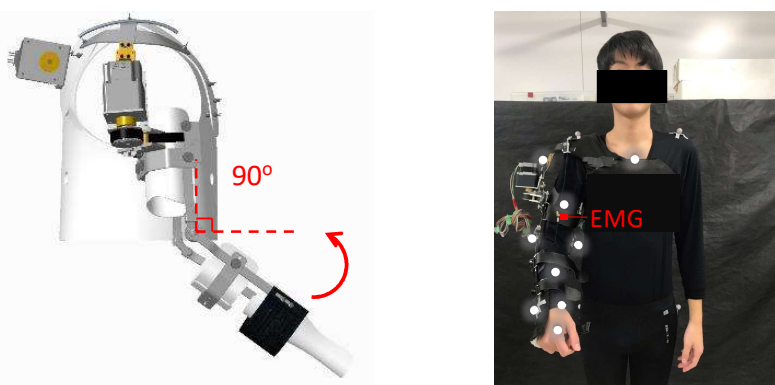


Figure 2. Elbow flexion motion with markers and EMG electrode positions

Musculoskeletal Model

Open source platform called OpenSim has been used and this platform allows the dynamic simulation on musculoskeletal system with motion capture data. An upper limb model (Fig.3) is available in this platform. It has realistic movements and precise muscular topology for the joints. Two simulations has been conducted with the motions data of subject performing arm movement with/without using assistive device.

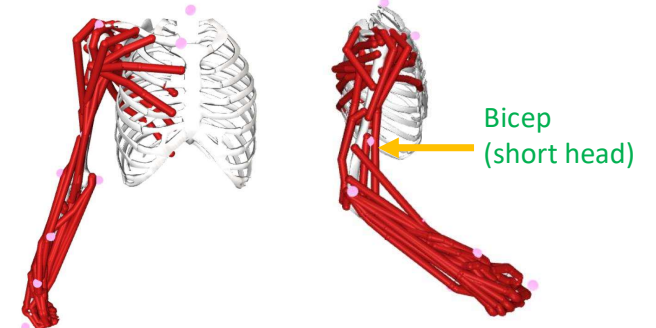


Figure 3. 7 degree of freedom of dynamic musculoskeletal model of the upper limb

Results & Discussions

Fig. 4 shows that the model used could estimate the muscle activation generated by a targeted muscle during movement. (a) shows result from measured EMG and (b) shows estimated EMG using OpenSim model. The assistive movement (blue) produced less muscle activities resulting the muscle force excitation lowered compare to non-assisting movement (green).

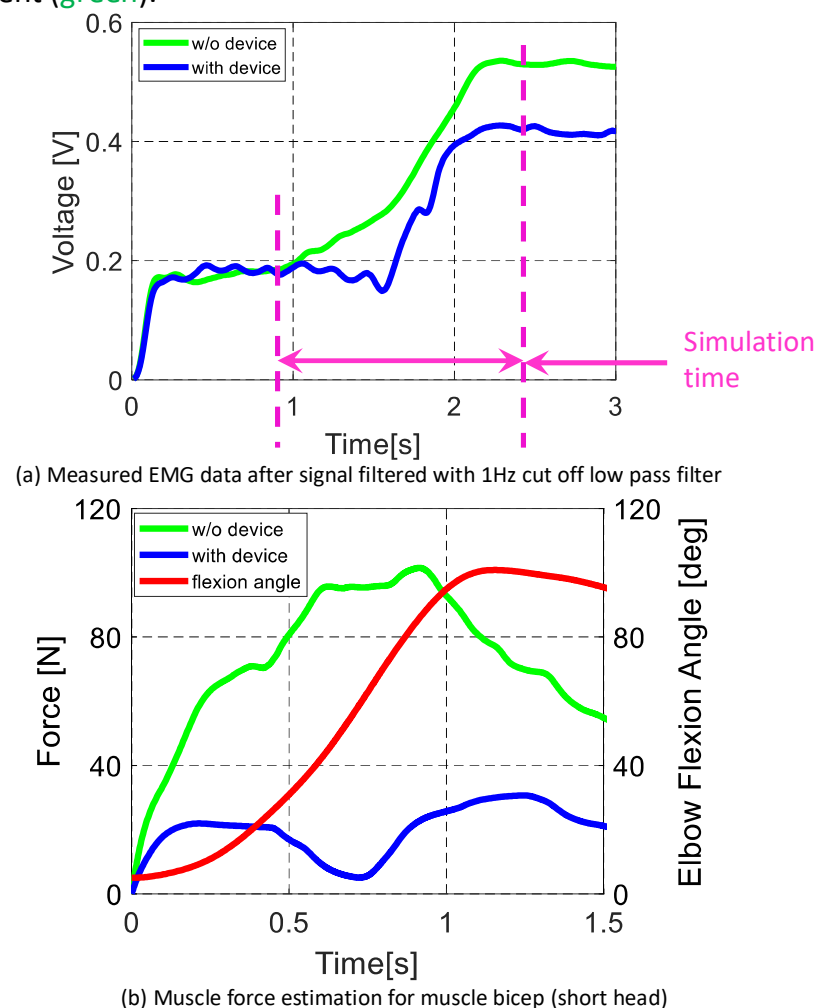


Figure 4. Filtered EMG data and estimation of muscle force for individual muscle during elbow flexion with and without assistive device

Conclusions

- ❑ The good agreement in recorded EMG data pattern and estimation muscle force data proved that this method could be used to identify muscle activity during arm movement.
- ❑ Few improvements to the model such as dynamic validation should be focused to have accurate muscle force results.
- ❑ The muscle force estimation method can be used for improvement of the assistive device.

Study of Muscle Force Estimation for Upper Limb Rehabilitation Device for Home Setting

Muhamad Fadzli Bin Ashari¹, Akihiko Hanafusa¹, Yuji Kubota¹, Daigo Nishimori¹

1. Shibaura Institute of Technology, Japan

Introduction & Objective

The number of stroke survivor are considerably huge numbers in this world and most of the survivor have impairment impact on upper limb function. Some patients may recover some functionality of the upper limb function following the rehabilitation. However, most of the high technology assistive device were placed at the rehabilitation center and must be operated with the therapist. Recently, the needs of the assistive device with cost effective and home user friendly could help the patients with the rehabilitation training at home. The development and improvement of the assistive device need to come together with the understanding of the muscle activation of the target muscle during the rehabilitation training.

Objective:

This study presents a method using musculoskeletal model focusing on upper limb to predict muscle activation during motion using the assistive device. Through this approach, the specific functional muscle involve during the movement could be known, making it possible to conduct improvement in the assistive device for rehabilitation training purpose.

Methodology

Assistive Device

As shown in Fig.1 below, a light weight assistive device which is wired driven by 2 servo motors has been developed in our laboratory. The device can generate the motions of elbow flexion/extension and internal/external rotation.

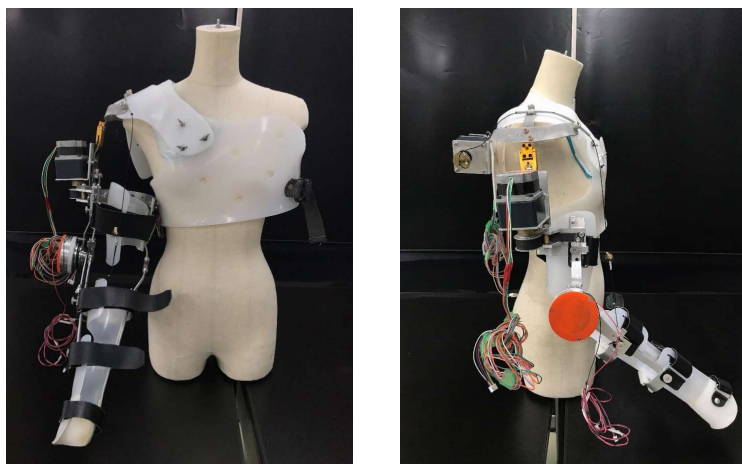


Figure 1. Upper limb right hand assistive device

Upper Limb Musculoskeletal Model

Open source platform called OpenSim has been used and this platform allows the dynamic simulation on musculoskeletal system with motion capture data. An upper limb model for the right hand (Fig.2) is available in this platform. It has realistic movements and precise muscular topology for the joints. Two simulations has been conducted with the motions data of subject performing arm movement with and without using assistive device.

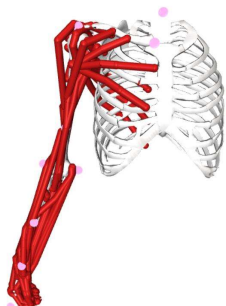


Figure 2. 7 degree of freedom of upper limb dynamic musculoskeletal model

Simulation Setup

One motion is designed where the elbow flexion from natural position to close to 100 degree. The motion data is produced from Motion Capture 3D data available at our laboratory. Two separate simulation have been designed where the model performing the motions with and without assistive device. Torque of 4Nm is applied to the musculoskeletal model simulating the model with assistive device. A target muscle which is bicep (short) is investigated for muscle activity.

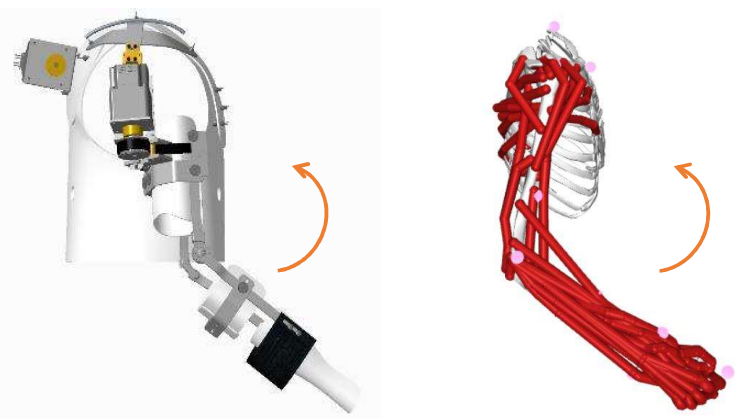


Figure 3. Elbow flexion motion

Results & Discussion

Fig. 4 shows that the model used could estimate the muscle activation generated by a targeted muscle during movement. The assistive movement (blue) produced less muscle activities resulting the muscle force excitation lowered compare to non-assisting movement (green).

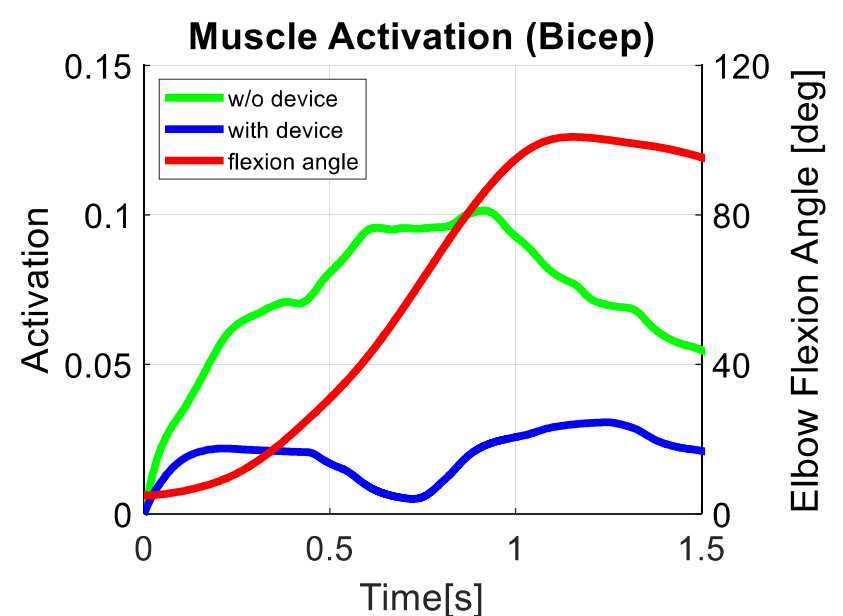


Figure 4. Estimation of muscle activation during elbow flexion with and without assistive device

Conclusion

- ❑ The muscle force estimation method used could further the improvement of the assistive device.
- ❑ Few improvements to the model such as dynamic validation should be focused to have accurate muscle activation results.
- ❑ The muscle estimation data should be compared to EMG data of the targeted muscle experimentally to ensure the reliability of the approach as well as the simulation results.
- ❑ This approach could deepen the understanding of human movement focusing on stroke patient with upper limb impairment to accelerate the development of rehabilitative treatments and assistive devices.

APPENDIX

(SUPPLEMENTAL MATERIAL)

Sample Model's File coding used in OpenSim

```
1 <?xml version="1.0" encoding="UTF-8" ?>
2 <OpenSimDocument Version="30000">
3   <Model name="Upperlimb Model with device">
4     <defaults>
5       <ControlLinear name="default">
18       <CoordinateActuator name="default">
30       <PointActuator name="default">
50       <TorqueActuator name="default">
68       <Thelen2003Muscle name="default">
133       <CMC Joint name="default">
161     </defaults>
162     <length_units>Meters</length units>
163     <force_units>N</force units>
164     <!--Acceleration due to gravity.-->
165     <gravity> 0 -9.80665 0</gravity>
166     <!--Bodies in the model.-->
167     <BodySet>
168       <objects>
169         <Body name="ground">
242         <Body name="clavicle">
424         <Body name="clavphant">
589         <Body name="scapula">
913         <Body name="scapphant">
1096        <Body name="humphant">
1243        <Body name="humphant1">
1408        <Body name="humerus">
1533        <Body name="ulna">
1600        <Body name="radius">
1658        <Body name="proximal row">
1716        <Body name="hand">
1787        <Body name="upperdevice">
1858        <Body name="lowerdevice">
1929        <Body name="sphere1">
1930        <Body name="sphere2">
1931        <Body name="trunk1">
1932      </objects>
1933      <groups />
1934    </BodySet>
1935    <!--Constraints in the model.-->
1936    <ConstraintSet>
1937      <objects>
1938        <CoordinateCouplerConstraint name="sternoclavicular r2 con">
1952        <CoordinateCouplerConstraint name="sternoclavicular r3 con">
1969        <CoordinateCouplerConstraint name="unrotscap r2 con">
1986        <CoordinateCouplerConstraint name="unrotscap r3 con">
2003        <CoordinateCouplerConstraint name="acromioclavicular r1 con">
2020        <CoordinateCouplerConstraint name="acromioclavicular r2 con">
2037        <CoordinateCouplerConstraint name="acromioclavicular r3 con">
2054        <CoordinateCouplerConstraint name="unrothum r1 con">
2071        <CoordinateCouplerConstraint name="unrothum r2 con">
2088        <CoordinateCouplerConstraint name="unrothum r3 con">
2105        <CoordinateCouplerConstraint name="shoulder1 r2 con">
2122        <CoordinateCouplerConstraint name="wrist hand r1 con">
2139        <CoordinateCouplerConstraint name="wrist hand r3 con">
2156      </objects>
2157    </ConstraintSet>
2158  </Model>
2159 </OpenSimDocument>
```

```
4929 |         </objects>
4930 |         <groups />
4931 |     </BodySet>
4932 |     <!--Constraints in the model.-->
4933 |     <ConstraintSet>
4934 |         <objects>
4935 |             <CoordinateCouplerConstraint name="sternoclavicular r2 con">
4952 |             <CoordinateCouplerConstraint name="sternoclavicular r3 con">
4969 |             <CoordinateCouplerConstraint name="unrotscap r2 con">
4986 |             <CoordinateCouplerConstraint name="unrotscap r3 con">
5003 |             <CoordinateCouplerConstraint name="acromioclavicular r1 con">
5020 |             <CoordinateCouplerConstraint name="acromioclavicular r2 con">
5037 |             <CoordinateCouplerConstraint name="acromioclavicular r3 con">
5054 |             <CoordinateCouplerConstraint name="unrothum r1 con">
5071 |             <CoordinateCouplerConstraint name="unrothum r2 con">
5088 |             <CoordinateCouplerConstraint name="unrothum r3 con">
5105 |             <CoordinateCouplerConstraint name="shoulder1 r2 con">
5122 |             <CoordinateCouplerConstraint name="wrist hand r1 con">
5139 |             <CoordinateCouplerConstraint name="wrist hand r3 con">
5156 |         </objects>
5157 |         <groups />
5158 |     </ConstraintSet>
5159 |     <!--Forces in the model.-->
5160 |     <ForceSet>
5161 |         <objects>
11329 |         <groups />
11330 |     </ForceSet>
11331 |     <!--Markers in the model.-->
11332 |     <MarkerSet>
11333 |         <objects>
11334 |             <Marker name="R.Clavicle">
11342 |             <Marker name="C7">
11350 |             <Marker name="R.Shoulder">
11358 |             <Marker name="R.Bicep">
11366 |             <Marker name="R.Elbow.Lateral">
11374 |             <Marker name="R.Forearm">
11382 |             <Marker name="R.Radius">
11390 |             <Marker name="Handle">
11398 |             <Marker name="R.Elbow.Medial">
11406 |             <Marker name="R.Ulna">
11414 |         </objects>
11415 |         <groups />
11416 |     </MarkerSet>
11417 |     <!--ContactGeometries in the model.-->
11418 |     <ContactGeometrySet>
11419 |         <objects />
11420 |         <groups />
11421 |     </ContactGeometrySet>
11422 | </Model>
11423 | </OpenSimDocument>
11424 |
```